Supervisor: Dr. Vijay K. Bhargava

ABSTRACT

In the design of the third generation of multi-media wireless networks, we are primarily concerned with the greatly varying information source rates, the quality requirements of various traffic types, the characteristics of the wireless environment, as well as the complexity and cost. Code Division Multiple Access (CDMA) cellular system is one of the most important candidates for supporting the future universal communications services. The objective of this research is to improve the capacity and the quality of service (QOS), as well as to reduce the complexity of cellular CDMA with integrated services, through improving or optimizing the design of system level operations.

To facilitate the system performance and capacity evaluation, the multi-cell multi-user interference is analyzed through a new approach. The area averaged probability density function (PDF) of interference power from one active user is evaluated. The Gamma distribution is proposed for modelling the area averaged PDF of the interference power. An efficient method for evaluating system performance is developed. Differing from the Gaussian approximation, this method is very effective and accurate for both a large number and a small number of users.

In this research, differing from the distance membership determination, the statistical effect of hand-off is considered. The effects of soft handoff operation on multi-cell multi-user interference are analyzed. Membership statistics which are determined by soft handoff are investigated. A simple binomial model is proposed for modelling the distribution of the number of users belonging to a base station.

Considering the call arrival statistics, user membership statistics and a finite number of channels available at a base station, we evaluate the call blocking/dropping rate. The minimum number of channels required at a base-station, which ensures a specified quality of service at a given capacity requirement, is determined. System capacity is further evaluated considering both outage probability limited by interference and call blocking/drop-

ping rate limited by finite number of channels. A pilot assisted channel allocation method is proposed to minimize the number of channels required at a base station.

Based on the analysis of a CDMA cellular system with a single traffic type, the design issues in developing a multi-media wireless networks are further discussed. The capacity of a CDMA cellular system with high quality requirements and mixed stream and packet types of traffic is assessed. The impact of the choice of a line rate (bit transmission rate through channel) on the system capacity is investigated. It is also shown that the power allocated to different types of traffic can be optimized to achieve maximum capacity. The optimum power allocation suggests that the power assignments to different traffic types are mainly determined by their quality requirements.

Examiners:

Dr. Vijay K. Bhargava, Supervisor

Dr. Qiang Wang, Departmental Member

Dr. Fayez El-Guibaly, Departmental Member

Dr. Frank Ruskey, Outside Member

Dr. Norman P. Secord, External Examiner

Table of Contents

List of Tables

List of Figures

Acknowledgments

I am deeply grateful to my supervisor, Dr. Vijay K. Bhargava, for offering me the opportunity to pursue my Ph. D. program in the University of Victoria. Your sustained support, encouragement and advice greatly assist me in not only completing this work, but also building up a solid foundation for my professional career. For all what you have done for me, please accept my deep appreciation from the bottom of my heart.

I would like to thank Dr. Qiang Wang for his valuable comments and suggestions on my research, Dr. Norman P. Secord for his detailed suggestions on my thesis, which lead to a great improvement of the quality of my thesis.

I would also like to extend my sincere appreciation to my colleagues at the Telecommunication Research Lab. for their friendship, support, discussion, proof-reading, ... In particular, I wish to thank Dr. Muzhong Wang for his great assistance in system simulations, Ms. Mo-Han Fong and Mr. Roman Pichna for the fruitful cooperation in the project for the Canadian Institute for Telecommunication Research (CITR).

This work is supported by the CITR under the NCE program of the Government of Canada, and the Natural Science and Engineering Research Council of Canada through research grants to Dr. Vijay K. Bhargava.

Finally, I feel deeply indebted to my family, specifically, to my wife Ms. Danhong Wu for all your sacrifices, love, persistent support and bearing, to my son Daniel Weiben Zou for the joy that you bring to me, and my parents Mr. Yizhi Zou and Ms. Qiyun Wang for your care, understanding and encouragement. Without your love, sacrifices and full support, this work would not have been completed.

To my grandmother and grandfather-

Wanyi Zhang and Chunzuo Zou

I miss you.

Chapter 1

Introduction

1.1 Background and Motivation

Nowadays, digital communication is undergoing a great revolution: the globalization of wireless communications. Over the past several years, the demand for wireless personal communications services has increased exponentially. The demand is not only from the developed countries, but also from the developing countries. Great opportunities appear to the wireless communications industry.

The ultimate service goal of universal personal communications is to allow reliable multi-media communications between any person, from anywhere, at anytime via a pocket-size handset [1]. To achieve this target, VLSI and advanced power supply technologies have been improved continuously to reduce the terminal size. Large scale wireless networks with cellular structure are being developed to provide the full coverage for accessing by any one from anywhere at anytime. Macro, micro, and pico cells, as well as satellite cells are involved to support the globalization of wireless personal communications. Integrated services will support multi-media traffic, which means that various traffic types will be fully integrated into one network and the service requirements of different types of traffic will be met.

A great amount of research activity has been devoted to developing third generation universal communications networks [2]-[4]. One of the major projects in the world which is at the leading edge in this area is the R & D in Advanced Communications Tech-

nologies in Europe (RACE) program. There are two sub-projects under RACE: the Advanced TDMA project and the COde DIvision Testbed (CODIT) project. CDMA is employed as the principle access technology in the CODIT project [2]. A similar project is also being conducted by the Canadian Institute for Telecommunications Research (CITR) in Canada. Both universities and industry are heavily involved [3], [5].

The next generation of wireless networks will accommodate a variety of traffic types. Different traffic types may have different source rates, different delay requirements and different quality requirements [3], [4], [6]. Typical future service requirements are shown in Table 1.1. The service requirements are considered in terms of transmission rate, delay and bit error rate.

Table 1.1 The characteristics of various traffic types

Traffic types	Bit rate range	Maximum BER	Delay
Speech	8-64 Kbps	10^{-3}	Sensitive
General computer data	0.1-1 Mbps	10^{-9}	Insensitive
Facsimile	20 Kbps or less	10^{-4}	Insensitive
High speed data (file transfer, multimedia)	1-10 Mbps	10^{-9}	Insensitive
Low Resolution Video	64-384 Kbps	10^{-4}	Sensitive
TV quality video	1-6 Mbps	10^{-4}-10^{-5}	Sensitive

To realize the goal of universal personal communications, there are several design objectives for the multi-media cellular network that telecommunications engineers must observe:

1. Managing our communication resources, such as energy, bandwidth, time and space, as efficiently as possible.

2. Full traffic integration over a wide range of source rates.

3. Real-time and high quality service performance.

4. Quality of services (QOS) meeting various quality requirements.

5. Capacity improvement for high rate users with high quality requirements.

6. Seamless support of fixed and mobile users with different speeds.

7. Flexibility of application/service development.

8. Minimize the complexity and cost.

There are several key techniques that are under development for the next generation of multi-media wireless networks. These techniques include: advanced multiple access techniques, cellular and mobility management techniques, error control techniques, resource management techniques, and system management techniques at the higher layer [1]. Among them, multiple access techniques are of the most concern in the physical layer.

Code Division Multiple Access (CDMA) has many inherent features which make it one of the best multiple access techniques for the next generation of wireless networks [1], [7]-[9]. There are several advantages to use CDMA in a cellular network. For example:

1. The entire bandwidth is used in each cell. Complex frequency planning is avoided, making a CDMA network more flexible for future system expansion.

2. The inherent interference averaging feature of CDMA allows for system design based on the average interference, which provides more capacity than the worst case design.

3. Frequency diversity and voice activity exploitation are inherent features of CDMA, therefore no extra effort is required to get high bandwidth efficiency in this regard.

4. CDMA is interference limited and any suppression of the interference can be directly translated into an increase in the capacity.

5. Finally, CDMA provides soft capacity and soft handoff features.

6. There is a great potential for performance improvement of cellular CDMA when the error control coding techniques are employed [10].

Soft capacity means that there is no hard limit on the number of users that can be accommodated in a CDMA cellular system. In a CDMA system which is already fully loaded, more users can still be added in at the expense of the communication quality of all currently active users in the system. Soft handoff means that there is no frequency switching during a handoff and seamless handoff is realized by employing the diversity combining techniques. Due to the advantages of CDMA, we focus our study on a CDMA cellular system with integrated services. Our research also includes cellular techniques and resource management techniques which are specifically related to CDMA.

IS-95 [10]-[13] is the first standard for cellular CDMA in North America. It is designed mainly for voice users. In the design of a CDMA cellular system with integrated services, special considerations must be made to deal with various traffic types with different source rates and quality requirements. Capacity and the QOS are two of the most important criteria for wireless cellular system design. They are closely related. The QOS determines the capacity. In order to provide design recommendations, the capacity of a system with various traffic types needs to be assessed. An efficient method for capacity evaluation should be developed. Here, we consider that the QOS includes the error probability, delay, blocking and dropping rate. Detailed analysis is necessary to determine the QOS of a system so as to provide design guidelines.

There is a large amount of literature related to performance analysis and capacity evaluation of Direct Sequence CDMA (DS-CDMA) cellular systems with a single type of traffic. Gilhousen et al. [14] have evaluated the capacity of a cellular CDMA system for voice users. A relatively simple approximation was applied with an assumption that the cell membership is determined by the minimum distance to a base-station and power control is perfect. Viterbi, Gilhousen et al. further analyzed the multi-cell, multi-user

interference of a CDMA cellular system with ideal soft handoff and power control [15], [16]. In [15], [16], the mean power of the interference is obtained and an interference factor has been given. This factor is the area averaged mean power of the inter-cell (or other cell's) interference divided by the corresponding average number of users per sector.

Since the capacity of a CDMA cellular system is interference limited, understanding the multi-cell, multi-user interference with various traffic types is necessary. The multi-cell, multi-user interference is largely determined by the performance of the system level operations such as resource management, handoff and power control which are tightly coupled to one another. Not only the mean but also the variance of the interference affects the system performance. Therefore, in addition to the mean, the variance must be determined by the analysis of system level operations. In order to maximize the capacity, interference must be minimized by improving the performance of those operations and techniques [17].

In [15], [16], the cell membership of a user is determined by the highest pilot power received by the user. However, the membership statistics have not yet appeared in the literature. Since the membership statistics determine the intra-cell interference and the QOS, a careful study of these statistics should be carried.

Most capacity evaluation work that appears in the literature utilizes the Gaussian assumption for multi-cell and multi-user interference. This assumption is accurate when the number of users per cell is sufficiently large. In a system with multiple traffic types, there may be users with very high bit rates and very high quality requirements. For these types of users, the number of users need not be large for the CDMA cellular system to reach its capacity. The performance of a system with a small number of users becomes very important for this case. Thus, an effective model and/or method is required for capacity evaluation when there are a small number of users.

In practice, the number of call arrivals at a base station is a random variable. To evaluate the actual capacity that can be supported by a system, the call arrival statistics

should be included. The Erlang capacity should therefore be evaluated. The Erlang capacity is calculated in [18] with an assumption that the number of physical channels at a base station is infinite. Actually, the number of channels is finite at a base station. The effect of a limited number of channels on QOS should therefore be evaluated.

For multiple traffic types, sources of differing rates should be efficiently integrated before transmission. In order to integrate a wide range of source rates, the application of a limited number of line rates is proposed to simplify the system design [3], [19]. A line rate is the actual bit transmission rate in the channel. The determination of the line rate becomes a design issue [20]. In addition, different levels of error control must be applied to different traffic types with specific quality requirements. To increase the overall capacity and improve the QOS, our communication resources such as channels, power and bandwidth should be carefully allocated to different types of users.

In the next generation of wireless networks, it is possible that all types of traffic will be transmitted in the form of packets. The nature of a packet CDMA network should be further investigated. The major issues of concern for a packet CDMA network are: throughput, error probability and delay. New design considerations should be made for the packet CDMA in a cellular environment with multiple traffic types.

1.2 Contributions of the Dissertation

The objective of this research is to improve the capacity and the quality of service of a multi-media cellular CDMA network, as well as to reduce the complexity and the cost of the network operations, through improving or optimizing the design of the system level operations. A careful study of a CDMA cellular system with a single type of traffic is performed. Based on the results obtained from the single type of traffic, the performance of a system with multiple traffic types is evaluated. Design guidelines are also provided. The contributions of this dissertation are in the following aspects.

We developed an analytical method to calculate both the mean and variance of the

total interference, as well as the area averaged probability density function (PDF) of inter-cell interference. We also analyzed the cell membership statistics of active users in a cell. Our results show that due to soft handoff, the area covered by a base station is enlarged and the inter-cell interference is greatly reduced.

To evaluate the system performance when the number of users per cell is small and the Gaussian model is inaccurate, we have developed a modelling method to calculate multi-cell, multi-user interference. An effective approach is developed to evaluate the performance of cellular CDMA systems for both a small and a large number of users. It is found that the Gamma distribution can be applied to model multi-cell, multi-user interference. Due to the effect of the soft handoff operation, the multi-user interference approaches the Gaussian distribution very quickly, especially when the Activity Factor (ACF) is large. The Gaussian model can therefore be applied in many cases, but it is inaccurate for a very small number of users, especially when the ACF is small.

The dependency of cell membership statistics on soft handoff is a very important factor affecting system performance, and has been investigated in detail. We have proposed a simple binomial model for the conditional distribution of the number of users due to soft handoff; the results closely agree with simulation. From the results obtained, it can also be seen that imperfect hand-off and power control reduce the capacity of a system.

Based on our analysis, we show that when there is soft handoff and cell site diversity, the number of channels required at a base station is much larger than the average number of users per cell. We have shown that with a limited number of channels, the call dropping rate increases drastically as the offered traffic increases. The minimum number of channels required at a base station for supporting a specific traffic is determined as a suggested design parameter. Pilot assisted channel allocation is proposed to reduce the number of channels required and control the cost.

To provide a guideline for the transmission line rate selection, we show that the

choice of line rate determines the Processing Gain (PG) and ACF. The capacity non-linearly increases as the PG increases and linearly increases as the ACF decreases. The increase of PG is more efficient in increasing the capacity.

For the traffic with different source rate and quality requirement, we show that the power allocated to different types of traffic can be optimized to achieve maximum capacity. An approach for determining the optimum power allocation for different types of traffic in a CDMA cellular system is developed. Optimum power allocation suggests that the different power assignments to different traffic types are mainly determined by their quality requirements.

1.3 Outline of the Dissertation

In this chapter, we provide an introduction to this thesis. The motivation and contribution of this research are addressed.

In Chapter 2, we give the basic principle, system model, and background on which this research is based on. The major related techniques in the IS-95 standard [10]-[13] and the basic channel model are described.

In Chapter 3, we analyze the multi-cell, multi-user interference in a CDMA cellular system with a single type of traffic. Ideal soft handoff and perfect power control are assumed at first.

In Chapter 4, we examine the effect of non-ideal soft handoff operations and imperfect power control. Based on a careful analysis of the effects of soft handoff operation in a multi-cell environment, the interference characteristics, system capacity and service quality are examined. The multi-cell, multi-user interference level highly depends on power control switching. In general, a highly sensitive power control handoff mechanism which is synchronized with cell site diversity selection is required.

In Chapter 5, we obtain a closed-form solution for the radio capacity, the Erlang capacity and the throughput of a packet CDMA cellular system. The capacity of a system

with typical parameters is evaluated. Various factors which affect the system capacity are examined. The capacity of a slotted ALOHA packet CDMA system is also assessed in this chapter. We show that the capacity of packet CDMA in a cellular environment is approximately 5 times larger than a conventional FDMA system. This result supports Qaulcomm's frequency reuse efficiency of a conventional CDMA system. We also show the effect of stream type of traffic on the throughput of packet traffic.

In Chapter 6, the performance of a CDMA cellular system with various traffic types is evaluated. This chapter examines issues such as traffic integration and resource management. To provide design guidelines for the line rate selection, the effects of PG and ACF on capacity are compared. The effect of the choice of line rate on system capacity for low rate, high rate and mixed rate traffic is evaluated. In this chapter, we also address how to assign suitable power levels to different traffic types. A method for optimizing the power assignment for multiple traffic types is developed and optimized power allocation is determined.

In chapter 7, several efficient simulation methods are discussed with an emphasis on the importance sampling. An analysis on the optimum biasing is shown in this chapter. Some simulation results of a CDMA cellular system are also given.

In chapter 8, conclusions and suggestions of future work are presented.

Chapter 2

Fundamental Principles and System Model

With the maturing of CDMA techniques, CDMA is often proposed for commercial applications. The first CDMA standard in North America, IS-95, has already been endorsed [7]-[14] and several field tests have been carried out [21], [22]. In this chapter, we provide an overview on several key aspects or techniques of an IS-95 CDMA cellular system. The IS-95 standard is the starting point of this research. The requirements of a system with integrated services are also discussed in this chapter.

2.1 Spread Spectrum and Code Division Multiple Access

The primary objectives of improving the performance of communication systems are to use our communication resources, such as energy, bandwidth, time and space, as efficient as possible. We want to increase the capacity and to improve the communication quality under the restrictions of the resources available and the consideration of decreasing the cost of the communication systems. The conventional methods of a communication system to allow multiple users to share the common resources are frequency division multiple access (FDMA) and time division multiple access (TDMA). Basically, they can be classified as one dimensional division operations, thus FDMA makes its division operation in the frequency domain and TDMA makes its operation in the time domain. This suggests that if a two-dimensional operation is possible, thus if we can assign different users different small frequency slots within different small time slots, the system capacity would be greatly increased. Although an ideal two dimensional opera-

tion is very difficult in practice, spread spectrum technology makes a non-ideal two dimensional operation possible. That is the code division multiple access (CDMA).

There are two distinct classes of spreading techniques. The first is direct sequence (DS) or pseudo-noise (PN) spread spectrum. The spreading is achieved via multiplication by a binary pseudo-random sequence whose symbol rate is many times the binary data bit rate. The spreading sequence symbol rate is called the chip rate. The second class of spreading technique employs a frequency hopping carrier. The spreading signal remains at a given frequency for each bit or even for several bits. Thus, locally it is no wider than the data signal, but it hops to any frequency over the entire spreading bandwidth. The start point of this thesis is IS-95 which is a DS-CDMA cellular system.

With DS-CDMA, each signal consists of a different pseudo-random binary sequence which modulates the carrier, spreading the spectrum of the waveform. A large number of CDMA signals share the same frequency spectrum. If one looks at CDMA in either the frequency or the time domain, the multiple access signals appear to be on top of each other. The signals are separated in the receivers by using a correlator which accepts only signal energy from the selected binary sequence and de-spreads its spectrum. The other users' signals, whose codes do not match that of the desired signal, are not de-spread in bandwidth and as a result, contribute only to the noise. The signal-to-interference ratio is determined by the ratio of desired signal power to the sum of the powers of the other user's signals, which is enhanced by the system processing gain (PG). PG is equal to the number of chips per information symbol.

CDMA is inherently a form of frequency diversity by spreading the signal energy over a wide bandwidth. The received signal coming from multiple paths can be discriminated by a RAKE receiver, provided that the delay spread is larger than the DS chip duration. Thus, assisted by multipath combining techniques, CDMA itself has great advantage in mitigating multipath fading. In general, diversity is the favored approach to combat fading. The quality of communication is normally improved significantly by

employing diversity at the expense of complexity and the resources for communications such as time, frequency and space. Correspondingly, there are three major types of diversity: time diversity, frequency diversity and space diversity. As mentioned before, CDMA is an example of frequency diversity. Time diversity can be obtained by the use of error control coding. Space diversity is obtained by providing multiple signal paths through simultaneous links from the mobile to two or more base stations (cell-site diversity) by allowing signals arriving with different propagation delays to be received separately, and by providing multiple antennas at the cell-site. Cell-site diversity is a very important part of an IS-95 system. It will be discussed in details later.

The capacity of an IS-95 system is given in [8], [10], [14]. The major factors that determine the capacity of a CDMA cellular system are: the PG, the required E_b/N_o, the activity factor (ACF) of voice, and the frequency reuse factor which is determined by the multi-cell, multi-user interference in cellular CDMA. To measure the quality of service (QOS), the outage probability is used more often than the average error probability. The outage probability is a more conservative and reasonable criterion for capacity evaluation.

E_b/N_o is the ratio of energy per bit to the noise power spectral density and is a very important parameter by which different coding and modulation schemes are compared. The required E_b/N_o or the minimum E_b/N_o that ensures an accepted bit error rate is often used as a criterion for performance evaluation of different schemes. A low E_b/N_o can be achieved by CDMA when powerful and high redundancy error correction coding techniques are employed. For the forward link, the CDMA signal design uses a convolutional code with a constraint length of 9 and a code rate of 1/2. The required minimum E_b/N_o in the forward link is 5 dB [14].

In the reverse link, the modulation scheme employs 64-ary orthogonal signalling based on the set of Walsh function sequences. Again, a convolutional code with Viterbi

decoding is used. A constraint length of 9, code rate 1/3 decoder determines the most likely information bit sequence. For each data block, a signal quality estimate is obtained and transmitted along with the data. The quality estimate is the average signal-to-noise ratio over the frame interval. The required E_b/N_o in the reverse link is 7 dB [14]. The details for determining the required E_b/N_o with selected coding scheme are shown in [19].

Due to the advantages discussed above, the capacity of a CDMA system can be expected to be better than a FDMA or a TDMA system. Along with other merits, such as flexibility of subscription, immunization of channel fading, its low cost and simplicity in realization, CDMA systems are certainly becoming a good candidate for the next generation of cellular mobile digital communications.

To have an overall image of CDMA, however, we also point out the drawbacks of CDMA: The performance of DS-CDMA is very sensitive to the accuracy of the power control. A relatively low data rate can be supported by CDMA comparing with TDMA (currently). More research in this aspect is required. The ability to support high data rate traffic is considered essential for the wireless personal communication system (PCS) to provide multimedia services.

2.2 Cellular Environment

Past experience has shown that to build up a mobile telecommunication system based on a cellular structure is the most efficient way to deal with large scale wireless communication systems. Also we can see that the cellular structure is basically a space division strategy. Due to this structure, frequency reuse becomes a reality. The capacity of a system is greatly increased.

One of the most important aspects of mobile communications is the channel characteristics. In general, mobile communication channels experience multipath fading and lognormal shadowing [23]-[25].

With multipath fading, if a signal is transmitted between a base station and a mobile station that is moving through a multipath environment, wave interference among the multipath components results in severe fading of the received signal. This fading is rapid and its rate is a function of the frequency of operation and the velocity of the receiving antenna. The fading channel is characterized as having multiple propagation paths and there is a propagation delay and an attenuation factor associated with each path. Both the propagation delays and the attenuation factors are time-variant due to the structural changes within the propagation medium.

The fading channels can be classified into frequency-selective and frequency-nonselective types [23]. In conception, if a signal is transmitted through a fading channel and the different frequency components experience different degrees of fading, then the fading is classified as frequency selective fading. Otherwise, the fading is nonselective. To facilitate the practical applications and academic research, there are several models introduced for multi-path fading which are widely accepted and used [23].

2.2.1 Rayleigh Distribution

The multipath delay, which is denoted as τ, is a random variable. The range of possible values for τ is called the multipath or delay spread of the channel and is denoted as T_m. The bandwidth within which fading is correlated is called the coherence bandwidth and is denoted as Δf_c. We have that

$$\Delta f_c \approx \frac{1}{T_m} \tag{2.1}$$

When the signal bandwidth W is much smaller than the coherence bandwidth Δf_c of the channel, the received signal is simply the transmitted signal multiplied by a complex-valued Gaussian random process $C(0;t)$, which presents the time-variant characteristics of the channel. The transfer function $C(0;t)$ for a frequency-nonselective channel may be expressed in the form

$$C(0;t) = \gamma(t)\, e^{-j\phi(t)} \tag{2.2}$$

where $\gamma(t)$ is the amplitude and $\phi(t)$ is the phase of channel frequency response. If $C(0;t)$ is modeled as a zero mean complex valued Gaussian random process, $\gamma(t)$ is Rayleigh-distributed for any instant of t and $\phi(t)$ is uniformly distributed over the interval $(-\pi, \pi)$.

For a frequency-selective fading channel, it can be shown that the time-variant frequency-selective channel can be modelled as a tapped delay line with tap spacing $1/W$ and tap coefficients $c_n(t)$. Thus the low-pass impulse response for the channel is

$$c(\tau;t) = \sum_{n=-\infty}^{\infty} c_n(t)\, \delta\left(\tau - \frac{n}{W}\right) \tag{2.3}$$

The corresponding transfer function is

$$C(f;t) = \sum_{n=-\infty}^{\infty} c_n(t)\, e^{-j2\pi fn/W} \tag{2.4}$$

Since the total multipath spread is T_m, for practical purposes the tapped delay line model can be truncated at $L = \lfloor T_m \cdot W \rfloor + 1$. The received signal can then be written as

$$r(t) = \sum_{n=1}^{L} c_n(t)\, u\left(t - \frac{n}{W}\right) \tag{2.5}$$

where $u(t)$ is the transmitted signal. If the time variant tap weights $c_n(t)$ are samples from a zero mean complex-valued, stationary Gaussian random process, the magnitudes $|c_n(t)|$ are also Rayleigh-distributed and the phases $\phi_n(t) = 2\pi fn/W$ are uniformly distributed.

The Rayleigh distribution was derived by Lord Rayleigh in 1880. As the real part and the imaginary part of $c_n(t)$ (which is $C(0;t)$ for frequency-nonselective fading) are

zero mean statistically independent Gaussian random variables each having a variance σ^2, then $\gamma = |c_n(t)|$ follows the Rayleigh distribution

$$p(\gamma) = \frac{\gamma}{\sigma^2} e^{-\gamma^2/2\sigma^2}. \tag{2.6}$$

It follows that the corresponding cumulative distribution function (CDF) is:

$$f(\gamma) = \int_0^{\gamma} \frac{x}{\sigma^2} e^{-x^2/2\sigma^2} dx = 1 - e^{-\gamma^2/2\sigma^2} \tag{2.7}$$

It is also known that if γ is Rayleigh distributed, its power form γ^2 is Chi-square distributed

$$p(\gamma^2) = \frac{1}{2\sigma^2} e^{-\gamma^2/2\sigma^2}. \tag{2.8}$$

It is common in the current literature to derive the Rayleigh PDF based on the assumption that $c_n(t)$ can be decomposed into two orthogonal Gaussian random processes that have zero mean and the same standard deviation σ. However, it has already been shown that the constraints of the complex Gaussian model are unnecessary. It is shown in the literature that the relationship between the Rayleigh PDF and its underlying physical assumption is not unique. Physically, this means that if a received signal amplitude follows a Rayleigh curve, it does not necessarily mean that there are a large number of interfering waves, or that the complex Gaussian decomposition is accurate. But if the amplitude and phase of each component wave are statistically independent, and the phase of each component wave is a random variable which is uniformly distributed on $(0, 2\pi)$, the relationship will be unique.

2.2.2 The Rice Distribution

If the channel condition is relatively good, there is a line-of-sight path for the desired signal transmission. The real part and the imaginary part of $c_n(t)$ are statisti-

cally independent Gaussian random variables with means m_1 and m_2, and common variance σ^2. Then $\gamma = |c_n(t)|$ is Rician distributed

$$p(\gamma) = \frac{\gamma}{\sigma^2} e^{-\left(\gamma^2 + s^2\right)/2\sigma^2} I_0\left(\frac{\gamma s}{\sigma^2}\right) \tag{2.9}$$

where $s^2 = m_1^2 + m_2^2$ and I_0 is the modified Bessel function of zero order. It can be shown that this PDF characterizes the statistics of the envelope of a signal corrupted by additive narrow-band Gaussian noise. The cumulative distribution function is given by

$$f(\gamma) = 1 - Q\left(\frac{s}{\sigma}, \frac{\gamma}{\sigma}\right) \tag{2.10}$$

where

$$Q(x, y) \equiv e^{-\left(x^2 + y^2\right)/2} \sum_{k=0}^{\infty} \left(\frac{x}{y}\right)^k I_k(xy) \qquad y > x > 0 \tag{2.11}$$

with I_k being the kth order Bessel function.

When γ is Rician distributed, the distribution of γ^2 is:

$$p\left(\gamma^2\right) = \frac{1}{2\sigma^2} e^{-\left(\gamma^2 + s^2\right)/2\sigma^2} I_0\left(\frac{\gamma s}{\sigma^2}\right). \tag{2.12}$$

This is a non-central Chi-square distribution with non-centrality parameter $s^2 = m_1^2 + m_2^2$.

2.2.3 The Nakagami Distribution

The Nakagami distribution was developed in the early 1940's by Nakagami et al. who performed an experiment in which the fading of HF signals received over long propagation paths was monitored by connecting the same fading signal input to both the horizontal and vertical deflection plates of a cathode ray tube (CRT) [27]. The received

signal amplitude probability distribution was then determined by measuring the emulsion density of CRT photographs taken after carefully controlled monitoring periods. The distributions were then plotted on log-log paper and compared with the results of a mathematical expression, the form of which was arrived at by inspection. Agreement between the measured and theoretical distributions was found to be reasonable, and after normalization and a change of variable, the corresponding probability density function was written as

$$p(\gamma) = \frac{2m^m \gamma^{2m-1}}{\Gamma(m)\,\Omega^m} e^{-(m/\Omega)\gamma^2} \tag{2.13}$$

where $\Omega = \overline{\gamma^2}$ is the time averaged power of the received signal and $m = (\overline{\gamma^2})^2 / \overline{(\gamma^2 - \overline{\gamma^2})^2}$ is the inverse of the normalized variance of γ^2. The parameter m is named the shape factor, and has a lower bound of 1/2, which has been mathematically derived, as well as ascertained from experiment.

The Nakagami PDF can be shown to be a more general expression of other well known density functions. For $m = 1$, the Rayleigh probability function is obtained. For $m = 1/2$, Equation (2.13) describes a one-sided Gaussian distribution. It can also be shown that the Nakagami expression can approximate both the Rice and the lognormal distributions under certain conditions.

Note that the power form of the Nakagami model is the Gamma distribution. Letting $\Re = \gamma^2/2$, we have

$$p(\Re) = \frac{1}{\Gamma(m)} \left(\frac{2m}{\Omega}\right)^m \Re^{m-1} e^{-\frac{2m}{\Omega}\Re}. \tag{2.14}$$

This distribution is very important and will be used for our modelling work.

2.2.4 Lognormal Shadowing

In addition to multipath fading, another important phenomenon in mobile channels is shadowing. Shadowing is mainly caused by the terrain configuration and the built environment between the base station and the mobile unit. It is generally accepted that shadowing is lognormally distributed [14], [28]-[31]. The shadowing affects the local mean of the total channel attenuation and multipath fading is on top of the lognormal shadowing.

In [14], it is shown that the attenuation of the shadowing and the path loss can be expressed as $\bar{\alpha} = r^{-\nu} \times 10^{\xi/10}$, where r is the distance from a subscriber to a cell site, ν is the path loss factor and ξ is a Gaussian random variable with zero mean and standard deviation σ_L. The PDF of $\bar{\alpha}$ is given by

$$f_L(\bar{\alpha}) = \frac{10}{\sqrt{2\pi}\sigma_L \ln 10 \bar{\alpha}} \exp\left\{\left(-\frac{10^2}{2\sigma_L^2 \ln^2 10}\right) \ln^2\left(r_i^{\nu} \bar{\alpha}\right)\right\}. \tag{2.15}$$

Due to the Rayleigh fading, the conditional PDF of the channel attenuation is exponentially distributed given that the local mean is a lognormal random variable. We have

$$f(\alpha|\bar{\alpha}) = \frac{1}{\bar{\alpha}} \exp\left(-\frac{\alpha}{\bar{\alpha}}\right). \tag{2.16}$$

Then the PDF of the channel attenuation is given by

$$f(\alpha) = \int_0^{\infty} f(\alpha|\bar{\alpha}) \cdot f_L(\bar{\alpha})\, d\bar{\alpha} = \int_0^{\infty} \frac{1}{\bar{\alpha}} \exp\left(-\frac{\alpha}{\bar{\alpha}}\right) \cdot f_L(\bar{\alpha})\, d\bar{\alpha} \tag{2.17}$$

where α is the channel attenuation, $\bar{\alpha}$ is the local mean of the channel attenuation and is a lognormal random variable, and $f_L(\bar{\alpha})$ is the lognormal PDF.

2.3 Reverse Link Power Control

Since there are always non-zero cross-correlations between the spreading sequences of the different users, co-channel multi-user interference is a dominate factor limiting the capacity of a DS-CDMA system. Due to the propagation path loss, in the reverse link a user located close to the base station could be received at a higher power level than other users. If the difference between the received levels is too large, one user may cause a disastrous interference to the other users. This is the so called near-far effect. Therefore, a power control system is employed that attempts to maintain an equal received power level from all users independently on their distance/location.

In the IS-95 standard, both open loop and closed loop power control are used. In a CDMA mobile cellular system, the objective of the mobile transmitter power control process is to produce, at the base station receiver, a nominal received signal power from each mobile transmitter operating within the cell.

It is very desirable to maximize the capacity of the CDMA system in terms of the number of simultaneous calls that can be handled in a given system bandwidth. It can readily be seen that the system capacity is maximized if each mobile transmitter's power is controlled so that its signal arrives at the base station with the minimum required signal-to-interference ratio. If a mobile's signal arrives at the base station with too low a value of received power, the bit-error-rate will be too high to permit high quality communications. If the received power is too high, the performance of this mobile unit will be acceptable, but interference to all the other mobile transmitters that are sharing the channel will be increased, possibly resulting in unacceptable performance to other users unless their number is reduced.

2.3.1 Open loop Power Control

Each mobile unit attempts to estimate the path loss from cell-site to the mobile unit. In the CDMA approach to multiple access, all the base stations in a region transmit, on the same frequency, a pilot signal that is used by all mobiles for initial synchroniza-

tion and as a frequency and time reference for demodulation of digital speech signals.

A mobile station measures the power level of both the pilot signal from the base station to which it is connected and also the sum of all the base station signals receivable at the mobile. In the latter case, the mobile might temporarily obtain a better path to a more distant base station than to its current reference base station which is normally the one close by.

Based on these measurements, the fluctuation of the channel attenuation is estimated. This estimate is then used to permit a rapid response to a sudden improvement in the channel while disallowing a rapid response to a sudden degradation in the channel. This is a conservative approach to limit the interference generated due to suddenly increasing power from a mobile.

A typical example of a sudden improvement occurs when a mobile is moving through an area that is shadowed by a large building or other large obstruction and then drives out of the shadow. This can take place in a few tens of milliseconds. As the mobile drives out of the shadow, the signal received by the mobile will increase in strength.

The reverse link path loss estimate at the mobile is used by the mobile to adjust its own transmitter power. The stronger the received signal, the lower will be the mobile's transmitter power. The reception of a strong signal from the base station indicates that the mobile is either close to the base station or has an unusually good path to the base station. This means that a relatively small amount of power is required to produce a nominal received power at the base station from this mobile transmission. In the case of a sudden improvement in the channel, the open loop power control mechanism, which is analog in nature and has about 85 dB or more dynamic range, provides for a very rapid response over a period of just a few microseconds. It adjusts the mobile transmit level downward, preventing the mobile transmitter power from being at too high a level.

In the IS-95 standard, the rate of increase of mobile transmit power is generally limited to the rate at which the closed loop power control from the base station can reduce

the power. This prevents a sudden degradation which affects only the individual quality temporarily from causing a mobile transmit power to increase to a level significantly higher than required for communication.

The base station transmits information as to its characteristics and number of active users on its setup channel. The mobile receives this information when first obtaining system synchronization and continues to monitor the messages being transmitted.

In addition to measuring the received signal strength in the mobile, it is also desirable for the microprocessor in the mobile to know the base station's transmit power and antenna characteristics and the number of active users from the base station. This capability allows the system to have base stations with differing transmit power levels and antenna gains corresponding to the size of the cells.

2.3.2 Closed-Loop Power Control

In a CDMA cellular system, a full-duplex radio channel is provided by using one frequency band for transmission from the base station to the mobile user and a different frequency band for transmission from the mobile user to the base station. The frequency separation allows a mobile user's transmitter and receiver to be active simultaneously without feedback or interference from the transmitter into the receiver. The frequency separation has very important implication for the power control process. It causes the multipath fading on the forward and reverse link channels to be independent processes. This means that a mobile unit cannot measure the path loss of a received signal and assumes that exactly the same path loss is present on its transmitted signal, particularly when the mobile is stationary. The above measurement technique provides the correct transmit power on the average, but additional provisions must be made for the effects of independent Rayleigh fading.

To account for the independence of the Rayleigh fading on the forward and the reverse link, which the mobile cannot estimate, the mobile transmitter power is also controlled by a signal from the base station. Each base station demodulator measures the

received signal strength from each mobile. The measured signal strength is compared to the desired signal strength for that mobile and a power adjustment command is sent in the forward link channel addressed to that mobile user. This power adjustment command is combined with the mobiles' open loop estimate to obtain the final value of the mobile's transmit power.

In the IS-95 standard, the cell-site power adjustment command instructs the mobile unit to increase or decrease its transmitted power by a predetermined amount, nominally about 0.5-1.0 dB. The power adjustment command is transmitted at a relatively high rate, on the order of one command every millisecond. The transmission rate of the power adjustment command must be high enough to permit the Rayleigh fading on the reverse link channel to be tracked. It is also desirable for the forward link Rayleigh fading to be tracked. One command per millisecond is adequate to track fading processes for vehicle speeds of 20-100 miles per hour for the 850 Mhz frequency band used in mobile communications. It is important that the latency in determining the power control signal and in the transmission process be kept small so that the channel conditions will not change significantly before the control bit can be received and acted upon.

The system controller residing at the mobile telephone switching office (MTSO) provides each cell-site controller with a value for the desired signal strength of each user based on the overall system information available. The cell-site controller maintains the desired signal strength information for each mobile that is active within that cell. This level is passed to each of the cell-site demodulators where it is used along with the available information on instantaneous vs. the expected value of the bit error rate of the received signal to determine whether to command a particular mobile to increase or to decrease its transmitter power. This mechanism is called the CDMA closed-loop power control.

The nominal power level can be adjusted up or down to accommodate variations from the average conditions. For example, a base station in an unusually noisy location

might be allowed to use a higher than normal targeted power level. This will result in a higher level of interference to the immediate neighbors of this cell. A trade-off must be made. For a system with heterogeneous traffic, different traffic types may also be assigned different power levels to maximize the overall capacity while ensuring the quality requirements of the different traffic types.

2.4 Forward Link Power Control

It is also desirable to provide a means for controlling the relative power used in each data signal transmitted by the base station in response to control information transmitted by each mobile. The primary reason for forward link power control is that in certain locations, the link from a base station to a mobile may be unusually weak. Unless the power being transmitted to this mobile is increased, the quality may become unacceptable. For example, if a mobile locates at a point where the path loss to the closest two or three base stations is nearly the same, the total interference would be increased by three times over the interference seen by the mobile at a point relatively close to its reference base station.

To realize forward link power control, the received signal-to-noise ratio is measured at a mobile. If the measured ratio is less than a predetermined value, the mobile transmits a request for additional power to the base station. If the ratio exceeds the predetermined value, the mobile transmits a request for a reduction in power. The base station receives the power adjustment requests from each mobile and responds by adjusting the power allocated within the total transmitted power of the corresponding base station by a predetermined amount. The base station also considers the power demands being made on it by all the mobiles in deciding whether to comply with the requests of any particular mobile. When the system approaches its capacity, certain constraints must be placed on the total transmitted power of a base station to ensure the stability of the entire power control system.

2.5 Soft Handoff and Diversity

In cellular CDMA, the same entire bandwidth available is used by all cells. Different subscribers are distinguished by the use of spreading codes. This means that the mobile unit need not switch frequencies when being handed-off from one base station to another. Therefore, there is a smaller probability that the call will be dropped if the handoff command is received in error.

The new base station assigns a modulator/demodulator (modem) unit, consisting of digital modulator and data receiver functions, to the user while the old base station continues to handle the user. When the mobile is located in the transition region between the two base stations, the mobile user can be switched back and forth between them as signal strength dictates with no disrupting effects on the mobile. Only when the mobile is firmly established in the new cell will the original base station discontinue handling the call. In this regard, the conventional system (FDMA and TDMA) can be said to provide a break-before-make switching while the CDMA based soft handoff system provides a make-before-break switching.

A mobile unit also plays an important role in soft handoff operations. The mobile can be permitted to initiate the handoff request and to determine the best new base station from the old station's neighbors. After a call is initiated, the mobile continues to scan the neighboring station's pilots to determine if one of these signals becomes stronger than the first station's pilot. When it happens, it indicates to the mobile that it has entered the new base station's coverage area and that a handoff could be initiated. The mobile transmits a control message to the base station handling the mobile with the information that a new base station's pilot is now stronger along with the identity of the new base station.

The system controller can now begin the handoff process. The system controller begins the handoff process by assigning a modem located in the new base station to the mobile. The modem is given the PN address of the mobile. The cell-site modem searches

for and finds the mobile's signal. The cell-site modem also begins transmitting the signal to the mobile. The mobile searches for this signal. When the new cell-site signal is found, the mobile can switch over to listening to this signal. The mobile then transmits a control message indicating that the handoff is complete. The system controller then switches the call over to the new base station and allows the old cell-site modem to enter the pool of idle modems available for reassignment.

One of the important parts of the soft handoff operation is cell-site diversity. In addition to the above, cell-site diversity reception is obtained by having two or three cell-sites demodulate the signal from the mobile. All base stations forward their demodulated data signals to the system controller along with an indication of the signal quality in the receiver. The system controller then compares the two or three versions of the mobile's signal and selects the signal with the best quality indication. It is also possible to use more efficient diversity combining techniques instead of diversity selection, but the complexity will be increased significantly.

With cell-site diversity, the process is initiated by the mobile determining that a neighboring base station has a signal strength high enough to allow good quality demodulation. The mobile transmits a control message to the new base station indicating the identity of this base station and requesting the cell-site diversity mode. The system controller responds by connecting the mobile to a modem in the new base station. The system controller then performs diversity combining of the signals received by the two (or three) base stations and the mobile performs diversity combining of the signals received from the base stations.

The cell-site diversity continues as long as good signals are received from all the base stations. The mobile continues to search for other base stations. If a new base station becomes stronger than one of the original base stations, a control message will be transmitted indicating the identity of this base station. The system controller will then drop the weakest base station and continue with the strongest base stations. Note that if

the mobiles are equipped with three data demodulators, then a triple cell-site diversity mode results. The diversity is terminated when the mobile determines that only one base station is providing adequate signals for quality reception. The mobile sends a control message indicating the base station which it wishes to remain with at the end of cell-site diversity mode. Cell-site diversity might be terminated by the system controller if the system were to become overloaded and an insufficient number of modems were available to support all requests for diversity.

Soft handoff is tightly coupled with power control. In IS-95, during soft handoff, multiple base stations are involved in the power control of a mobile. If the requests from all base stations are to increase power then the mobile will increase its transmission power. As long as there is one base station requesting reduced power, the mobile will reduce its transmission power.

2.6 Cellular CDMA Supporting Integrated Services

In the third generation of universal wireless communication networks, a user will be allowed to communicate with anyone, in a variety of formats --- voice, data, image, and full motion video --- from virtually any geographic location.

A DS-CDMA wireless system structure for multi-media transmission is proposed in the CITR project. Multiple data rates from 1 Kbps up to 2 Mbps are considered. The low rate traffic would be voice and low rate data, while the high rate traffic would be high speed data and video. The bandwidth available for the proposed system could be 5, 10 or 15 MHz. The signals from a user are spread over the whole bandwidth available to achieve a high bandwidth efficiency. High degree of compatibility with Broadband-Integrated Services Digital Networks (B-ISDN) and Asynchronous Transfer Mode (ATM) will be a requirement for integration of wireless and wired networks. Different traffic types will be fully integrated with various techniques at both the physical layer and higher layer. Efficient resource management will be realized to improve the system capacity and the QOS.

Chapter 3

Interference Analysis for Cellular CDMA

3.1 Introduction

Since the capacity of a CDMA cellular system is determined by multi-cell, multi-user interference, and since there are a number of factors affecting not only the mean but also the variance of the interference, understanding of multi-cell, multi-user interference incorporating various traffic types is necessary. Power control and handoff are two key techniques in a cellular CDMA system. The multi-cell, multi-user interference level is largely determined by the performance of the handoff and power control which are tightly coupled with each other. One of the most important advantages of cellular CDMA is that the soft handoff can be realized. With a soft handoff, the multi-cell, multi-user interference is reduced by approximately 50% compared a hard handoff. As a result, the capacity is increased by over 100% [16].

Since DS-CDMA has great advantages in saving power and bandwidth, combating multi-path fading and as a result increasing the system capacity, it becomes one of the most promising techniques for supporting the next generation of wireless PCS with high transmission rates and high quality requirements for multi-media applications [3], [6]

Gilhousen et al. [14] have evaluated the capacity of a cellular CDMA system for voice users with a relatively simple approximation. In [15], [16], the membership of a user is determined by the highest pilot power received at the user and the mean power of the interference is obtained. There are many further works related to this issue e.g., [32],

[33]. Most of the analytical results of these papers are obtained through the Gaussian approximation for a large number of users. Prasad et al. [32] model the total inter-cell interference as a lognormal random variable. This approach simplifies the analysis when power control error is considered. In this chapter and the next, we will develop a new approach different from the Gaussian approximation for not only a large number of users but also a small number of users [17], [34].

The works [35]-[38], concentrate more on the multi-path combining techniques. The effects of wide band signalling techniques on the system performance and system capacity are examined. In [40], the performance of a CDMA system in a micro-cellular environment is investigated. There are also a lot of efforts on improving power control techniques [33], [41].

For wireless cellular systems, the multi-user co-channel interference problem always attracts a lot of attention. If the number of independent random variables is large enough, the PDF of the sum of the variables approaches the Gaussian distribution. For a small number of variables, the problem becomes very complicated. There have been many works which deal with the sum of interference variables e.g., [29], [31]. Nakagami has developed a general model for multi-path fading and lognormal shadowing [27]. One of the most convenient properties of this model is that, in many cases, there is a closed form solution for the PDF of the sum of Nakagami random variables.

In this chapter, we develop a new approach to analyze multi-cell, multi-user interference. The area averaged PDF of the interference of an active user is introduced. Differing from the distance membership determination, we take the statistical effect of soft hand-off into consideration. An analytical method for calculating the mean and variance of multi-cell, multi-user interference is developed. The membership statistics are also analyzed.

The rest of this chapter is organized as follows. The second section is devoted to a discussion on system structure, traffic profile and mobile channel characteristics of a

cellular CDMA system. In the third section, inter-cell interference is analyzed. A method for calculating the mean and variance of the inter-cell interference is developed in the fourth section. The mean and variance of intra-cell interference are calculated in the fifth section. The membership statistics are also analyzed in this chapter. The last section presents a summary and remarks.

3.2 System Model

We consider a CDMA cellular system consisting of equal-size hexagonal cells. The base stations are located at the centers of all cells and employ directional antennas separating a cell into three sectors as shown in Fig. 3.1. All base stations are connected to a central switching office. Each base station transmits a pilot tone to mobiles for hand-off, power control and synchronization.

Since both the forward link and the reverse link are very complicated and very different techniques are employed in the different links, a separate study is required for each. We concentrate in this thesis work on the performance analysis and evaluation of the reverse link.

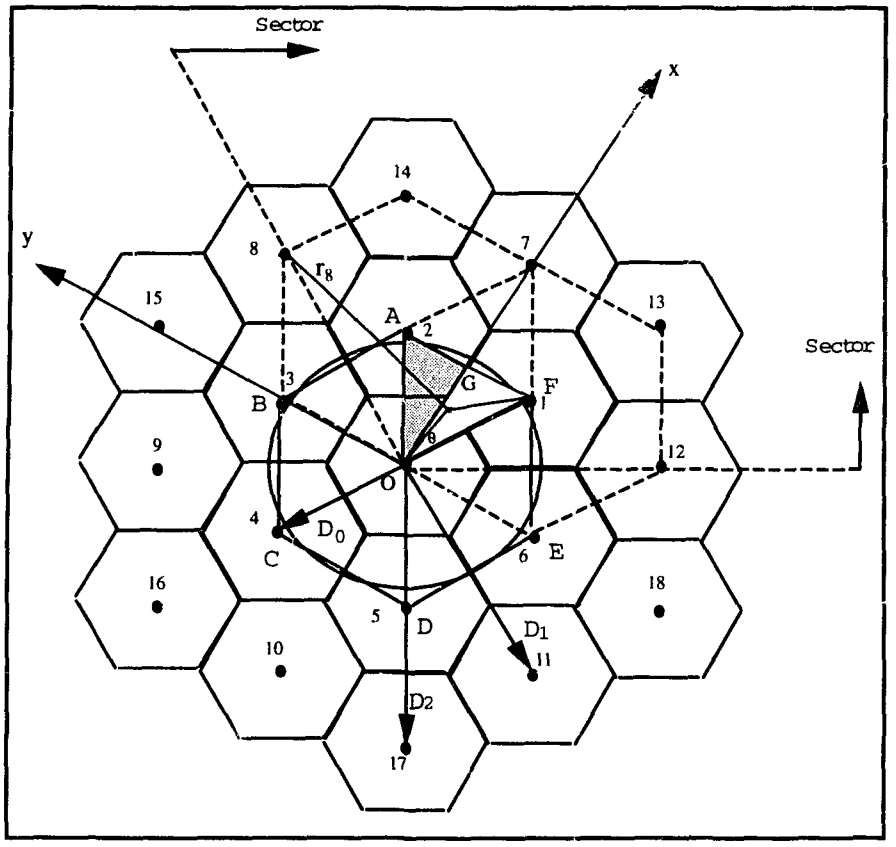

Fig. 3.1 Cellular structure and coverage.

3.2.1 Traffic Profile

At first, we examine a CDMA cellular system with a single type of traffic. The user distribution over the service area is defined by the user density function $D(r, \theta)$. It is a the number of users per unit area. The $D(r, \theta)$ represents how users are distributed over the area covered by the cellular system. The total number of users within an area A is

$$N_A = \iint_A D(r, \theta)\, r dr d\theta \tag{3.1}$$

where N_A is the number of users within area A. If the users are uniformly distributed all

over the area to be considered, the average user number per sector is N_s and the hexagonal cell radius is normalized to unity, we have

$$D(r,\theta) = \frac{2}{\sqrt{3}} N_s . \tag{3.2}$$

Based on the user density function, we define a user position distribution function as

$$f_A(r,\theta) = \frac{1}{N_A} D_A(r,\theta) \tag{3.3}$$

where N_A is the user number within A and $D_A(r,\theta)$ is the density function defined over the area A to be considered.

The meaning of a user position distribution function can be explained by

$$P_{A_k} = \int\int_{A_k} f_A(r,\theta)\, r dr d\theta \tag{3.4}$$

where P_{A_k} is the probability that a user is located in area A_k which is within the area A to be considered. Note that Equation (3.3) is a general formula and is not only for the uniform distribution of users. Since a uniform distribution of users is an important case, without loss the generality of our method, we calculate the numerical results assuming that users are uniformly distributed in our study.

3.2.2 Channel Characteristics

In a mobile environment, the signal power is typically attenuated by multi-path fading and shadowing. In addition, there is a path loss for radio propagation. It is generally accepted that shadowing is lognormally distributed and if there is no line of sight path, the multipath fading is Rayleigh distributed [28], [29]. The channel attenuation can be considered as the multiplication of two independent random variables: the Rayleigh fading and lognormal shadowing. The Rayleigh fading is on top of the lognormal shadow-

ing and the local mean of the Rayleigh fading is lognormally distributed [28], [29]. The attenuation of shadowing and the path loss can be expressed as $\bar{\alpha} = r^{-\nu} \times 10^{\xi/10}$, where r is the distance from a subscriber to a cell site, ν is the path loss factor and ξ is a Gaussian random variable with zero mean and standard deviation σ_L. Values of $\nu = 4$ and $\sigma_L = 8dB$ are normally used in a typical cellular environment [14].

3.2.3 Power Control and Soft Handoff

Power control is employed for compensating the propagation path loss and the channel attenuation due to shadowing and fading. Perfect power control and ideal soft handoff are assumed in this chapter at first. If perfect power control is assumed, the received power at the base station will be the same for each user which are power controlled by the reference station. For simplicity, we normalize this nominal power to 1. In reality, power control error always exists. The details of the effect of power control error can be found in [32], [33], [17].

With ideal soft handoff, the best of the involved base stations' receptions will be utilized at the switching center. A mobile in the handoff zone is controlled by all involved adjacent cells. Its power level is always set to match the lowest power requirements among these cells by responding to the pilot received with the highest power [42], [16]. Since during soft handoff operation, the best received signal is selected and, ideally, power control always works on the best received signal, there is an internal switching of the user membership. We say that a mobile belongs to a base station when the mobile has a power control connection with the base station and the best reception selected at the switching center is from this base station. This base station is identified as the current reference base station.

The interference generated by users that are power controlled by the reference base station is defined as intra-cell interference. The interference from users that are controlled by other base stations is defined as inter-cell interference. The effects of multipath

fading are considered separately for inter-cell and intra-cell interferences. For inter-cell interference, we assume that multipath fading is Rayleigh distributed on top of the log-normal shadowing. For intra-cell interference, we consider that the channel conditions in terms of fading and shadowing are much better in a lot of cases; path loss and shadowing are perfectly compensated by power control, and multipath fading can be greatly reduced by employing multi-path combining techniques and fast power control [43]. The final effect of fading is factored into the signal-to-noise ratio (SNR) requirement. A conventional signal to noise ratio (SNR) requirement is $E_b/N_o = 7dB$ as suggested in [14] for coded voice. In this chapter, we first consider a system in the lognormal shadowing environment.

Since propagation path loss is severe, the possibility that a subscriber belongs to a distant base station is very small. In order to simplify the problem, we investigate the performance of a system in which the three closest base stations are involved in the soft handoff operation of a mobile. Analysis and simulation results show that the effect of this simplification on the overall system performance is negligible [16], [19], [44]. Due to soft handoff, the area covered by a base station is extended. We call this extended area an enlarged cell area, for instance, the hexagonal area ABCDEF in Fig. 3.1; it has three times the area of a cell.

3.3 Analysis of the Area Averaged PDF of inter-cell Interference

It can be shown that the output of a correlation detector at the reference station is

$$R_p = P_0 + n_T + I_{ita} + I_{ite} \tag{3.5}$$

where P_0 is the received power from the desired user, n_T is the thermal noise with power σ_T^2, I_{ita} is the intra-cell interference, and I_{ite} is the inter-cell interference

Since power control is mainly for compensating path loss and shadowing, it works based on the measurement of the path loss and shadowing. In addition, the power that a

mobile is required to transmit should also be minimized. With perfect power control, the transmitted power from a mobile power controlled by the ith base station is

$$I_{tr,i} = r_i^{\nu} 10^{\frac{x_i}{10}} \tag{3.6}$$

where r_i is the distance between the reference mobile and the ith base station, and x_i is a Gaussian random variable with zero mean and standard deviation σ_L. For J different base stations, the PDFs of $I_{tr,i}$ are

$$f(I_{tr,i}) = \frac{10}{\sqrt{2\pi}\sigma_L \ln 10 I_{tr,i}} \exp\left\{-\frac{10^2}{2\sigma_L^2 \ln^2 10} \ln^2\left(\frac{I_{tr,i}}{r_i^{\nu}}\right)\right\} \qquad i = 0, 1, \ldots, J\text{-}1. \tag{3.7}$$

Ignoring the handoff operation, $I_{tr,0}$, $I_{tr,1}$, ..., $I_{tr,i}$, ... are independent and their joint PDF is

$$f(I_{tr,0}, I_{tr,1}, \ldots, I_{tr,J-1}) = \left(\frac{10}{\sqrt{2\pi}\sigma_L \ln 10}\right)^J \times \prod_{i=0}^{J-1} \frac{1}{I_{tr,i}} \exp\left\{-\frac{10^2}{2\sigma_L^2 \ln^2 10} \ln^2\left(\frac{I_{tr,i}}{r_i^{\nu}}\right)\right\}. \tag{3.8}$$

Taking the effects of the soft handoff into consideration, here we assume diversity selection and power control are ideal. There are J base stations involved in the power control of a mobile. Ideally, the transmission power level of a mobile is adjusted following the instructions from one of the involved base stations whose pilot power is the highest received by the mobile. A mobile power controlled by the 0th reference station has transmitted power $I_{tr,0}$ which meets $I_{tr,0} \le I_{tr,1} \cap I_{tr,0} \le I_{tr,2}$.

Taking $J = 3$ in Equation (3.8), the PDF of the transmitted power of an active user is

$$f_{I_{tr,0}}(I_{tr,0}) = F(I_{tr,0}, I_{tr,0} \le I_{tr,1} \cap I_{tr,0} \le I_{tr,2})$$
$$= F(I_{tr,0}, I_{tr,0} \le I_{tr,1} \le I_{tr,2}) + F(I_{tr,0}, I_{tr,0} \le I_{tr,2} \le I_{tr,1}) \quad (3.9)$$

where

$$F(I_{tr,0}, I_{tr,0} \le I_{tr,1} \le I_{tr,2}) = \int_{I_{tr,0}}^{\infty}\int_{I_{tr,1}}^{\infty}\left(\frac{10}{\sqrt{2\pi}\sigma_L \ln 10}\right)^3 \times \prod_{i=0}^{2}\frac{1}{I_{tr,i}}\exp\left\{\left(-\frac{10^2}{2\sigma_L^2 \ln^2 10}\right)\ln^2\left(\frac{I_{tr,i}}{r_i^v}\right)\right\} dI_{tr,2}dI_{tr,1}$$
$$= \frac{10^2}{2\pi\sigma_L^2 \ln^2(10) I_{tr,0}}\exp\left\{-\frac{10^2}{2\sigma_L^2 \ln^2(10)}\ln^2\left(\frac{I_{tr,0}}{r_0^v}\right)\right\}$$
$$\times \int_{I_{tr,0}}^{\infty}\frac{1}{I_{tr,1}}\exp\left\{-\frac{10^2}{2\sigma_L^2 \ln^2(10)}\ln^2\left(\frac{I_{tr,1}}{r_1^v}\right)\right\}$$
$$\times\left(\frac{1}{2} - \frac{1}{2}\mathrm{erf}\left(\frac{10}{\sqrt{2}\sigma_L \ln(10)}\ln\left(\frac{I_{tr,1}}{r_2^v}\right)\right)\right) dI_{tr,1}, \quad (3.10)$$

$$F(I_{tr,0}, I_{tr,0} \le I_{tr,2} \le I_{tr,1}) = \frac{10^2}{2\pi\sigma_L^2 \ln^2(10) I_{tr,0}}\exp\left\{-\frac{10^2}{2\sigma_L^2 \ln^2(10)}\ln^2\left(\frac{I_{tr,0}}{r_0^v}\right)\right\}$$
$$\times \int_{I_{tr,0}}^{\infty}\frac{1}{I_{tr,2}}\exp\left\{-\frac{10^2}{2\sigma_L^2 \ln^2(10)}\ln^2\left(\frac{I_{tr,2}}{r_2^v}\right)\right\}$$
$$\times\left(\frac{1}{2} - \frac{1}{2}\mathrm{erf}\left(\frac{10}{\sqrt{2}\sigma_L \ln(10)}\ln\left(\frac{I_{tr,2}}{r_1^v}\right)\right)\right) dI_{tr,2} \quad (3.11)$$

The area averaged interference from a reference mobile in the triangular area AOF in Fig. 3.1 to base stations 1 to 6 is equivalent to the inter-cell interference from a first tier neighbor cell to the reference station. Similarly, its interference to base stations 7 through 12 is equivalent to the inter-cell interference from cell 7 (or 8, 12) to the reference station; the interference to base station 13 through 18 is equivalent to the inter-cell interference

from cell 13 (or 14) to the reference station, and so on. Given that a reference user belongs to the reference station, the path attenuation from the user to the surrounding base stations, except base stations 0, 1 and 2, is independent of the mobile transmitted power. Considering this independent case, the interference power generated by a reference user to the ith base station is

$$I_i = \frac{I_{tr,0}}{r_i^{\nu}} 10^{\frac{x_i}{10}} = I_{tr,0} I_{pi} \qquad i = 3, 4, \ldots \tag{3.12}$$

where x_i represents the lognormal shadowing and r_i is the distance from the reference user to the ith base station. We denote I_{pi} as the total attenuation of path i including path loss and lognormal shadowing. The PDF of I_i can be obtained for $i = 3, 4, \ldots$, as

$$f_{I_i}(I_i) = \int_0^{\infty} \frac{1}{I_{tr,0}} f_{I_{pi}}\left(\frac{I_i}{I_{tr,0}}\right) f_{I_{tr,0}}(I_{tr,0})\, dI_{tr,0} \tag{3.13}$$

where $f_{I_{tr,0}}(I_{tr,0})$ is given by Equation (3.9) and the PDF of I_{pi}, $f_{I_{pi}}(I_{pi})$, is given by

$$f_{I_{pi}}(I_{pi}) = \frac{10}{\sqrt{2\pi}\sigma_L \ln 10 I_{pi}} \exp\left\{\left(-\frac{10^2}{2\sigma_L^2 \ln^2 10}\right) \ln^2\left(r_i^{\nu} I_{pi}\right)\right\}, \tag{3.14}$$

When the interference of an active user is received at base station 1 or 2, the path attenuation is correlated with user transmitted power. Now, we consider two random variables

$$I_{01} = \left(\frac{r_0}{r_1}\right)^{\nu} 10^{\frac{x}{10}} = \left(\frac{r_0}{r_1}\right)^{\nu} 10^{\frac{x_1 - x_0}{10}} \tag{3.15}$$

where I_{01} is the interference received at base station 1 given that the mobile is power controlled by base station 0, and

$$I_{21} = \left(\frac{r_2}{r_1}\right)^{\nu} 10^{\frac{y}{10}} = \left(\frac{r_2}{r_1}\right)^{\nu} 10^{\frac{x_1 - x_2}{10}} \tag{3.16}$$

where I_{21} is the interference received at base station 1 given that the mobile is power controlled by base station 2. Note that I_{01} and I_{21} are lognormally distributed. Variables x_0, x_1,and x_2 are independent Gaussian random variables with zero mean and standard deviation σ_L. Then, x and y are correlated Gaussian random variables. The joint PDF of x and y can be obtained as [23]

$$f(x, y) = \frac{1}{2\pi\sigma^2\sqrt{1-\rho^2}} \exp\left\{-\frac{1}{2(1-\rho^2)}\left(\frac{x^2}{\sigma_x^2} - 2\rho\frac{(xy)}{\sigma_x\sigma_y} + \frac{y^2}{\sigma_y^2}\right)\right\} \tag{3.17}$$

where ρ is the correlation coefficient and $\sigma_x = \sigma_y = \sigma = \sqrt{2}\sigma_L$ is the standard deviation. In our case, the exact ρ can be obtained

$$\begin{aligned} E(x, y) &= E((x_1 - x_0)(x_1 - x_2)) \\ &= E\left(x_1^2\right) - E(x_1x_2) - E(x_0x_1) + E(x_0x_2) = \sigma_L^2 \end{aligned} \tag{3.18}$$

and

$$\rho = \frac{E(x, y)}{\sigma_x\sigma_y} = \frac{1}{2}. \tag{3.19}$$

If hand-off is ideal, we have $I_{01} < I_{21}$ given that an active user belongs to base station 0. Then the conditional PDF of x can be obtained as

$$f(x|I_{01}<I_{21}) = f\left(x|\ \frac{10v}{\ln 10}\ln\frac{r_0}{r_2}+x<y\right)$$
$$= \frac{1}{\sqrt{2\pi}\sigma}\exp\left\{-\frac{x^2}{2\sigma^2}\right\}\left(\frac{1}{2}-\frac{1}{2}\mathrm{erf}\left(\frac{\frac{10v}{\ln 10}\ln\frac{r_0}{r_2}+(1-\rho)x}{\sqrt{2(1-\rho^2)}\sigma}\right)\right) \tag{3.20}$$

and the conditional PDF of I_{01} is

$$f(I_{01}|I_{01}<I_{21}) = \frac{10}{\sqrt{2\pi}\ln 10\sigma I_{01}}\exp\left\{-\left(\frac{10}{2\sigma\ln 10}\ln\left(I_{01}\left(\frac{r_1}{r_0}\right)^v\right)\right)^2\right\}$$
$$\times\left(\frac{1}{2}-\frac{1}{2}\mathrm{erf}\left(\frac{\frac{10v}{\ln 10}\ln\frac{r_0}{r_2}+(1-\rho)\frac{10}{\ln 10}\ln\left(I_{01}\left(\frac{r_1}{r_0}\right)^v\right)}{\sqrt{2(1-\rho^2)}\sigma}\right)\right) \tag{3.21}$$

Due to the symmetric nature of the hexagonal cell structure, the conditional PDF of the interference at base station 2 is the same as at station 1, thus $f(I_{01}|I_{01}<I_{21}) = f(I_{02}|I_{02}<I_{12})$. Then, the area averaged PDF of the interference power of an active user j from a cell in the first tier (e.g. cell 1) and two cells (e.g. cells 7 and 13) in the second tier can be obtained as

$$f_{avj}(I_{avj}) = \sum_{i=1}^{18}\int_0^{r_c}\int_0^{\frac{\pi}{3}} f_{I_i}(I_i|r_0,\theta)f_{A_k}(r_0,\theta)\,r_0 dr_0 d\theta \tag{3.22}$$

where the conditional PDF, $f_{I_i}(I_i|r_0,\theta) = f_{I_i}(I_i)$ for $i = 3, 4, \ldots$, is given by Equation (3.13), $f_{I_1}(I_1|r_0,\theta) = f_{I_2}(I_2|r_0,\theta) = f(I_{01}|I_{01}<I_{21}) = f(I_{02}|I_{02}<I_{12})$ are given by Equation (3.21), and $f_{A_k}(r_0,\theta)$ is the position distribution given by Equation (3.3) defined over the effective area covered by a base station, e.g. the hexagonal area ABCDEF in Fig. 3.1. Two tiers of cells, 19 cells in total, are considered. It is generally accepted that interference from outside the second tier is negligible [14].

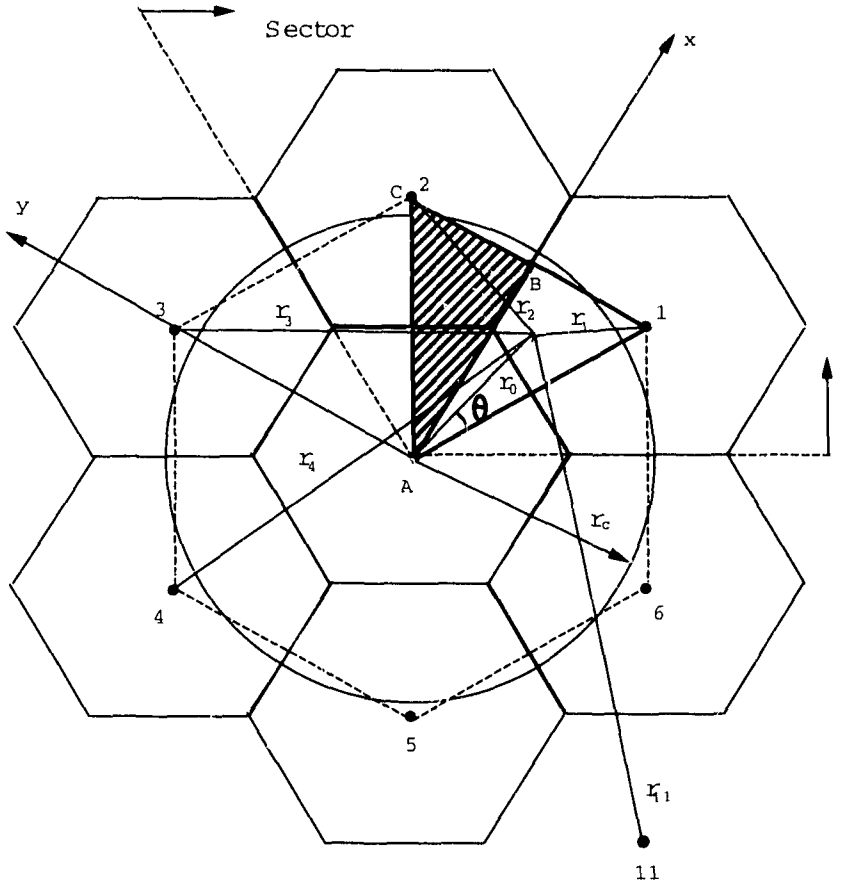

Fig. 3.2 The effective area covered by a base station.

We call the hexagonal area ABCDEF an enlarged cell area. If users are uniformly distributed, $f_{A_k}(r_0, \theta) = \frac{2}{9\sqrt{3}}$. Let r_c denote the radius of a circle that has the same area as a enlarged hexagonal cell area (three times the area of a cell), as shown in Fig. 3.2. We use r_c to calculate the area of the enlarged cell area. r_c is obtained as $r_c = \sqrt{\frac{9\sqrt{3}}{2\pi}}$. As shown in Fig. 3.1, the integration is calculated over the shadowed triangular area due to the symmetry nature. The relations between r_0, r_1, r_2, ... are

$$\begin{cases} r_1^2 = d_0^2 + r_0^2 - 2r_0 d_0 \cos\theta \\ r_2^2 = d_0^2 + r_0^2 - 2r_0 d_0 \cos\left(\frac{\pi}{3} - \theta\right) \\ r_3^2 = d_0^2 + r_0^2 - 2r_0 d_0 \cos\left(\frac{2\pi}{3} - \theta\right) \\ r_4^2 = d_0^2 + r_0^2 - 2r_0 d_0 \cos(\pi - \theta) \\ r_7^2 = d_1^2 + r_0^2 - 2r_0 d_1 \cos\left(\theta - \frac{\pi}{6}\right) \\ r_8^2 = d_1^2 + r_0^2 - 2r_0 d_1 \cos\left(\frac{\pi}{2} - \theta\right) \\ r_9^2 = d_1^2 + r_0^2 - 2r_0 d_1 \cos\left(\frac{5\pi}{6} - \theta\right) \\ r_{10}^2 = d_1^2 + r_0^2 - 2r_0 d_1 \cos\left(\frac{7\pi}{6} - \theta\right) \\ r_{14}^2 = d_2^2 + r_0^2 - 2r_0 d_2 \cos\left(\frac{\pi}{3} - \theta\right) \\ r_{15}^2 = d_2^2 + r_0^2 - 2r_0 d_2 \cos\left(\frac{2\pi}{3} - \theta\right) \\ r_{16}^2 = d_2^2 + r_0^2 - 2r_0 d_2 \cos(\pi - \theta) \end{cases} \tag{3.23}$$

where $d_0 = \sqrt{3}$, $d_1 = 3$ and $d_2 = 2\sqrt{3}$. The r_i given by Equation (3.23) are those required in further calculations due to the symmetry property of hexagonal cell structure.

3.4 Mean and Variance Analysis of Inter-cell Interference

From Equation (3.12), the interference from one user received at the base station is the multiplication of two independent random processes: the path attenuation, I_{pi}, and the mobile transmitted power, $I_{tr,0}$. Let $I_i = I_{tr,0} I_{pi}$, then, for the ith base station, $i = 3, 4, \ldots$, the mean interference power from an active reference user is

$$
\begin{aligned}
E(I_i) &= \int_0^{1}\int_0^{\infty} \frac{I_i}{I_{tr,0}} f_{I_{pi}}\left(\frac{I_i}{I_{tr,0}}\right) f_{I_{tr,0}}(I_{tr,0})\, \mathrm{d}I_{tr,0}\mathrm{d}I_i \\
&= \int_0^{\infty}\int_0^{1} \frac{I_i}{I_{tr,0}} f_{I_{pi}}\left(\frac{I_i}{I_{tr,0}}\right) \mathrm{d}\left(\frac{I_i}{I_{tr,0}}\right) \cdot I_{tr,0} f_{I_{tr,0}}(I_{tr,0})\, \mathrm{d}I_{tr,0} \\
&= \int_0^{\infty} M_{pi} I_{tr,0} f_{I_{tr,0}}(I_{tr,0})\, \mathrm{d}I_{tr,0} \cdot
\end{aligned}
\tag{3.24}
$$

Letting $I_i' = I_i / I_{tr,0}$, we have that for $i = 3, 4, \ldots,$

$$
\begin{aligned}
M_{pi} &= \int_0^{\frac{1}{I_{tr,0}}} I_i' f_{I_{pi}}(I_i')\, \mathrm{d}I_i' \\
&= \frac{1}{r_i^{\nu}} \exp\left\{\frac{\sigma_L^2 \ln^2 10}{200}\right\}\left(\frac{1}{2} + \frac{1}{2}\mathrm{erf}\left(\frac{10\nu \ln\left(\frac{r_i}{I_{tr,0}}\right)}{\sqrt{2}\sigma_L \ln 10} - \frac{\sigma_L \ln 10}{10\sqrt{2}}\right)\right),
\end{aligned}
\tag{3.25}
$$

where $f_{I_{tr,0}}(I_{tr,0})$ is the PDF of the transmitted power given by Equation (3.9) and r_i represents the distance from the reference mobile to the ith base station.

Given that an active user belongs to base station 0, the mean interference from an active user (at position (r, θ)) to base station 1 is

$$
\begin{aligned}
E(I_{01}) &= \int_{-\infty}^{b} \left(\frac{r_0}{r_1}\right)^{\nu} \frac{1}{2\sqrt{\pi}\sigma_L} \exp\left\{\frac{x \ln 10}{10} - \frac{x^2}{4\sigma_L^2}\right\} \\
&\quad \times \left(\frac{1}{2} - \frac{1}{2}\mathrm{erf}\left(\frac{\frac{10\nu}{\ln 10}\left(\ln\frac{r_0}{r_2}\right) + (1-\rho)x}{2\sqrt{(1-\rho^2)}\sigma_L}\right)\right)\mathrm{d}x \cdot
\end{aligned}
\tag{3.26}
$$

Since the upper bound of I_{01} is

$$I_{01} = \left(\frac{r_0}{r_1}\right)^{\nu} 10^{\frac{x}{10}} \leq 1, \tag{3.27}$$

the b in Equation (3.26) has value

$$b = \frac{10\nu}{\ln 10}\left(\ln\frac{r_1}{r_0}\right). \tag{3.28}$$

Due to symmetry in the hexagonal cells, we have that $E(I_{02}) = E(I_{01})$ for base station 2. Denote $E(I_{01})$ as $E(I_1)$ and $E(I_{02})$ as $E(I_2)$. The definition of r_i and θ, is shown in Fig. 3.2. The details of calculation of r_i are given by Equation (3.23). Since in a macro-cellular environment path loss is severe, interference from cells outside of the two tiers is negligible [14]. Therefore, we consider multi-user interference within these two tiers of cells. In a sector, there are 6 interference cells within these two tiers. We can pair these cells such that each pair of cells has the same relative location to the reference station. Since the area of an enlarged cell is three times that of a normal cell, there are $k = 18N_s$ users generating inter-cell interference in a cell pair. Then, the area averaged mean of inter-cell interference power is given by [17]

$$\overline{E(I_s)} = 18\int_0^{r_c}\int_0^{\frac{\pi}{3}}\sum_{i=1}^{18} E(I_i) f_{A_0}(r_0, \theta)\, r_0 dr_0 d\theta \cdot \tag{3.29}$$

We call $\overline{E(I_s)}$ the mean factor of inter-cell interference.

Similarly, we can also obtain the area averaged variance of the interference power of an active user. We first examine the independent case:

$$\begin{aligned} E\left(I_i^2\right) &= \int_0^{1}\int_0^{\infty} \frac{I_i^2}{I_{tr,0}} f_{I_{pi}}\left(\frac{I_i}{I_{tr,0}}\right) f_{I_{tr,0}}(I_{tr,0})\, dI_{tr,0} dI_i \\ &= \int_0^{\infty} Msq_{qi} \cdot I_{tr,0}^2 \cdot f_{I_{tr,0}}(I_{tr,0})\, dI_{tr,0} \end{aligned} \tag{3.30}$$

where for $i = 3, 4, \ldots,$

$$Msq_{pi} = \frac{1}{r_i^{2\nu}} \exp\left\{\frac{\sigma_L^2 \ln^2 10}{50}\right\} \cdot \left(\frac{1}{2} + \frac{1}{2}\operatorname{erf}\left(\frac{10\nu \ln\left(\frac{r_i}{I_{tr,0}}\right)}{\sqrt{2}\sigma_L \ln 10} - \frac{\sqrt{2}\sigma_L \ln 10}{10}\right)\right), \tag{3.31}$$

For base station 1 and 2, correlation exists and the second moment can also be obtained in a manner similar to the first moment in Equation (3.26).

$$E\left(I_1^2\right) = \int_{-\infty}^{b} \left(\frac{r_0}{r_1}\right)^{2\nu} \frac{1}{2\sqrt{\pi}\sigma_L} \exp\left\{\frac{(\ln 10)x}{5} - \frac{x^2}{4\sigma_L^2}\right\} \times \left(\frac{1}{2} - \frac{1}{2}\operatorname{erf}\left(\frac{\frac{10\nu}{\ln 10}\left(\ln\frac{r_0}{r_2}\right) + (1-\rho)x}{2\sqrt{(1-\rho^2)}\sigma_L}\right)\right) dx \cdot \tag{3.32}$$

where b is given by Equation (3.28). Similarly, we have also $E\left(I_1^2\right) = E\left(I_2^2\right)$. Then

$$\overline{E(I_s^2)} = 18 \int_0^{r_c} \int_0^{\frac{\pi}{3}} \sum_{i=1}^{18} E\left(I_i^2\right) f_{A_0}(r_0, \theta)\, r_0 dr_0 d\theta \tag{3.33}$$

and

$$\overline{E^2(I_s)} = 18 \int_0^{r_c} \int_0^{\frac{\pi}{3}} \sum_{i=1}^{18} E^2(I_i) f_{A_0}(r_0, \theta)\, r_0 dr_0 d\theta \cdot \tag{3.34}$$

We call $\overline{E(I_s^2)}$ the second moment factor and $\overline{E^2(I_s)}$ the mean square factor.

Since a traffic type may not has a continuous source rate, we consider transmission activity as an independent on/off random process represented by an ACF, υ. For example voice has an ACF of 0.375. This random process has a mean of υ and a variance of $\upsilon - \upsilon^2$. Considering the ACF and employing the parameters $\overline{E(I_s)}$, $\overline{E(I_s^2)}$ and

$E^2\overline{(I_s)}$, we obtain the total mean inter-cell interference of N_s users per sector to be

$$E(I_{ite}) = N_s \cdot \upsilon \cdot E\overline{(I_s)} \tag{3.35}$$

and the variance of inter-cell interference is

$$D(I_{ite}) = N_s \cdot \left(\upsilon E\overline{(I_s^2)} - \upsilon^2 E^2\overline{(I_s)} \right) \tag{3.36}$$

In addition, we consider the inter-cell interference fluctuation caused by the Rayleigh fading as an independent random variable I_{Ry}. The total inter-cell interference is $I_{Rite} = I_{ite} \cdot I_{Ry}$ and I_{Ry} is Chi-square distributed with mean equal to 1. Therefore, with the Rayleigh fading the mean of the inter-cell interference is

$$E(I_{Rite}) = E(I_{ite}) \tag{3.37}$$

and its variance increases to

$$\begin{aligned} D(I_{Rite}) &= N_s \cdot \left(E\left(I_{ite}^2\right) E\left(I_{Ry}^2\right) - E^2(I_{ite})\, E^2(I_{Ry}) \right) \\ &= N_s \cdot \left(2\upsilon\overline{E(I_s^2)} - \upsilon^2 E^2\overline{(I_s)} \right) \cdot \end{aligned} \tag{3.38}$$

3.5 intra-cell Interference Analysis

It is difficult to calculate the PDF of the intra-cell interference directly, but the mean and variance can be obtained. To obtain the mean and variance of intra-cell interference, we first evaluate the probability that a mobile belongs to a base-station, which can be determined by a comparison of pilots strength. The internal membership switching process of an active user can be presented as a binomial random variable φ

$$\varphi = \begin{cases} 1 & \text{User belongs to the reference base station with probability } p(\varphi = 1 | r_0, \theta), \\ 0 & \text{Otherwise.} \end{cases}$$

Then, we have that

$$\begin{aligned} \varphi = 1 | r_0, \theta) &= p\left((I_{tr,0} \le I_{tr,1}) \cap (I_{tr,0} \le I_{tr,2}) \,\middle|\, r_0, \theta \right) \\ &= p(I_{tr,0} \le I_{tr,1} \le I_{tr,2} | r_0, \theta) + p(I_{tr,0} \le I_{tr,2} \le I_{tr,1} | r_0, \theta) \end{aligned} \tag{3.39}$$

where

$$p\left(I_{tr,0} \le I_{tr,1} \le I_{tr,2} \middle| r_0, \theta\right) = \int_0^{\infty} \int_0^{I_{tr,2}} \left(\frac{10}{\sqrt{2\pi}\ln 10\sigma_L}\right)^2 \cdot \frac{1}{I_{tr,1} I_{tr,2}} \times \exp\left\{-\frac{10^2}{2\sigma_L^2 \ln^2 10}\left(\ln^2\left(\frac{I_{tr,1}}{r_1^v}\right) + \ln^2\left(\frac{I_{tr,2}}{r_2^v}\right)\right)\right\} \times \left(\frac{1}{2} + \frac{1}{2}\operatorname{erf}\left(\frac{10}{\sqrt{2}\ln 10\sigma_L}\ln\left(\frac{I_{tr,1}}{r_0^v}\right)\right)\right) dI_{tr,1} dI_{tr,2} \tag{3.40}$$

and

$$p\left(I_{tr,0} \le I_{tr,2} \le I_{tr,1} \middle| r_0, \theta\right) = \int_0^{\infty} \int_0^{I_{tr,1}} \left(\frac{10}{\sqrt{2\pi}\ln 10\sigma_L}\right)^2 \cdot \frac{1}{I_{tr,1} I_{tr,2}} \times \exp\left\{-\frac{10^2}{2\sigma_L^2 \ln^2 10}\left(\ln^2\left(\frac{I_{tr,1}}{r_1^v}\right) + \ln^2\left(\frac{I_{tr,2}}{r_2^v}\right)\right)\right\} \times \left(\frac{1}{2} + \frac{1}{2}\operatorname{erf}\left(\frac{10}{\sqrt{2}\ln 10\sigma_L}\ln\left(\frac{I_{tr,2}}{r_0^v}\right)\right)\right) dI_{tr,2} dI_{tr,1} \tag{3.41}$$

where $\operatorname{erf}(x)$ is the error function.

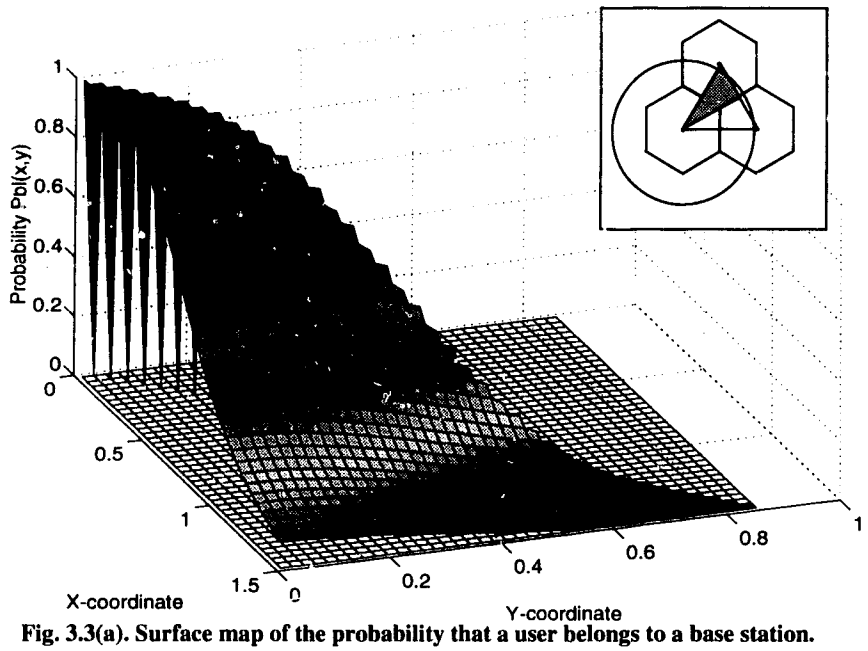

Fig. 3.3(a). Surface map of the probability that a user belongs to a base station.

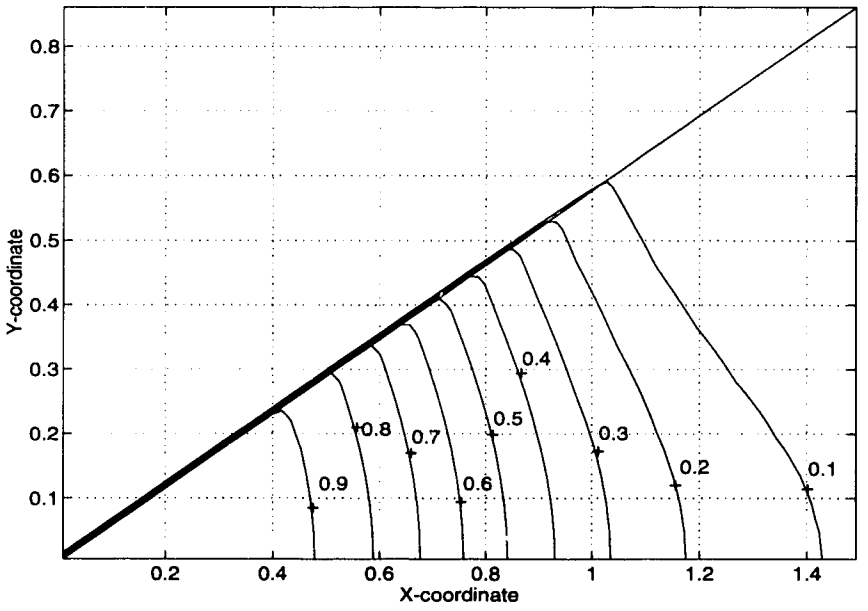

Fig. 3.3(b). Contour map of the probability that a user belongs to a base station.

Fig. 3.3 The surface and contour map of the probability distribution of a user which belongs to the reference base station. This triangular area is corresponding to the shadowed area shown in Fig. 3.1 and Fig. 3.2.

A contour map of the probability distribution that a user belongs to the reference base-station is given in Fig. 3.3. In this figure, the reference station is located at the origin, (0,0), and the probability distribution is represented over the triangular area AOG in Fig. 3.1. Given that there is an offered traffic of N_s calls per sector ($3N_s$ for an enlarged sector), the mean number of active users which belong to the reference base station can be obtained.

$$E(N_{bl}) = 3N_s \cdot E\overline{(\varphi)} = 3N_s \cdot \int\int_{A_0} p(\varphi = 1 | r_0, \theta) f_{A_0}(r_0, \theta)\, r_0 dr_0 d\theta \tag{3.42}$$

where N_{bl} is the number of users belonging to a base station and A_0 is the enlarged cell area covered by a base station. With uniformly distributed users, $E\overline{(\varphi)} = 1/3$ and Equation (3.42) reduces to N_s. The variance of the number of users is

$$D(N_{bl}) = 3N_s \cdot \left(E\left(\varphi^2\right) - E^2\overline{(\varphi)} \right) \tag{3.43}$$

where

$$E\left(\varphi^2\right) = \int\int_{A_0} p(\varphi = 1 | r_0, \theta) f_{A_0}(r_0, \theta)\, r_0 dr_0 d\theta, \tag{3.44}$$

and

$$E^2\overline{(\varphi)} = \int\int_{A_0} p^2(\varphi = 1 | r_0, \theta) f_{A_0}(r_0, \theta)\, r_0 dr_0 d\theta \cdot \tag{3.45}$$

Since the membership switching and user activity are independent random variables, the mean power of intra-cell interference can be expressed as

$$\begin{aligned} E(I_{ita}) &= (3N_s - 1)\upsilon \cdot E\overline{(\varphi)} \\ &= (3N_s - 1)\upsilon \cdot \int\int_{A_0} p(\varphi = 1 | r_0, \theta) f_A(r_0, \theta)\, r_0 dr_0 d\theta \end{aligned} \tag{3.46}$$

With uniformly distributed users, $E\overline{(\varphi)} = 1/3$ and Equation (3.46) reduces to

$$E(I_{ita}) = \left(N_s - \frac{1}{3}\right) \cdot \upsilon \tag{3.47}$$

Similarly, the area averaged variance of the intra-cell interference with one active user is

$$\begin{aligned} D(I_{ita}) &= (3N_s - 1)\left(\upsilon E\overline{(\varphi^2)} - \upsilon^2 E^2\overline{(\varphi)}\right) \\ &= (3N_s - 1)\left(\frac{1}{3}\upsilon - \upsilon^2 E^2\overline{(\varphi)}\right) \end{aligned} \tag{3.48}$$

Note that $E\overline{(\varphi^2)}$ is also 1/3 if users are uniformly distributed and we calculate $E^2\overline{(\varphi)}$ which is given as a parameter for interference calculation. The key parameters for calculating the total interference are the area averaged first and second moments. Values for these parameters, obtained under tne conditions of ideal handoff, perfect power control, user ACF of 1 and the path loss factor, $\nu = 4$, are given in Table 3.1.

Then the mean of total interference power is

$$M(I_t) = E(I_{ita}) + E(I_{Rite}) \tag{3.49}$$

and the variance of total interference power is

$$Var(I_t) = D(I_{ita}) + D(I_{Rite}) \tag{3.50}$$

where I_t is the total multi-user interference.

Table 3.1 The First and Second Moments for Evaluating The Total Interference and Membership Statistics

σ_L	$E\overline{(I_s)}$	$E\overline{(I_s^2)}$	$E^2\overline{(I_s)}$	$E^2\overline{(\varphi)}$
4.0	0.442	0.163	0.046	0.267
6.0	0.501	0.189	0.031	0.237
8.0	0.564	0.222	0.024	0.212

3.6 Summary

In this chapter, we analyzed the multi-cell, multi-user interference in a CDMA cellular system with a single type of traffic. Ideal soft handoff and perfect power control is assumed. We developed an analytical method to calculate the mean and variance of the total interference, as well as the area averaged PDF of inter-cell interference from one user. In this chapter, we also analyzed the membership statistics of an active user in a cell. The first and second moments for evaluating the total interference and membership statistics are given. From our results, we may see that due to soft handoff, the area covered by a base station is enlarged and the inter-cell interference is greatly reduced.

Chapter 4

The Effect of Imperfect Handoff and Power Control, Interference Modelling and Outage Analysis

4.1 Introduction

In a CDMA cellular system, soft handoff is tightly coupled with power control. In [16], the effect of ideal soft handoff was evaluated, revealing that the system capacity is doubled when an ideal soft handoff is used rather than a hard handoff that was studied in [45]. Here we consider soft handoff operations including cell site diversity and power control of one mobile by multiple base stations. For the cell site diversity, selection diversity is assumed in the reverse link since it is of low complexity and very effective.

Ideal soft handoff minimizes the interference by using the best signal reception of the involved base stations at the central office and synchronizing power control on this signal. In other words, ideal soft handoff means that when more than one base station is requested by a mobile, the best reception from one station is selected and power control is synchronized with the diversity selection. This operation compensates for the path loss and the channel attenuation on the path from the mobile to the base station which is obtaining the best reception.

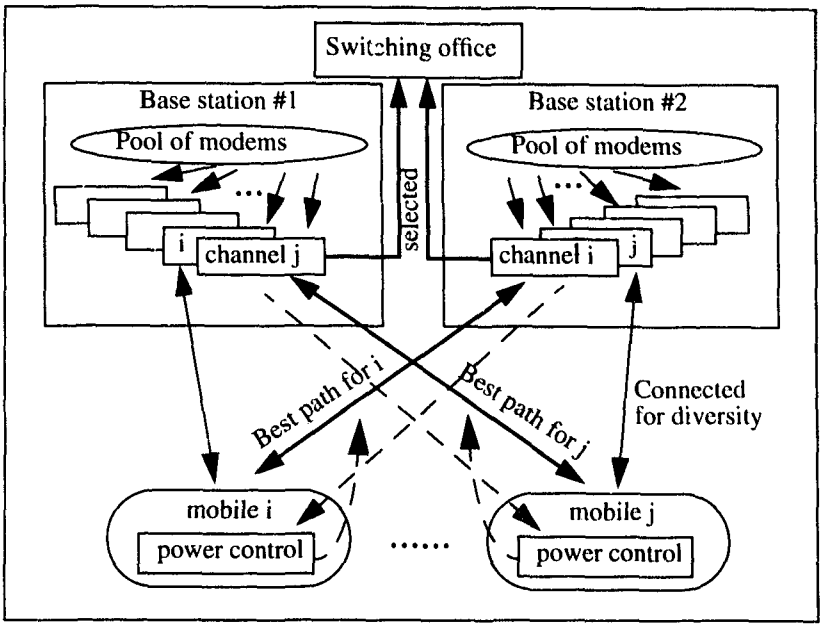

Fig. 4.1 Soft handoff operations. Soft handoff operations include diversity selection and power control switching. Due to cell site diversity, more channels are required at a base station.

In practice, reverse link power control consists of closed loop and open loop power control. Closed loop power control means that a base station measures the received power from a mobile and, based on this measurement, sends a feedback message to the mobile to adjust its transmitted power. Open loop power control means that a mobile measures the pilot power from surrounding base stations and tracks the strongest one for power control. Since the power control in the reverse link is different from that of the forward link, the objective of reverse link power control is to achieve a nominal received power, not a target SNR. There are two drawbacks to closed loop power control: 1. Feedback channel is not error free; 2. Closed loop power control relies on the measurement of the received signal power. In practice, it is very difficult to measure the desired signal power alone, typically one measures the signal power plus noise. Therefore, it is not enough to only employ closed loop power control in the reverse link. On the other hand, open loop

power control does not work well by itself. Open loop power control requires the datums provided by the closed loop power control. Therefore, both open loop and closed loop power control are necessary for the reverse link.

Since power control during soft handoff should ideally compensate for the attenuation of the path from the mobile to the base station with the best reception, there is an actually switching of power control connections among the involved base stations. This switching of power control connection is in terms of following the instruction from one specific base station with the best reception for closed loop power control and locking on the pilot power which is the strongest from that base station for open loop power control. A sensitive power control switching mechanism which is matched to the attenuation on the path to the best base station is required to minimize interference. In practice, the internal power control switching is not this perfect. Accordingly, we use a parameter H_p, within a range $0 < H_p \leq 1$, to represent the "hardness" or imperfectness of the power control switching mechanism. Due to the reciprocity of path loss and lognormal shadowing, switching the power control connection can be determined by pilot power measurement. When the pilot power of a nearby station is $1/H_p$ times greater than the pilot power of the current reference base station, a power control switching occurs [46].

After a power control connection is established, power control error always exists. The authors of [18], [32], [33] suggest that with non-ideal power control, the power control error is lognormally distributed. We adopt this lognormal assumption and treat power control error as an independent lognormal random variable in our analytical evaluation of the effect of imperfect power control.

In the last chapter, we divided the total interference into intra-cell and inter-cell. It is almost impossible to calculate this interference directly. In addition, it normally takes a long time to get simulation results. Modelling the interference is an effective way to solve this problem. Using a good model may make calculation much simpler and give very accurate results. The conventional model of multi-cell, multi-user interference is the

Gaussian model based on the Large Number Theorem. Here, we develop a model suitable for both a large and a small number of users.

The Gamma distribution which is closely related to the Nakagami model is employed to model the PDF of the area averaged inter-cell interference power of an active user and the PDF of the power control error. The validity of our model and the Gaussian approximation is verified via simulation. Since the next generation of PCS will support a variety of traffic types with very high transmission quality requirements, the performance of a system with a small number of users becomes very important, so we examine our model for a wide range of user number.

The rest of this chapter is organized as follows. The second and the third sections are devoted to a discussion on the effect of nonideal soft handoff and power control on interference. A model for inter-cell interference is developed in the fourth section. A model for intra-cell interference and membership statistics is proposed in the fifth section. Outage analysis and case studies are presented in the sixth section. The last section presents a summary and concluding remarks.

4.2 The Effect of Non-ideal Handoff Operation and Imperfect Power Control on inter-cell Interference

4.2.1 The effect of non-ideal handoff

Considering the hardness parameter H_p, we can see that when $H_p = 1$, soft handoff is perfect. If $H_p = 0$, there is no power control switching at all. Including in the hardness parameter H_p and taking $j = 3$ in Equation (3.8), we have the PDF of the transmitted power of an active user as

$$f_{I_{0,tr}}(I_{tr,0}) = F(I_{tr,0}, H_p I_{tr,0} \le I_{tr,1} \cap H_p I_{tr,0} \le I_{tr,2})$$
$$= F(I_{tr,0}, H_p I_{tr,0} \le I_{tr,1} \le I_{tr,2}) + F(I_{tr,0}, H_p I_{tr,0} \le I_{tr,2} \le I_{tr,1}) \quad (4.1)$$

where

$$F(I_{tr,0}, H_p I_{tr,0} \le I_{tr,1} \le I_{tr,2}) = \frac{10^2}{2\pi\sigma_L^2 \ln^2(10) I_{tr,0}} \exp\left\{-\frac{10^2}{2\sigma_L^2 \ln^2(10)} \ln^2\left(\frac{I_{tr,0}}{r_0^{\nu}}\right)\right\}$$
$$\times \int_{H_p I_{tr,0}}^{\infty} \frac{1}{I_{tr,1}} \exp\left\{-\frac{10^2}{2\sigma_L^2 \ln^2(10)} \ln^2\left(\frac{I_{tr,1}}{r_1^{\nu}}\right)\right\}$$
$$\times \left(\frac{1}{2} - \frac{1}{2}\mathrm{erf}\left(\frac{10}{\sqrt{2}\sigma_L \ln(10)} \ln\left(\frac{I_{tr,1}}{r_2^{\nu}}\right)\right)\right) dI_{tr,1} \tag{4.2}$$

and

$$F(I_{tr,0}, H_p I_{tr,0} \le I_{1,tr} \le I_{tr,2}) = \frac{10^2}{2\pi\sigma_L^2 \ln^2(10) I_{tr,0}} \exp\left\{-\frac{10^2}{2\sigma_L^2 \ln^2(10)} \ln^2\left(\frac{I_{tr,0}}{r_0^{\nu}}\right)\right\}$$
$$\times \int_{H_p I_{tr,0}}^{\infty} \frac{1}{I_{tr,2}} \exp\left\{-\frac{10^2}{2\sigma_L^2 \ln^2(10)} \ln^2\left(\frac{I_{tr,2}}{r_2^{\nu}}\right)\right\}$$
$$\times \left(\frac{1}{2} - \frac{1}{2}\mathrm{erf}\left(\frac{10}{\sqrt{2}\sigma_L \ln(10)} \ln\left(\frac{I_{tr,2}}{r_1^{\nu}}\right)\right)\right) dI_{tr,2} \,. \tag{4.3}$$

Using methods similar to Chapter 3, we obtain the mean interference power from an active reference user, including H_p and assuming perfect power control. Using Equation (3.12), for the ith base station, $i = 3, 4\ldots$, we have

$$E(I_i) = \int_0^{1/H_p} \int_0^{\infty} \frac{I_i}{I_{tr,0}} f_{I_{pi}}\left(\frac{I_i}{I_{tr,0}}\right) f_{I_{tr,0}}(I_{tr,0})\, dI_{tr,0} dI_i$$
$$= \int_0^{\infty} \int_0^{1/H_p} \frac{I_i}{I_{tr,0}} f_{I_{pi}}\left(\frac{I_i}{I_{tr,0}}\right) d\left(\frac{I_i}{I_{tr,0}}\right) \cdot I_{tr,0} f_{I_{tr,0}}(I_{tr,0})\, dI_{tr,0}$$
$$= \int_0^{\infty} M_{pi} I_{tr,0} f_{I_{tr,0}}(I_{tr,0})\, dI_{tr,0} \,. \tag{4.4}$$

Letting $I_i' = I_i / I_{tr,0}$, we obtain that, for $i = 3, 4, \ldots,$

$$M_{pi} = \int_0^{\frac{1}{I_{tr,0}H_p}} I_i f_{I_{pi}}(I_i)\,dI_i$$
$$= \frac{1}{r_i^{\nu}}\exp\left\{\frac{\sigma_L^2 \ln^2 10}{200}\right\}\left(\frac{1}{2}+\frac{1}{2}\mathrm{erf}\left(\frac{40\ln\left(\frac{r_i}{I_{tr,0}H_p}\right)}{\sqrt{2}\sigma_L \ln 10}-\frac{\sigma_L \ln 10}{10\sqrt{2}}\right)\right). \tag{4.5}$$

When the interference of an active user is received at base station 1 or 2, the path attenuation is correlated with the user's transmitted power. Considering power control switching, we have that $I_{01}H_p < I_{21}$, given that an active user belongs to base station 0. Then the PDF of x which was defined in Chapter 3, can be similarly obtained as

$$f(x|H_p I_{01} < I_{21}) = f\left(x\left|\frac{10}{\ln 10}\ln H_p + \frac{10\nu}{\ln 10}\ln\frac{r_0}{r_2} + x < y\right.\right)$$
$$= \frac{1}{\sqrt{2\pi}\sigma}\exp\left\{-\frac{x^2}{2\sigma^2}\right\}\left(\frac{1}{2}-\frac{1}{2}\mathrm{erf}\left(\frac{\frac{10}{\ln 10}\left(\ln H_p + \nu\ln\frac{r_0}{r_2}\right)+(1-\rho)x}{\sqrt{2(1-\rho^2)}\sigma}\right)\right). \tag{4.6}$$

Given that an active user belongs to base station 0, the mean interference from an active user (at position (r, θ)) to base station 1 is

$$E(I_{01}) = \int_{-\infty}^{b}\left(\frac{r_0}{r_1}\right)^{\nu}\frac{1}{2\sqrt{\pi}\sigma_L}\exp\left\{\frac{x\ln 10}{10}-\frac{x^2}{4\sigma_L^2}\right\}$$
$$\times\left(\frac{1}{2}-\frac{1}{2}\mathrm{erf}\left(\frac{\frac{10}{\ln 10}\left(\ln H_p + \nu\ln\frac{r_0}{r_2}\right)+(1-\rho)x}{2\sqrt{(1-\rho^2)}\sigma_L}\right)\right)dx. \tag{4.7}$$

Since the upper bound of I_{01} is

$$I_{01} = \left(\frac{r_0}{r_1}\right)^{\nu} 10^{\frac{x}{10}} \le \frac{1}{H_p}, \tag{4.8}$$

the b in Equation (4.7) has a value of

$$b = \frac{10}{\ln 10}\left(v\ln\frac{r_1}{r_0} - \ln H_p \right). \tag{4.9}$$

Like Chapter 3., we have that $E(I_{02}) = E(I_{01})$ for base station 2, and denote $E(I_{01})$ as $E(I_1)$ and $E(I_{02})$ as $E(I_2)$. The definition of r_i and θ, is shown in Fig. 3.2, the calculation of r_i is shown in (3.23).

Similarly, we can also obtain the area averaged variance of the interference power of an active user. We first examine the independent case:

$$\begin{aligned} E\left(I_i^2\right) &= \int_0^{\frac{1}{H_p}} \int_0^{\infty} \frac{I_i^2}{I_{tr,0}} f_{I_{pi}}\left(\frac{I_i}{I_{tr,0}}\right) f_{I_{tr,0}}(I_{tr,0})\, dI_{tr,0} dI_i \\ &= \int_0^{\infty} Msq_{qi} \cdot I_{tr,0}^2 \cdot f_{I_{tr,0}}(I_{tr,0})\, dI_{tr,0} \end{aligned} \tag{4.10}$$

where for $i = 3, 4, \ldots,$

$$Msq_{pi} = \frac{1}{r_i^{2v}} \exp\left\{\frac{\sigma_L^2 \ln^2 10}{50}\right\} \cdot \left(\frac{1}{2} + \frac{1}{2}\operatorname{erf}\left(\frac{10v\ln\left(\frac{r_i}{I_{tr,0}H_p}\right)}{\sqrt{2}\sigma_L \ln 10} - \frac{\sqrt{2}\sigma_L \ln 10}{10} \right) \right) \tag{4.11}$$

For base station 1 and 2, correlation exists and the second moment can also be obtained in a manner similar to the first moment in Equation (4.7). Therefore,

$$\begin{aligned} E\left(I_1^2\right) = \int_{-\infty}^{b} \left(\frac{r_0}{r_1}\right)^{2v} \frac{1}{2\sqrt{\pi}\sigma_L} \exp\left\{\frac{(\ln 10)x}{5} - \frac{x^2}{4\sigma_L^2}\right\} \\ \times \left(\frac{1}{2} - \frac{1}{2}\operatorname{erf}\left(\frac{\frac{10}{\ln 10}\left(\ln H_p + v\ln\frac{r_0}{r_2}\right) + (1-\rho)x}{2\sqrt{(1-\rho^2)}\sigma_L} \right) \right) dx \cdot \end{aligned} \tag{4.12}$$

where b is given by Equation (4.9). Similarly, we have also $E\left(I_1^2\right) = E\left(I_2^2\right)$.

With Equations (3.29), (3.33) and (3.34), we can obtain the first and second moments of area averaged inter-cell interference. The effects of handoff sensitivity, H_p, on the parameters $E\overline{(I_s)}$, $E\overline{(I_s^2)}$ and $E^2\overline{(I_s)}$ are shown in Fig. 4.2, Fig. 4.3 and Fig. 4.4. We can see that if power control does not match on the best path, the inter-cell interference level will increase significantly.

4.2.2 The Effect of Imperfect Power Control

After a power control connection is established, there is always power control error which can be modelled as a lognormal random variable [18], [32], [33]. Taking the power control error into consideration, we get

$$I_i' = I_i \cdot I_{pce} \qquad i = 1, 2, \ldots \tag{4.13}$$

where I_i is the interference generated by a user belonging to the reference base station and received at base station i, and $I_{pce} = 10^{x_e/10}$ represents the power control error with a standard deviation σ_e.

From Equation (4.13), we see that the total interference I_i' is formed by the multiplication of two independent random variables: I_i and power control error I_{pce}. Then, using the parameters in Table 3.1, we can easily factor the power control error and obtain the mean of the total inter-cell interference by modifying Equation (3.35). This gives

$$E(I_{ite}) = N_s \cdot \upsilon E(I_{pce}) \cdot E\overline{(I_s)} \tag{4.14}$$

where the mean power control error is

$$E(I_{pce}) = \exp\left\{\frac{\left(\sigma_e^2 \ln^2 10\right)}{200}\right\}. \tag{4.15}$$

As in Chapter 3, we consider the total inter-cell interference is as $I_{Rite} = I_{ite} \cdot I_{Ry}$

where I_{Ry} is Chi-square distributed with mean equal to 1. Therefore, with Rayleigh fading the mean of the inter-cell interference is $E(I_{Rite}) = E(I_{ite})$.

Taking the user Activity Factor and the power control error into consideration, we have that the area averaged variance of the total inter-cell interference is

$$D(I_{ite}) = N_s \cdot \left(\upsilon E\left(I_s^2\right) E\left(I_{pce}^2\right) - \upsilon^2 E^2\left(\overline{I_s}\right) E^2(I_{pce}) \right) \tag{4.16}$$

where $E\left(I_{pce}^2\right)$ is the second moment of the power control error given by

$$E\left(I_{pce}^2\right) = \exp\left\{ \frac{\left(\sigma_e^2 \ln^2 10\right)}{50} \right\}. \tag{4.17}$$

With Rayleigh fading the variance of the inter-cell interference increases to

$$\begin{aligned} D(I_{Rite}) &= N_s \cdot \left(E\left(I_{ite}^2\right) E\left(I_{Ry}^2\right) - E^2(I_{ite}) E^2(I_{Ry}) \right) \\ &= N_s \cdot \left(2\upsilon \overline{E(I_s^2)} E\left(I_{pce}^2\right) - \upsilon^2 E^2\left(\overline{I_s}\right) E^2(I_{pce}) \right). \end{aligned} \tag{4.18}$$

4.3 The Effect of Non-ideal Handoff Operation and Imperfect Power Control on intra-cell Interference

Non-ideal power control switching also affects the membership statistics. Taking the handoff sensitivity into consideration, we have

$$\begin{aligned} p(\varphi = i | r_0, \theta) &= p(I_{tr,0} H_p \le I_{tr,1} \cap I_{tr,0} H_p \le I_{tr,2} | r_0, \theta) \\ &= p(I_{tr,0} H_p \le I_{tr,1} \le I_{tr,2} | r_0, \theta) + p(I_{tr,0} H_p \le I_{tr,2} \le I_{tr,1} | r_0, \theta) \end{aligned} \tag{4.19}$$

where

$$p\left(I_{tr,0}H_p \le I_{tr,1} \le I_{tr,2} \middle| r_0, \theta\right) = \int_0^{\infty}\int_0^{I_{tr,2}} \left(\frac{10}{\sqrt{2\pi}\ln 10\sigma_L}\right)^2 \cdot \frac{1}{I_{tr,1}I_{tr,2}} \times \exp\left\{-\frac{10^2}{2\sigma_L^2 \ln^2 10}\left(\ln^2\left(\frac{I_{tr,1}}{r_1^{v}}\right) + \ln^2\left(\frac{I_{tr,2}}{r_2^{v}}\right)\right)\right\} \times \left(\frac{1}{2} + \frac{1}{2}\operatorname{erf}\left(\frac{10}{\sqrt{2}\ln 10\sigma_L}\ln\left(\frac{I_{tr,1}}{H_p r_0^{v}}\right)\right)\right) dI_{tr,1}dI_{tr,2} \tag{4.20}$$

and

$$p\left(I_{tr,0}H_p \le I_{tr,2} \le I_{tr,1} \middle| r_0, \theta\right) = \int_0^{\infty}\int_0^{I_{tr,1}} \left(\frac{10}{\sqrt{2\pi}\ln 10\sigma_L}\right)^2 \cdot \frac{1}{I_{tr,1}I_{tr,2}} \times \exp\left\{-\frac{10^2}{2\sigma_L^2 \ln^2 10}\left(\ln^2\left(\frac{I_{tr,1}}{r_1^{v}}\right) + \ln^2\left(\frac{I_{tr,2}}{r_2^{v}}\right)\right)\right\} \times \left(\frac{1}{2} + \frac{1}{2}\operatorname{erf}\left(\frac{10}{\sqrt{2}\ln 10\sigma_L}\ln\left(\frac{I_{tr,2}}{H_p r_0^{v}}\right)\right)\right) dI_{tr,2}dI_{tr,1} \tag{4.21}$$

Since the parameters $E\overline{(\varphi)}$, $\overline{E(\varphi^2)}$ and $E^2\overline{(\varphi)}$ are related to $p(\varphi = 1 | r_0, \theta)$ as shown in Chapter 3, we get

$$E\overline{(\varphi)} = \iint_{A_0} p(\varphi = 1 | r_0, \theta) f_{A_0}(r_0, \theta)\, r_0 dr_0 d\theta, \tag{4.22}$$

$$\overline{E(\varphi^2)} = \iint_{A_0} p(\varphi = 1 | r_0, \theta) f_{A_0}(r_0, \theta)\, r_0 dr_0 d\theta, \tag{4.23}$$

and

$$E^2\overline{(\varphi)} = \iint_{A_0} p^2(\varphi = 1 | r_0, \theta) f_{A_0}(r_0, \theta)\, r_0 dr_0 d\theta. \tag{4.24}$$

From Equation (3.43), we define the variance factor of user membership as

$$\overline{D(\varphi)} = 3 \cdot \left(\overline{E(\varphi^2)} - E^2\overline{(\varphi)}\right). \tag{4.25}$$

The effect of H_p on user membership statistics is plotted in Fig. 4.5. From this figure, we can see that the variance of N_{bl} increases as H_p increases. This results from the fact that a more sensitive membership handoff mechanism leads to more internal membership switching activity.

The received power of a reference user is P_0 as shown in Equation (3.5). If there is no power control error, P_0 is the nominal power, which is often normalized to 1. Now, we consider that power control is imperfect in combatting propagation path loss, shadowing and multi-path fading. When a power control system is in steady state, the received signal process is considered to be stationary and subject to a certain distribution. Under the lognormal assumption of power control error, the received power of a desired user at the base station is

$$P_0 = \frac{E_s}{T_s 10^{x_e/10}} \tag{4.26}$$

where E_s is the symbol energy, T_s is the symbol period and x_e represents the power control error which is Gaussian distributed with zero mean and the standard deviation σ_e about 0.5--3dB. Here, E_s/T_s can be normalized to 1 without loss of generality. Then the probability density function of the desired signal power, P_0, is

$$f_0(P_0) = \frac{10}{\ln 10 \sqrt{2\pi}\sigma_e P_0} \exp\left\{-\frac{1}{2\sigma_e^2}\left(\frac{10}{\ln 10}\ln P_0\right)^2\right\}. \tag{4.27}$$

Similarly, the PDF of the power of the ith active interference signal belonging to the reference cell is

$$f_{0i}(P_{0i}) = \frac{10}{\ln 10 \sqrt{2\pi}\sigma_e P_{0i}} \exp\left\{-\frac{1}{2\sigma_e^2}\left(\frac{10}{\ln 10}\ln P_{0i}\right)^2\right\}. \tag{4.28}$$

Since call arrival, membership switching, user activity and power control error are

independent random variables, the mean power of intra-cell interference can be expressed as

$$E(I_{ita}) = (3N_s - 1)\upsilon \cdot E(I_{pce}) \cdot E\overline{(\varphi)} \tag{4.29}$$

and if the active users are uniformly distributed, then

$$E(I_{ita}) = \left(N_s - \frac{1}{3}\right) \cdot \upsilon \cdot E(I_{pce}) \cdot \tag{4.30}$$

Similarly, the area averaged variance of the intra-cell interference with one active user is

$$\begin{aligned} D(I_{ita}) &= (3N_s - 1)\left(\upsilon E\left(I_{pce}^2\right)E\overline{(\varphi^2)} - \upsilon^2 E^2(I_{pce})\,E^2\overline{(\varphi)}\right) \\ &= (3N_s - 1)\left(\frac{1}{3}\upsilon E\left(I_{pce}^2\right) - \left(-\upsilon^2 E^2(I_{pce})\,E^2\overline{(\varphi)}\right)\right) \end{aligned} \tag{4.31}$$

where $E\left(I_{pce}^2\right)$, $E^2(I_{pce})$ and $E^2\overline{(\varphi)}$ can be obtained by using Equations (4.15), (4.17) and (4.24). Note that N_s is fixed when we consider radio capacity.

4.4 Modelling the intra-cell Interference

The intra-cell interference is mainly determined by hand-off, transmission duty cycle and power control error. From Equations (4.22) and (4.25), the mean and variance of the number of the users which belong to the reference station can be obtained, but the distribution of N_{bl} is difficult to calculate. Since it is important to the evaluation of system performance, we propose the following model to simplify the problem.

As shown in Fig. 3.3, the probability of a user belonging to a base-station is almost equal to 1 when the user is very close to the base station. Accordingly, we propose a model in which users are separated into two groups. Users in the first group are assumed to always belong to one of the three base stations. There are N_{rm} such users belonging to each base station. The remaining users may belong to any one of the three base stations.

We denote the total number of these users as N_{ef}. Then, the number of users belonging to a base station is the sum of a random variable m and N_{rm}

$$N_{bl} = m + N_{rm} \cdot \tag{4.32}$$

We model m with a binomial distribution which has the same mean and variance as N_{bl}, as given by Equations (3.42) and (3.43). This results in

$$p_m(m) = \binom{N_{ef}}{m} p_{bl}^{m} (1 - p_{bl})^{N_{ef} - m} \tag{4.33}$$

where N_{ef} is determined by the variance of N_{bl} given by Equation (3.43) and p_{bl} is the average probability that a user belongs to a base station. Let the variance of the binomial model be

$$Var_m(N_{bl}) = N_{ef} \cdot p_{bl}(1 - p_{bl}) = D(N_{bl}),$$

then

$$N_{ef} = \text{int}\left(\frac{D(N_{bl})}{p_{bl}(1 - p_{bl})} \right) \cdot \tag{4.34}$$

The number of users which always belong to a base-station is therefore

$$N_{rm} \approx N_s - \text{int}(p_{bl} \cdot N_{ef}) = N_s - \text{int}\left(\frac{D(N_{bl})}{1 - p_{bl}} \right) \cdot \tag{4.35}$$

Since there are three base stations closest to an active user involved in operation, if the users are uniformly distributed, the average probability of a user belonging to one of the base stations is 1/3. Therefore, we take $p_{bl} = 1/3$ in our model. The PDF of N_{bl} obtained with this binomial model agrees closely with the simulation results, as shown in Figures 4.6 to 4.9.

The active user number is determined not only by hand-off, but also by the Activity Factor. The distribution of the active user number k is

$$p(k|m) = \binom{m + N_{rm} - 1}{k} \upsilon^{k} (1 - \upsilon)^{m + N_{rm} - 1 - k}. \tag{4.36}$$

This is a conditional distribution given that there are $m + N_{rm}$ users belonging to the reference base station.

With the lognormal assumption of the power control error, calculating the PDF of the total intra-cell interference becomes a problem of calculating the PDF of a sum of lognormal random variables, which is usually quite difficult. To solve this problem, we use the Gamma distribution instead of the lognormal distribution. Note that the Gamma distribution is the power form distribution of the Nakagami model. The expression of the Gamma distribution is given by Equation (2.14). When the standard deviation of a log-normal variable is small, the lognormal distribution can be well approximated by the Nakagami model [27], [47]. Fig. 4.10 shows a comparison of the two PDFs. The main bodies of the Gamma and lognormal PDFs closely agree with each other. Since the Gamma model employed has the same mean and variance as the lognormal PDF, their tails, which are largely determined by the variance, must also be very close. This is justified by our final outage simulation results as shown in Fig. 4.20. Using the Gamma distribution, after power control and diversity combining, the PDF of received signal power of a user that belongs to the reference station can be expressed as

$$f'_{0i}(P_{0i}) = \frac{1}{\Gamma(\mu_0)} \left(\frac{\mu_0}{M_0} \right)^{\mu_0} P_{0i}^{\mu_0 - 1} \exp\left\{ -\frac{\mu_0}{M_0} P_{0i} \right\} \tag{4.37}$$

where $\Gamma(x)$ is the Gamma function, M_0 is the mean of P_{0i} and $\mu_0 = M_0 / Var(P_{0i})$.

When there are k independent active interfering users belonging to the reference station, the PDFs of the received power of every user that belongs to the reference base station are the same, with the same mean and variance. The total interference is therefore

$$I_{0k} = \sum_{i=1}^{k} P_{0i}.$$

Then the PDF of I_{0k} is the k-fold convolution of the $f'_{0i}\ (P_{0i})$

$$f_{I_{0k}}(I_{0k}) = f'_{01}\ (P_{01}) * f'_{02}\ (P_{02}) * \ldots * f'_{0k}\ (P_{0k})$$
$$= \frac{1}{\Gamma(\mu_0 k)}\left(\frac{\mu_0}{M_0}\right)^{\mu_0 k} I_{0k}^{\mu_0 k - 1} \exp\left\{-\frac{\mu_0}{M_0} I_{0k}\right\}. \tag{4.38}$$

Note that M_0 is the mean of the received power of an active user. Since the received power of a user belonging to the reference station is normalized, M_0 is the same as the mean of the power control error and it can be obtained from Equation (4.15), thus, $M_0 = E(I_{pce})$. μ_0 is a parameter given by $\mu_0 = M_0 / Var(P_{0i})$ where $Var(P_{0i}) = Var(P_0)$ is the variance of power control error.

$$Var(P_0) = Var(I_{pce}) = \exp\left\{\frac{\sigma_e^2 (\ln 10)^2}{100}\right\} \cdot \left(\exp\left\{\frac{\sigma_e^2 (\ln 10)^2}{100}\right\} - 1\right). \tag{4.39}$$

Both the mean and variance of the Gamma model are taken to be the same as the lognormal model and we use the σ_e of the lognormal PDF representing power control error to facilitate comparisons with other results in the literature.

Finally, the PDF of the total intra-cell interference is given by

$$f_{ita}(I_{ita}) = \sum_{m=N_1}^{N_{ef}} \sum_{k=0}^{m+N_{rm}-1} \binom{N_{ef}}{m} p_{bl}^{m} (1-p_{bl})^{N_{ef}-m}$$
$$\times \binom{m+N_{rm}-1}{k} \upsilon^k (1-\upsilon)^{m+N_{rm}-1-k} f_{I_{0k}}(I_{0k}) \cdot \tag{4.40}$$

In Equation (4.40), if N_{rm} as obtained from Equation (4.35) is less than 1, then we take $N_1 = 1$ and $N_{rm} = 0$. Otherwise, $N_1 = 0$ and N_{rm} is obtained from Equation (4.35). Fig. 4.12 shows the PDF of intra-cell interference with perfect power control, ideal hand-off and an ACF of 0.375.

4.5 Modelling the inter-cell Interference

For inter-cell interference, it can be shown that the area averaged PDF of an active user j can also be well approximated by the Gamma distribution with the same mean and variance. We have therefore

$$f'_{jav}(I_{avj}) = \frac{1}{\Gamma(\mu_j)}\left(\frac{\mu_j}{M_j}\right)^{\mu_j} I_{avj}^{\mu_j - 1} \exp\left\{-\frac{\mu_j}{M_j} I_{avj}\right\} \tag{4.41}$$

where $M_j = E(I_{Rite}) / (18N_s)$ is obtained from Equation (4.14) and is the area averaged mean power of an active interference user which is not power controlled by the reference station, the variance $Var_j = D(I_{Rite}) / (18N_s)$ can be obtained by employing Equation (4.18) and μ_j can be obtained via $\mu_j = M_j^2 / Var_j$. Fig. 4.11 shows the comparison of the area averaged PDF and the Gamma PDF with the same mean and variance.

To obtain the PDF of multi-user interference, we consider k users which belong to a base station other than the reference base station in the enlarged cell area. Their powers received at the reference station are $I_1, I_2, \ldots, I_k$, and their locations are $(r_1, \theta_1), (r_2, \theta_2), \ldots, (r_k, \theta_k)$, respectively. The conditional PDF of the sum of $I_1, I_2, \ldots, I_k$ is

$$f_m(I_m) = f_1(I_1|r_1, \theta_1) * f_2(I_2|r_2, \theta_2) * \ldots * f_k(I_k|r_k, \theta_k) \tag{4.42}$$

Over a long period, the users will travel over any location following the user distribution statistics. Therefore, the PDF of I_m is averaged over the area concerned giving,

$$\begin{aligned} f_{ite}(I_{ite}) = & \int_{A_1}\int \int_{A_2}\int \cdots \int_{A_k}\int f_1(I_1|r_1, \theta_1) * f_2(I_2|r_2, \theta_2) * \ldots * f_k(I_k|r_k, \theta_k) \\ & \times f_{A_1}(r_1, \theta_1) \cdot f_{A_2}(r_2, \theta_2) \cdot \ldots \cdot f_{A_k}(r_k, \theta_k)\, dA_1 dA_2 \ldots dA_k \end{aligned} \tag{4.43}$$

Equation (4.43) can be expressed as the convolution of the area averaged PDF of inter-cell interference

$$f_{ite}(I_{ite}) = f_{av1}(I_{av1}) * f_{av2}(I_{av2}) * \ldots * f_{avk}(I_{avk}) \tag{4.44}$$

where $f_{av1}(I_{av1}) = f_{av2}(I_{av2}) = \ldots = f_{avj}(I_{avj})$ is given by Equation (3.22). We model $f_{avj}(I_{avj})$ as the Gamma distribution given by Equation (4.41). Since there exists a closed form solution for the convolution of Gamma distributions [23], [27], the PDF of inter-cell interference can be expressed as

$$f_{ite}(I_{ite}) = \frac{1}{\Gamma(\mu_{ite})}\left(\frac{\mu_{ite}}{M_{ite}}\right)^{\mu_{ite}} I_{ite}^{\mu_{ite}-1} \exp\left\{-\frac{\mu_{ite}}{M_{ite}} I_{ite}\right\} \tag{4.45}$$

where $M_{ite} = E(I_{Rite})$ and $\mu_{ite} = M_{ite}^2 / Var(I_{Rite})$ can be obtained by Equations (4.14) and (4.18).

The total interference is the sum of intra-cell and inter-cell interference as well as the Gaussian background noise. This can be expressed as

$$I_{st} = I_{ita} + I_{ite} + \sigma_T^2 = I_t + \sigma_T^2 \tag{4.46}$$

where σ_T^2 is the normalized power of the Gaussian noise due to spurious interference as well as thermal noise contained in the total spread bandwidth. From [14], $\sigma_T^2 = 1.26\,(1dB)$ for voice traffic when the power of the reference user is normalized to 1. The PDF of the total interference is therefore given by

$$f_{I_{st}}(I_{st}) = \int_0^\infty f_{ita}\left(I_{st} - I_{ite} - \sigma_T^2\right) f_{ite}(I_{ite})\, dI_{ite} \tag{4.47}$$

Fig. 4.13 shows the calculated PDF of inter-cell interference. Figures 4.14 to 4.19 show the comparisons of the calculated PDF given by the Gamma and Gaussian model with simulation results. From the results, we see that our Gamma model closely agree

with simulation results for both a small number and a large number of users. The simulation results are obtained based on the simulation package that we developed for CRC and BC Science Council. More details can be found in [44], [48].

Fig. 4.20 shows the outage probabilities obtained by using the Gamma model and Gaussian model as well as simulation. It can be seen that the outage probability obtained by our method is very close to the simulation result even for small number of users. This means that our interference model closely agrees with both the main body and tail of the PDF of multi-cell, multi-user co-channel interference.

4.6 Outage Analysis

4.6.1 Outage Probability

Following [14], the final received E_b/N_0 is

$$\frac{E_b}{N_0} = \frac{W}{R}\frac{p_0}{I_{ita} + I_{ite} + \sigma_T^2} = PG\frac{P_0}{I_{st}} \quad . \tag{4.48}$$

If we denote E_b/N_0 as γ, then the PDF of γ can be obtained from

$$f_\gamma(\gamma) = \int_0^\infty \frac{I_{st}}{PG} f_0\left(\frac{\gamma I_{st}}{PG}\right) f_{I_{st}}(I_{st})\, dI_{st} \tag{4.49}$$

where $f_0(.)$ is given by Equation (4.27) and $f_{I_{st}}(.)$ is given by Equation (4.46).

In general, the error probability of a decoder and demodulator is a function of the received γ. If γ is larger than a certain threshold, say η, $p_e(\gamma)$ will be smaller than the system quality requirement $p_e(\eta)$ where $p_e(\eta) = \varepsilon$. The outage probability is the probability that $\gamma < \eta$, or the probability that $p_e(\gamma) < \varepsilon$. We have therefore

$$p(p_e(\gamma) < \varepsilon) = p(\gamma < \eta) = \int_0^{\eta} f_\gamma(\gamma)\, d\gamma. \tag{4.50}$$

From previous results, it can be seen that due to the effect of hand-off, more than N_s users are involved in power control by a base station. The multi-cell, multi-user interference quickly tends toward a Gaussian distribution, especially when the ACF is large. Using the Gaussian model to evaluate the outage probability is a simple and effective way when number of users is large. If we consider the total interference to be Gaussian, and assume power control to be perfect, the outage probability is

$$\begin{aligned} p_{out} = p(\gamma < \eta) = p(I_t > t) &= \int_t^{\infty} \frac{1}{\sqrt{2\pi Var(I_t)}} \exp\left\{ -\frac{(I_t - M(I_t))^2}{2Var(I_t)} \right\} dI_t \\ &= \frac{1}{2}\operatorname{erfc}\left(\frac{(t - M(I_t))}{\sqrt{2Var(I_t)}} \right) \end{aligned} \tag{4.51}$$

where $I_t = I_{ita} + I_{Rite}$,

$$t = \frac{PG}{\eta} = \frac{PG}{(E_b/N_0)_{QR}} - \sigma_T^2, \tag{4.52}$$

$$M(I_t) = E(I_{ita}) + E(I_{Rite}) \tag{4.53}$$

and

$$Var(I_t) = D(I_{ita}) + D(I_{Rite}) \tag{4.54}$$

$E(I_{Rite})$, $D(I_{Rite})$, $E(I_{ita})$ and $D(I_{ita})$ can be obtained by Equations (4.14), (4.18), (4.30) and (4.31), respectively. If power control is assumed to be imperfect, the outage probability is given by

$$p_{out} = p\left(\frac{p_0}{I_t} < \frac{\eta P_0}{PG} \right) = \int_0^{\infty} \frac{1}{2} P_0 f_0(P_0)\, erfc\left(\frac{\frac{P_0 PG}{\eta} - M(I_t) - \sigma_T^2}{\sqrt{2Var(I_t)}} \right) dP_0 \tag{4.55}$$

where P_0 is the received power of the reference user. It is a random variable due to the

power control error. $f(P_0)$ is the PDF of P_0 given by Equation (4.27).

We also evaluate the system performance when the traffic contains mixed traffic types. If there are N_t types of traffic (or users), they may have different transmission rates, different quality requirements and different duty cycles. Since there are a lot of cases where the mixed type of interference is likely to be Gaussian, we may simply use the Gaussian model for mixed traffic. The design issues for multiple traffic types will be discussed in detail in Chapter 6. As in the case of a single traffic type, we have

$$M(I_t) = \sum_{i=1}^{N_t} M(I_{ti}) \tag{4.56}$$

and

$$Var(I_t) = \sum_{i=1}^{N_t} Var(I_{ti}) . \tag{4.57}$$

Again, the outage probability can be calculated by Equation (4.51) if power control is perfect or by using Equation (4.55) if power control is imperfect.

4.6.2 Numerical Results: Case Studies

In this part, we examine a conventional CDMA system and a system proposed for supporting high rate communications with mixed traffic.

For the conventional system, we choose the parameters to be the same as in [14]. The spread bandwidth is $W = 1.25\,\text{MHz}$, the bit rate is $R = 8\,\text{Kbps}$ and as a result, the processing gain is 156. The normalized background noise power is $\sigma_T^2 = 1\,\text{dB}$. The quality requirement is $(E_b/N_0)_{QR} = 7\,\text{dB}$ for coded voice to ensure an outage probability less than 0.01. Fig. 4.21 and Fig. 4.22 show the PDFs of the multi-cell, multi-user interference. It can be seen that with an increasing of the number of users, multi-cell, multi-user interference tends toward the Gaussian distribution more quickly than one would

expect from a simple summation of the interference power generated by the same number of users. The reason is that soft handoff operations randomize the total interference. We also see that when the ACF is large, the interference approaches the Gaussian distribution even quickly.

Fig. 4.23 and Fig. 4.24 show the PDF of the interference when power control error exists. In this situation, the PDF of the interference matches more closer to the lognormal distribution with a long tail. The effect of imperfect power control on outage performance is shown in Fig. 4.25. From the figure, we can see that for an outage probability of 0.01 if σ_e = 1 dB, there is a 28% loss in capacity; if σ_e = 2 dB, capacity is reduced by 58%. Our results support the reported simulation and analysis results in [32], [33], [44].

From Fig. 4.26, we can see that imperfect hand-off also affects the system performance. Here the hand-off parameter H_p is the reference station pilot power divided by highest pilot power. Our results show that if H_p is reduced from 1.0 to 0.5, system capacity is reduced by about 30%. Fig. 4.27 shows the outage performance when the service quality requirement is very high. In this case, the number of users which can be supported by the system is small.

For the high rate system, we evaluate the system performance with mixed traffic of voice and video. Here we assume an ideal case where no overhead is added to the different traffic sources. The system configuration is: Total spread bandwidth W = 10 MHz, speech bit rate R_s = 8 Kbps and video bit rate R_v = 64 Kbps. Both speech and video are transmitted at a line rate R_l = 64 Kbps. This means the Activity Factor for voice is 0.375/8, and for video is 1.0. The transmission quality requirement is $p_b = 10^{-3}$ for voice, and for low resolution video, we assume that the requirement is $P_b = 10^{-5}$ at first. To meet the quality requirements, we set the outage thresholds at 7 dB for voice and 12

dB for video.

Fig. 4.28 shows the outage probabilities for video traffic given a certain number of mixed users, based on the quality requirement of the video users. In this case, the requirements for both traffic types are met.

Fig. 4.29 shows the outage probabilities for voice traffic based on the outage requirement of the voice users. Here, only the voice users meet their quality requirements.

The capacity of the system with mixed traffic is shown in Fig. 4.30. The calculation is based on the outage requirements of the video users. The results show that if more powerful error control techniques are employed such that the SNR requirement of video users can be reduced, the overall system capacity can be increased significantly.

4.7 Summary

In this Chapter, we have examined the effect of non-ideal soft handoff operations and imperfect power control. Based on the careful analysis of the effects of soft handoff operation in a multi-cell environment, the interference characteristics, system capacity and service quality have been examined. The multi-cell, multi-user interference level depends highly on power control switching. In general, a highly sensitive power control handoff mechanism which is synchronized with cell site diversity selection is required.

The dependency of membership statistics on the soft handoff is a very important factor affecting system performance, and has been investigated in detail. We have proposed a simple binomial model for the conditional distribution of the user number due to soft handoff; the results closely agree with simulation.

We develop a modelling method to calculate multi-cell, multi-user interference. An effective approach is developed to evaluate the performance of the cellular CDMA systems for both small and large number of users. It is found that the Gamma distribution can be applied to model multi-cell, multi-user interference. From the results obtained, it

can also be seen that imperfect hand-off and power control reduce the capacity of a system. Due to the effect of soft handoff operation, the multi-user interference approaches the Gaussian distribution very quickly, especially when the Activity Factor is large. The Gaussian model can therefore be applied in a lot of cases, but it is inaccurate for a very small number of users, especially when the Activity Factor is small. For mixed traffic, system capacity can be increased significantly if the high quality requirement of high rate users is reduced.

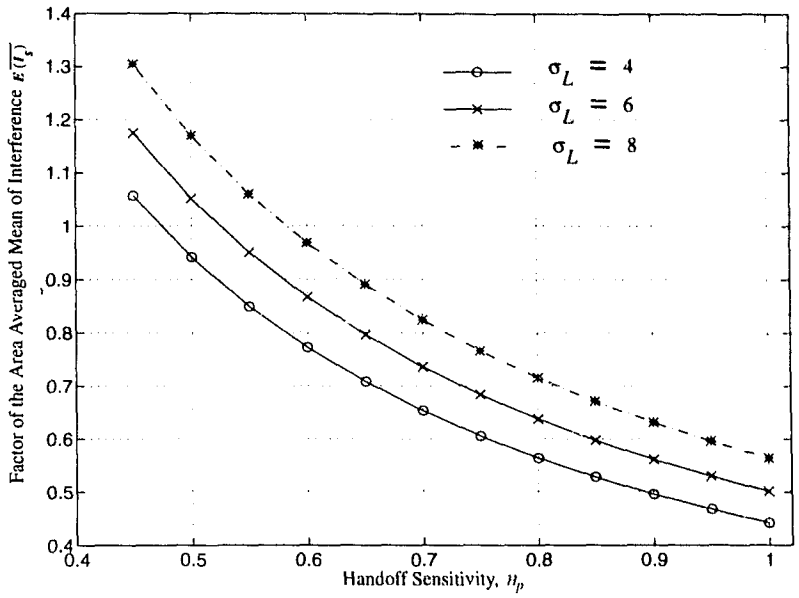

Fig. 4.2 The effects of the power control switching sensitivity on the mean factor of the inter-cell interference $\varepsilon(\overline{I_s})$.

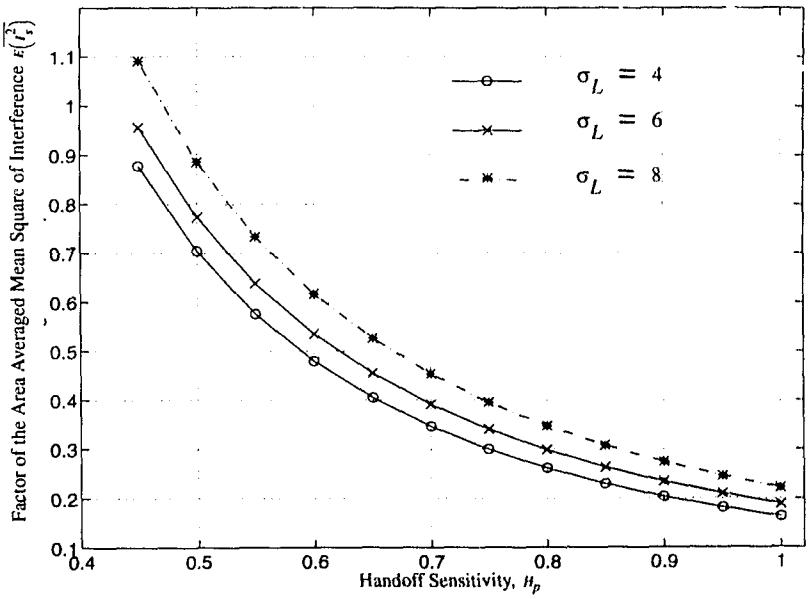

Fig. 4.3 The effects of the power control switching sensitivity on the factor of mean square of the inter-cell interference $\varepsilon(\overline{I_s^2})$.

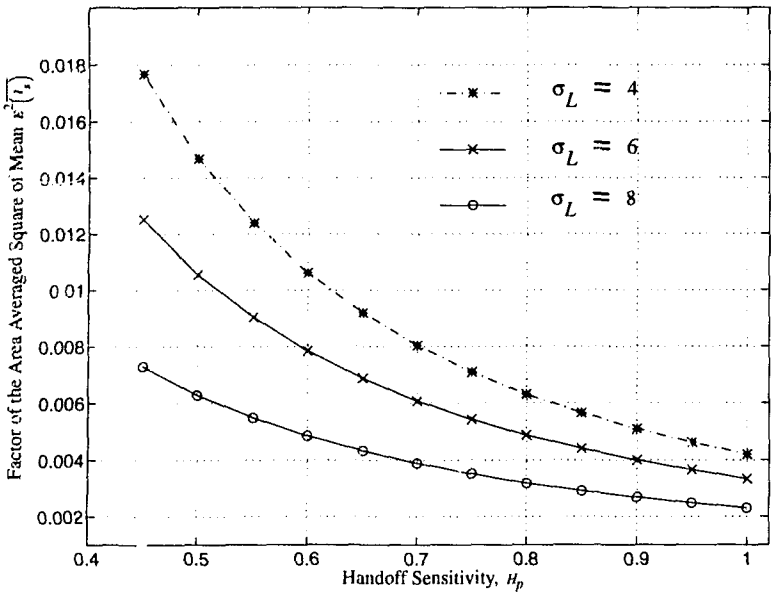

Fig. 4.4 The effects of the power control switching sensitivity on the factor of square of mean inter-cell interference $\varepsilon^2 \overline{(I_s)}$.

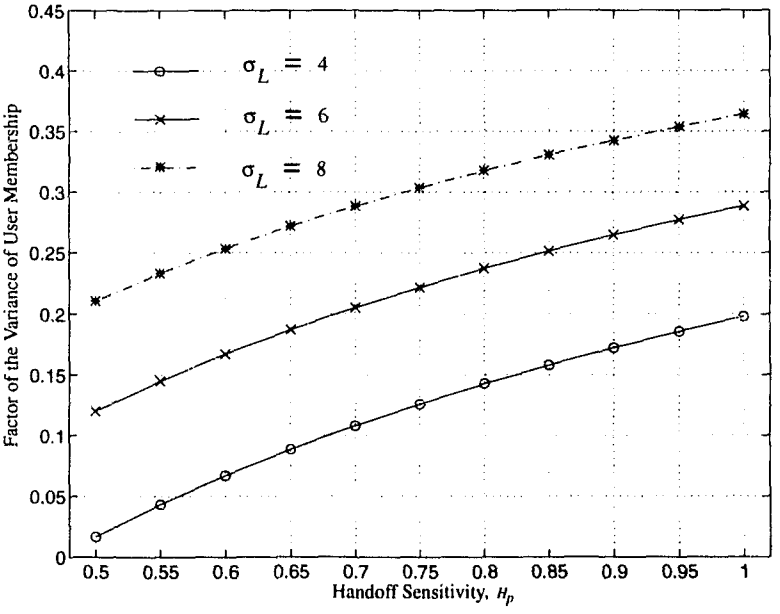

Fig. 4.5 The effect of power control switching on the user membership statistics.

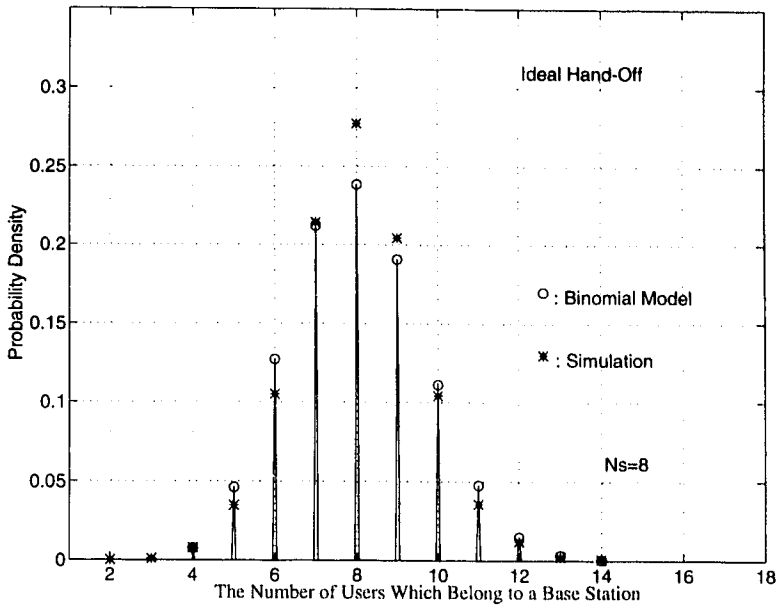

Fig. 4.6 Modelling and simulation results of the probability distribution of the number of users which belong to a base station with Ns=8.

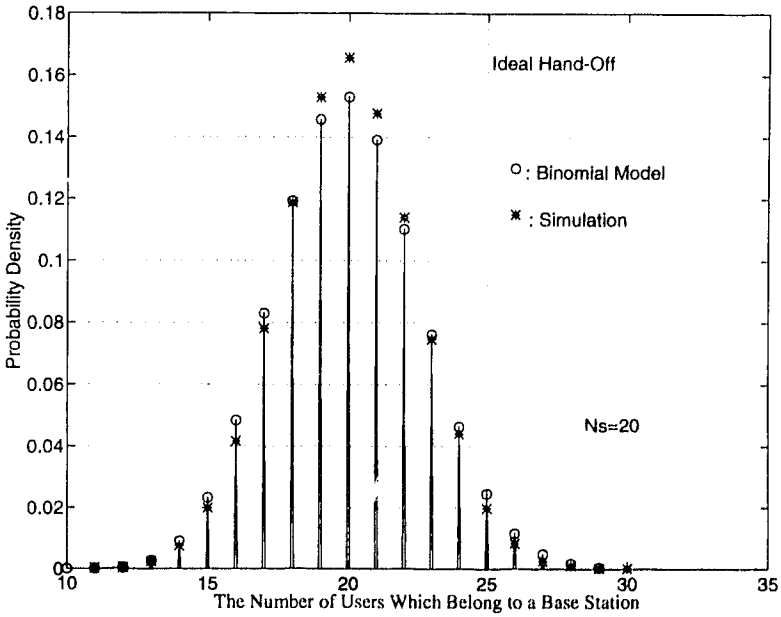

Fig. 4.7 Modelling and simulation results of the probability distribution of the number of users which belong to a base station with Ns=20.

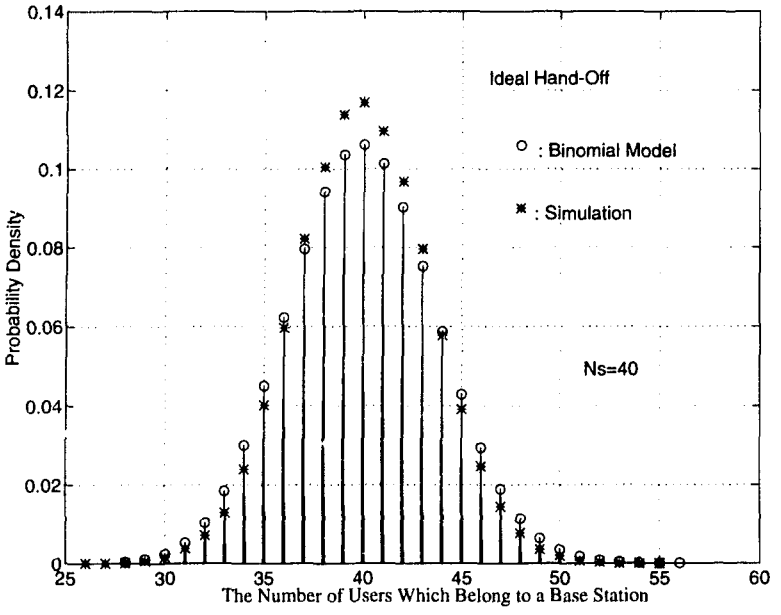

Fig. 4.8 Modelling and simulation results of the probability distribution of the number of users which belong to a base station with Ns=40.

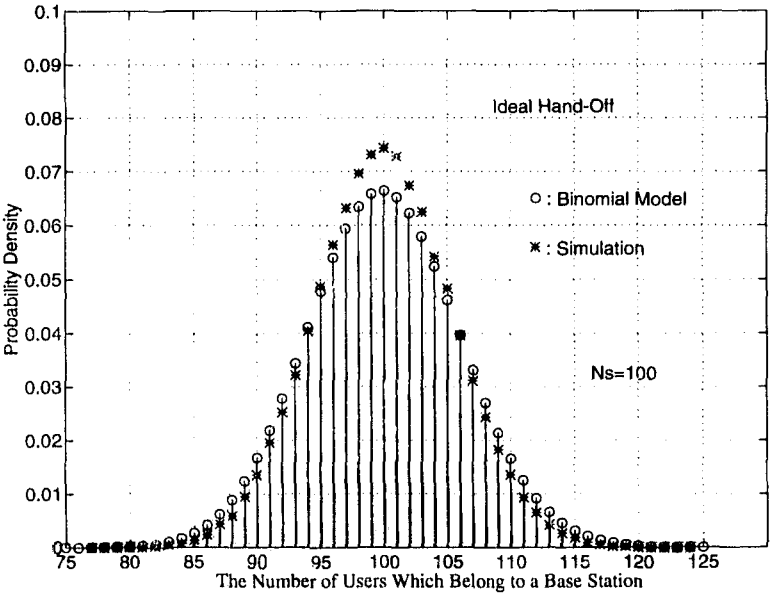

Fig. 4.9 Modelling and simulation results of the probability distribution of the number of users belonging to a base station with Ns=100.

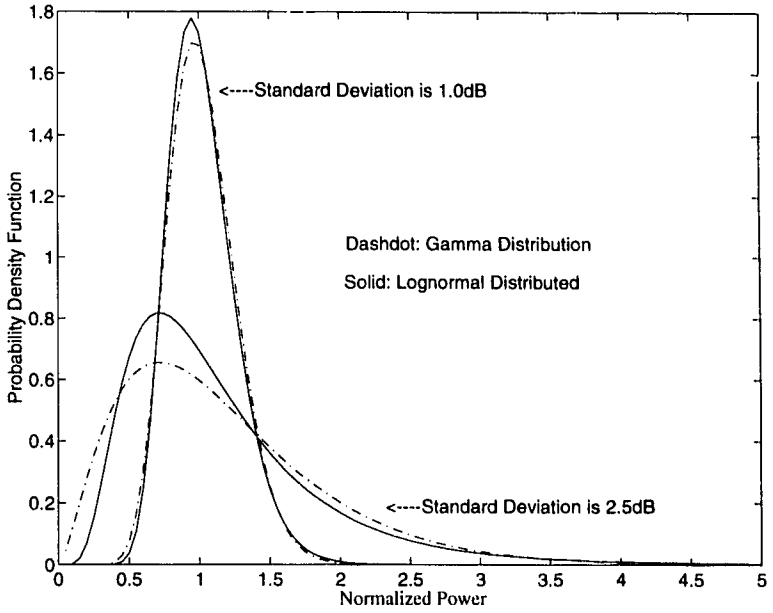

Fig. 4.10 Comparison of the Gamma PDF with lognormal PDF when they have the same mean and variance, and the standard deviation is small.

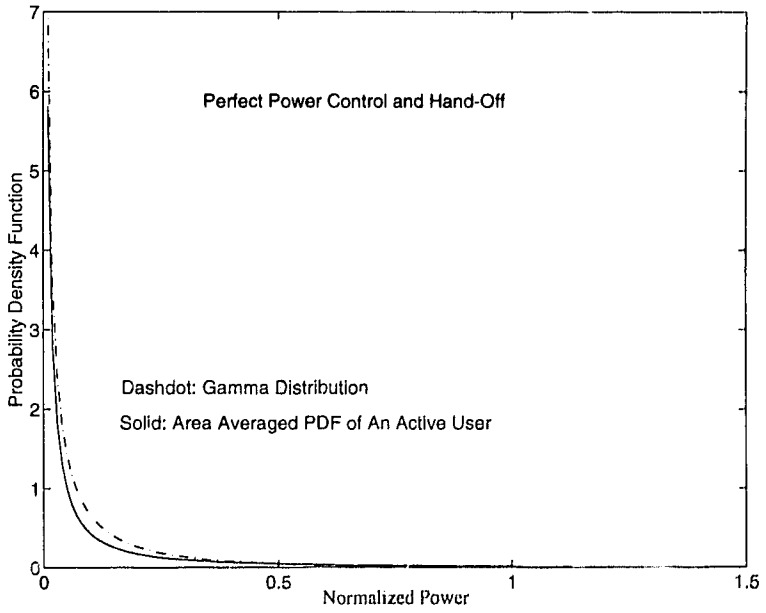

Fig. 4.11 Comparison of the area averaged PDF of an active user with the Gamma PDF. Both of them have the same mean and variance.

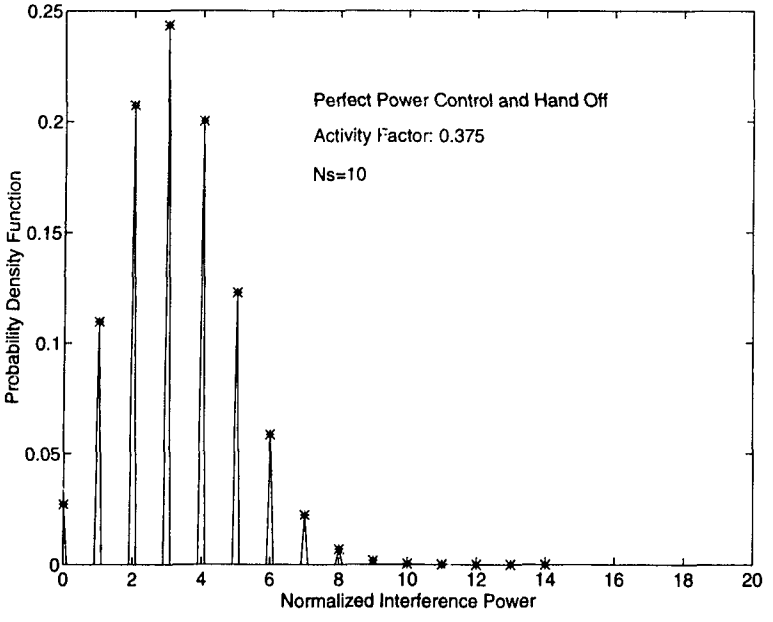

Fig. 4.12 The probability density function of intra-cell interference. Perfect power control and handoff assumed.

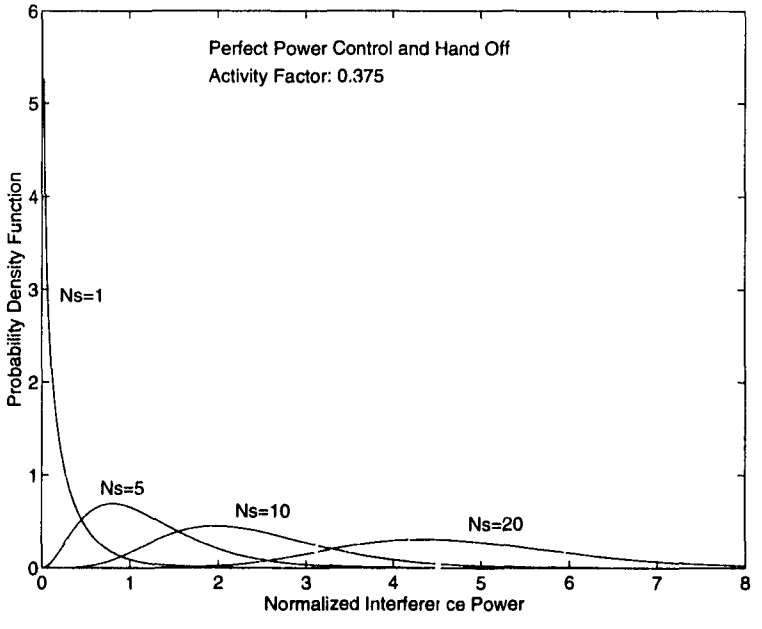

Fig. 4.13 The probability density function of inter-cell interference. Perfect power control and handoff assumed. Activity Factor is 0.375.

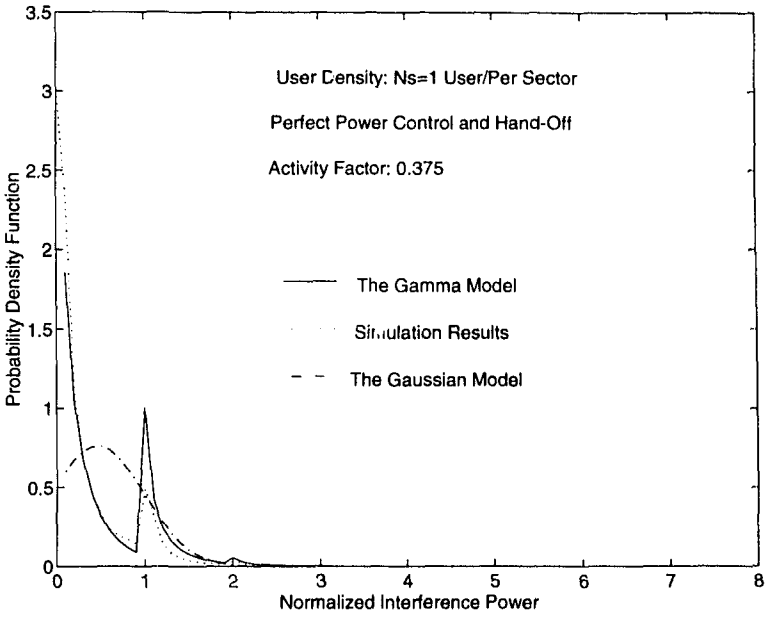

Fig. 4.14 Comparison of calculated PDF and simulation result for one user per sector. Perfect power control and handoff. Activity Factor is 0.375.

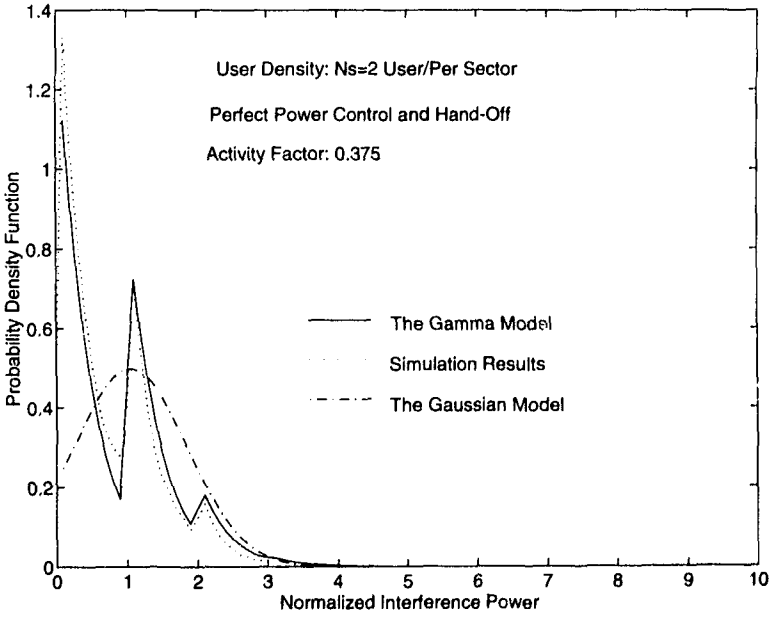

Fig. 4.15 Comparison of calculated PDF and simulation result for two users per sector. Perfect power control and handoff. Activity Factor is 0.375.

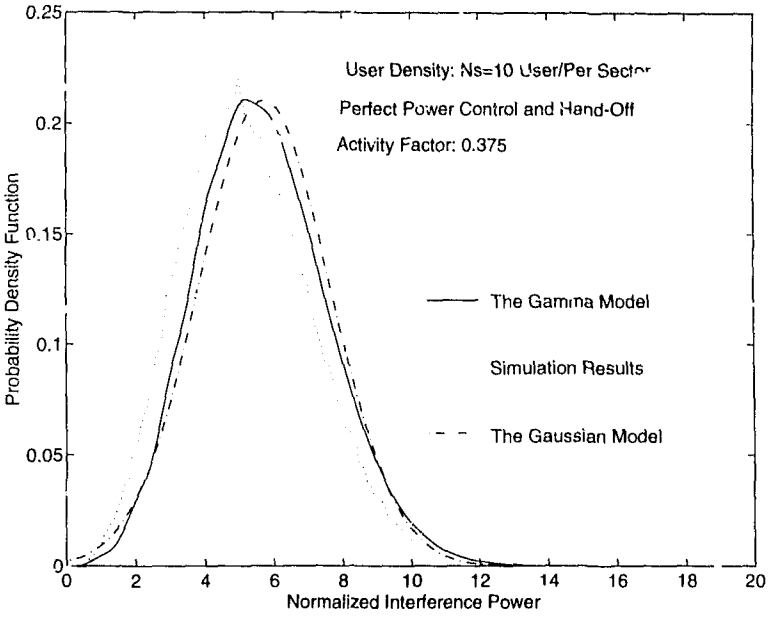

Fig. 4.16 Comparison of calculated PDF and simulation result for ten users per sector. Perfect power control and handoff. Activity Factor is 0.375.

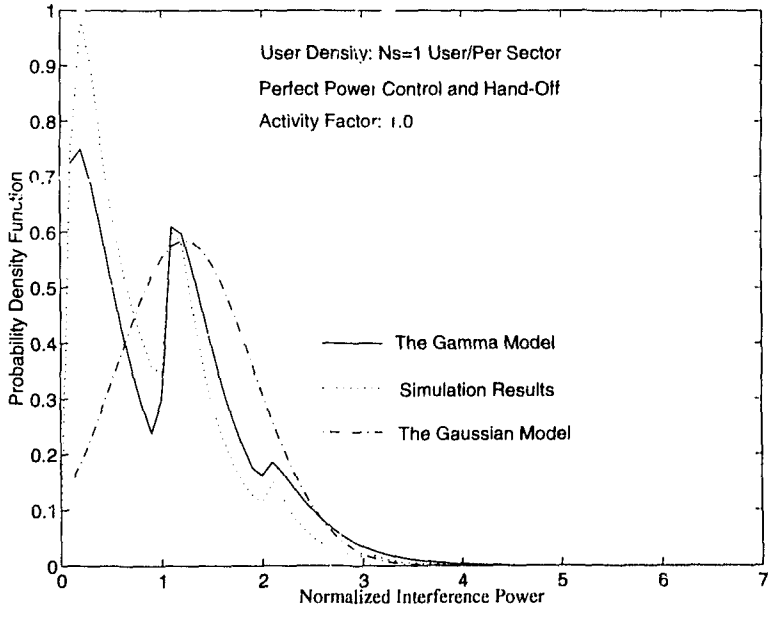

Fig. 4.17 Comparison of calculated PDF and simulation result for one user per sector. Perfect power control and handoff. Activity Factor is 1.0.

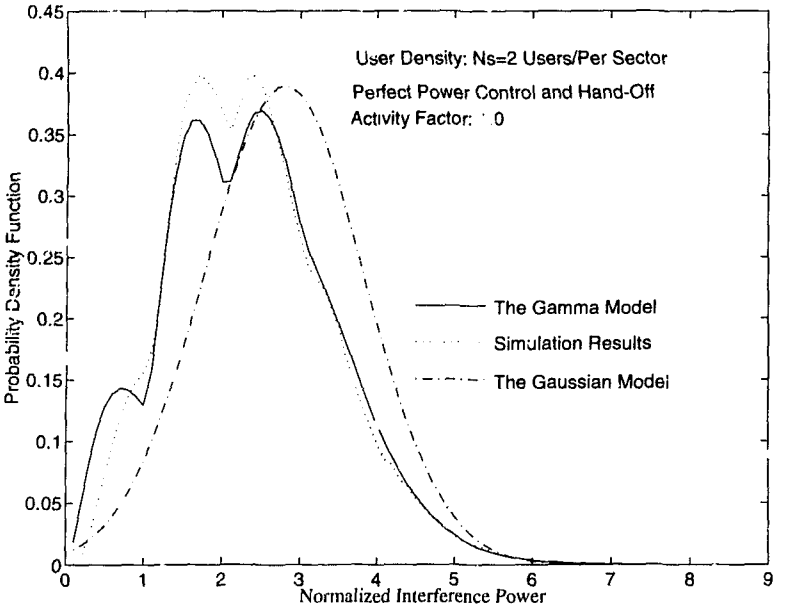

Fig. 4.18 Comparison of calculated PDF and simulation result for two users per sector. Perfect power control and handoff. Activity Factor is 1.0.

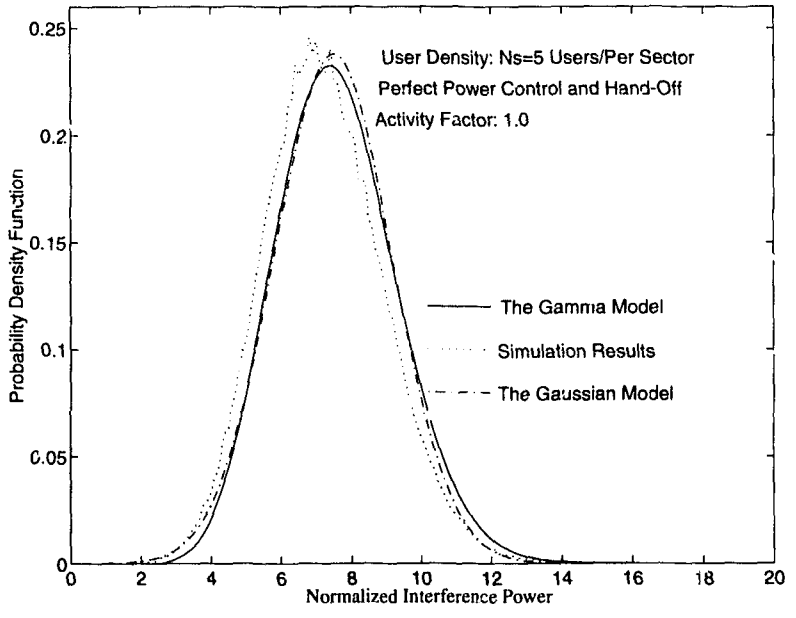

Fig. 4.19 Comparison of calculated PDF and simulation result for five users per sector. Perfect power control and handoff. Activity Factor is 1.0.

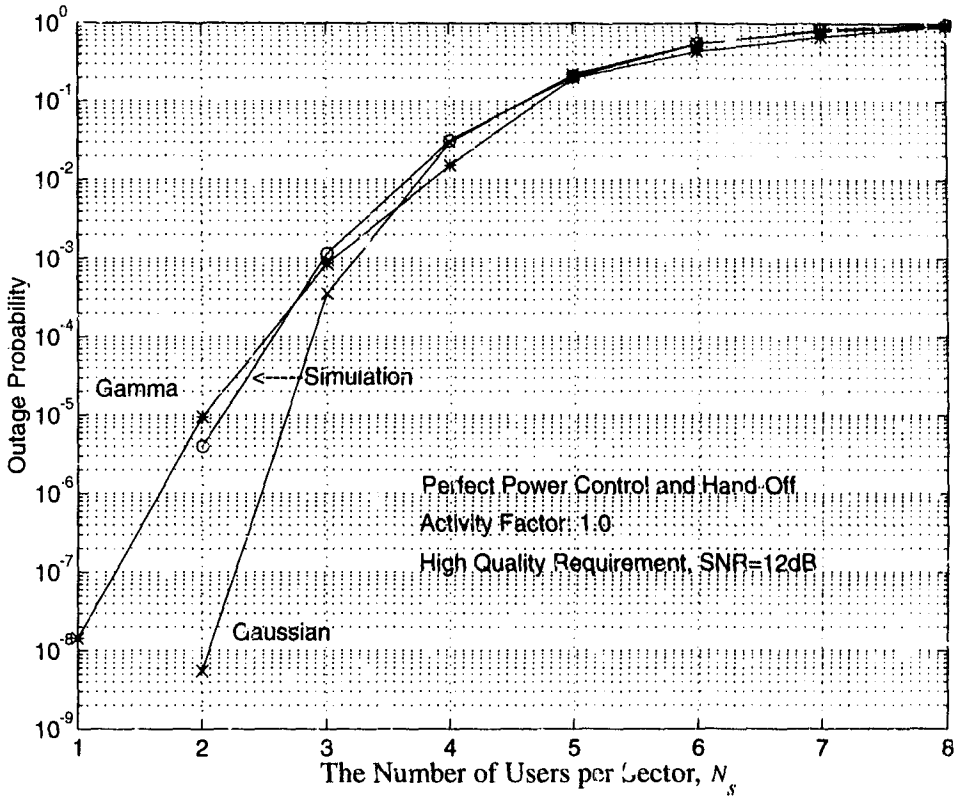

Fig. 4.20 The comparison of using the Gamma model, the Gaussian model and simulation to calculate outage probability.

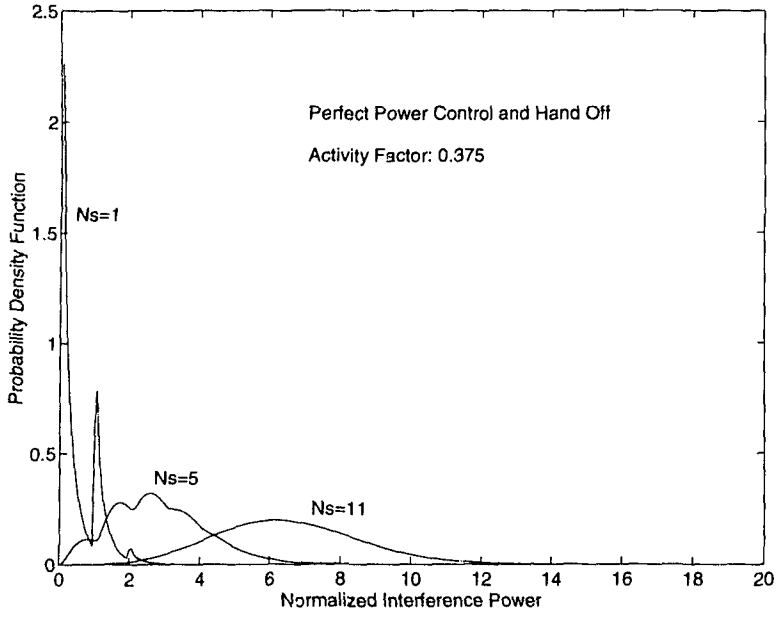

Fig. 4.21 The PDF of multi-user and multi-cell interference when the user number per sector is small. The traffic is voice only with an Activity Factor of 0.375.

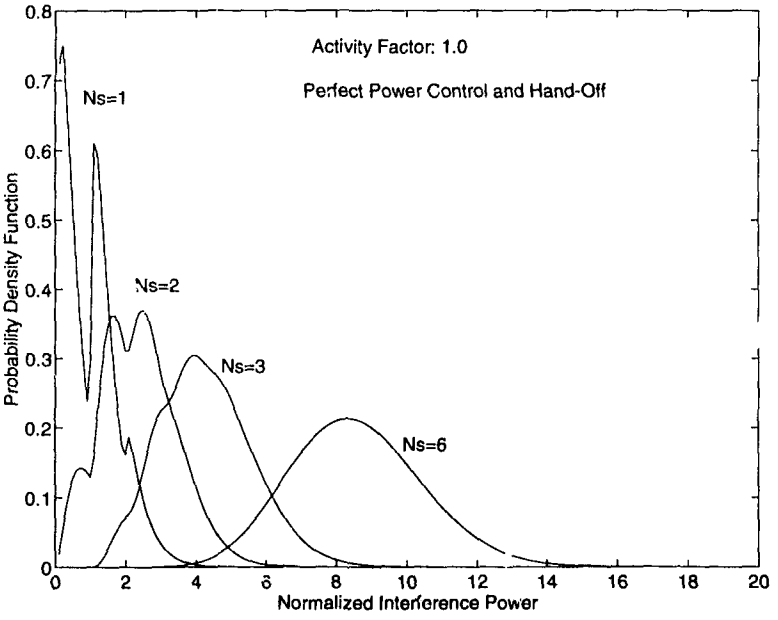

Fig. 4.22 The PDF of multi-cell and multi-user interference when there is single type of traffic with an Activity Factor of 1.0.

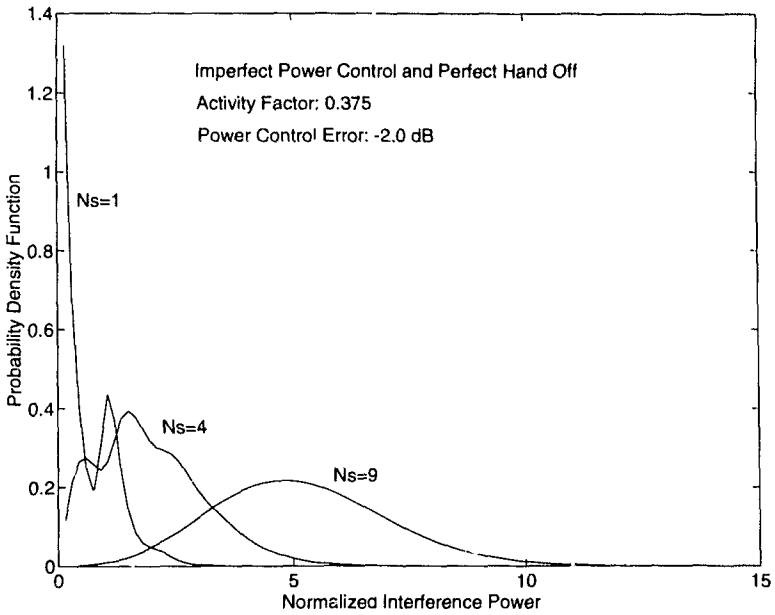

Fig. 4.23 The PDF of multi-user and multi-cell interference when power control error is small. The traffic is voice only with an Activity Factor of 0.375.

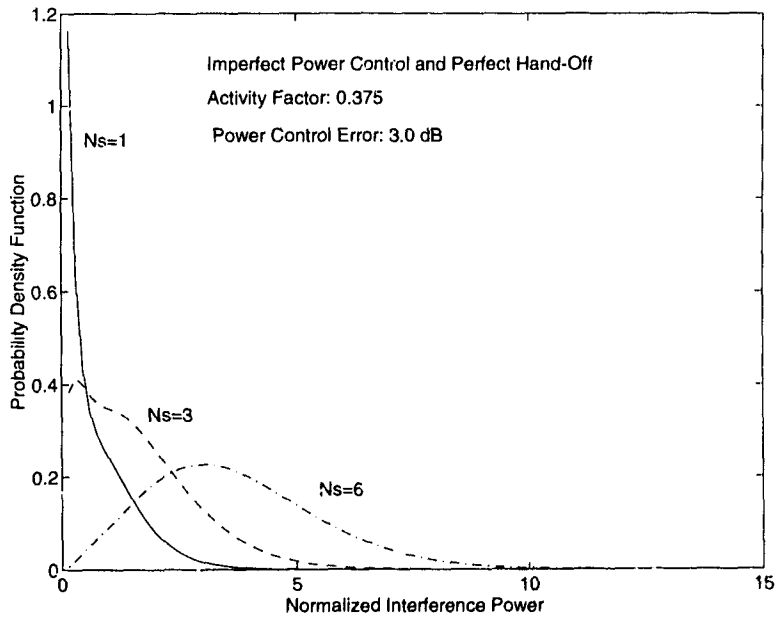

Fig. 4.24 The PDF of multi-user and multi-cell interference when power control error is large. The traffic is voice only with an Activity Factor of 0.375.

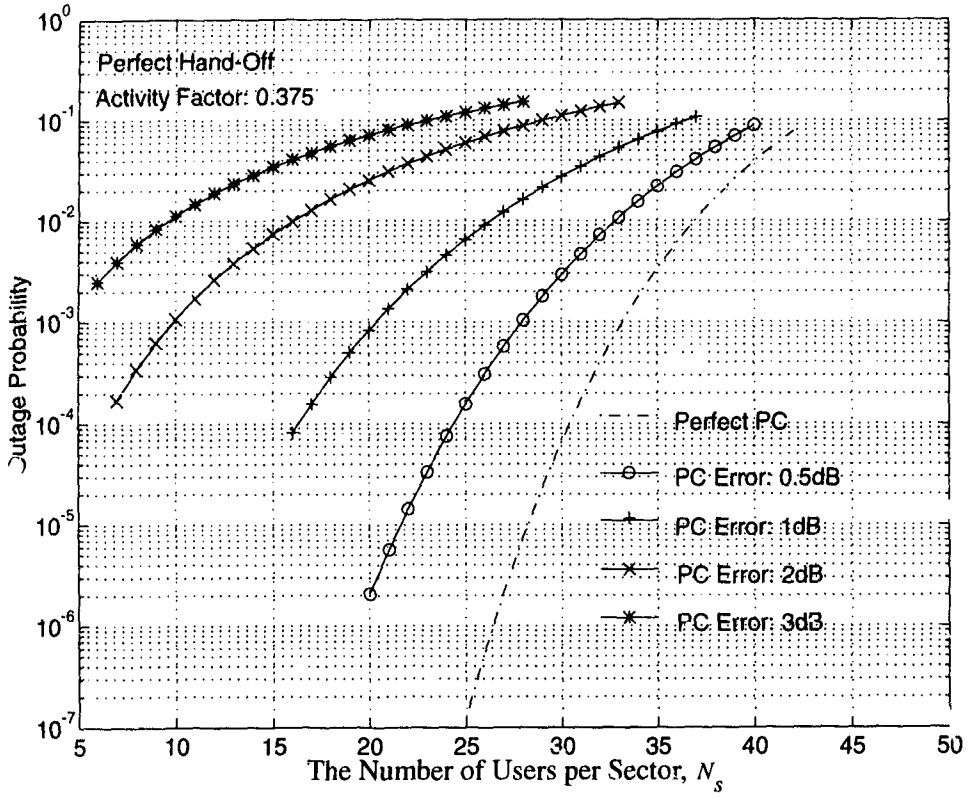

Fig. 4.25 The effects of imperfect power control (PC) on outage probability. The outage probabilities for different standard deviation of PC error are plotted. Single type of voice traffic is assumed. The quality requirement: Eb/No=7 dB.

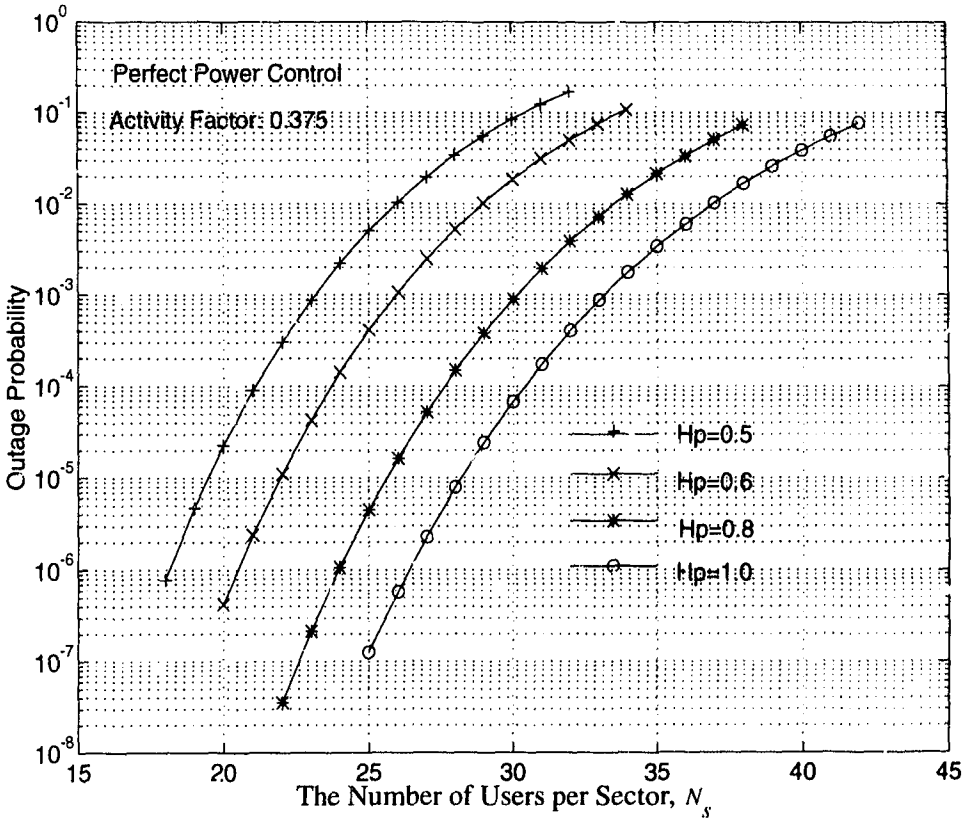

Fig. 4.26 The effects of imperfect handoff operation on outage probability. Voice traffic only. H_p = reference pilot power/highest pilot power. The quality requirement: Eb/ No=7dB.

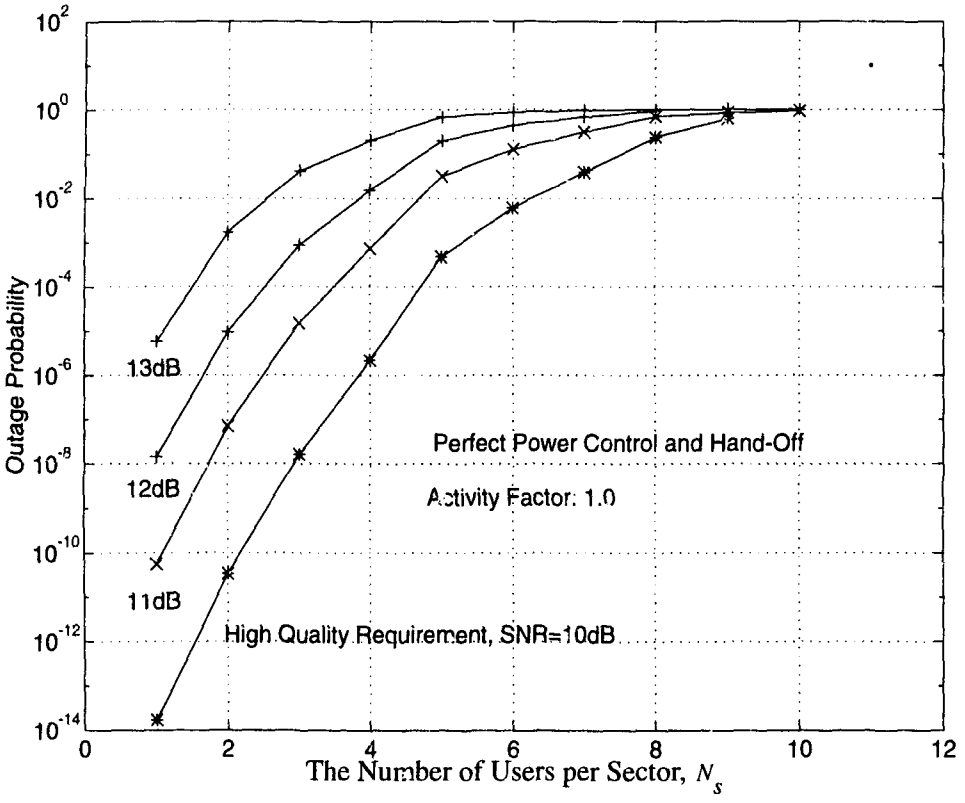

Fig. 4.27 The outage probabilities of single type of traffic with high service quality requirements. Activity Factor is 1.0. At the radio capacity of the system, number of users per sector is small.

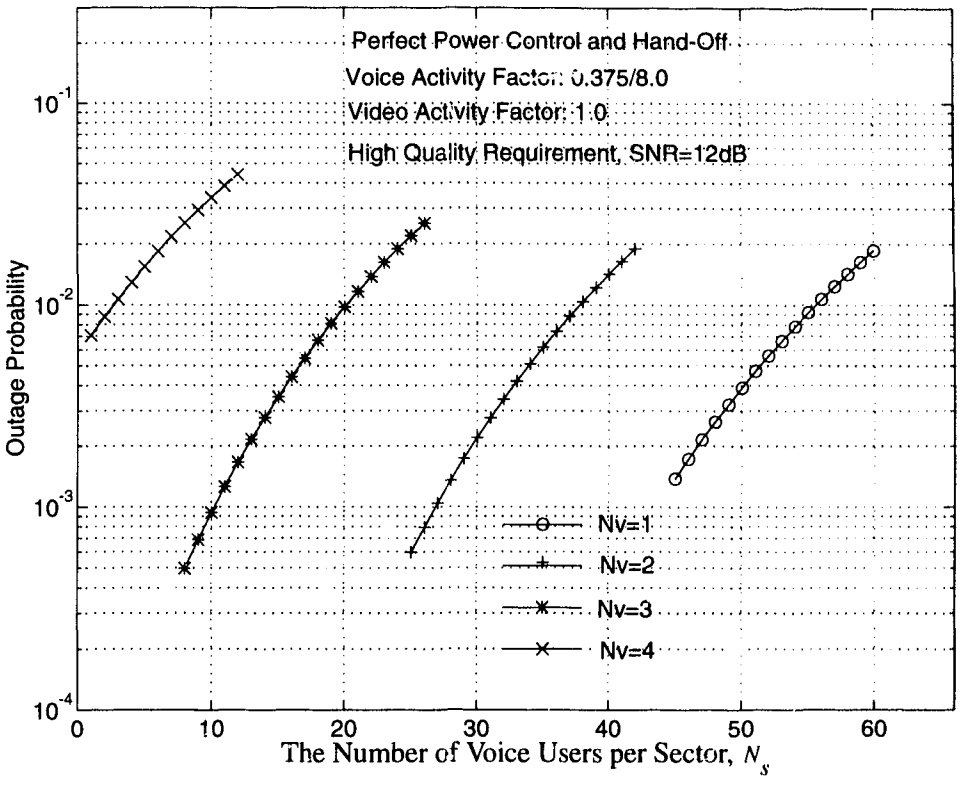

Fig. 4.28 The outage probabilities of video traffic given certain number of mixed voice and video users. Calculation is based on the quality requirement of video users. The quality requirement of Eb/No=12 dB is assumed for the video. Here, Nv is the number of video users.

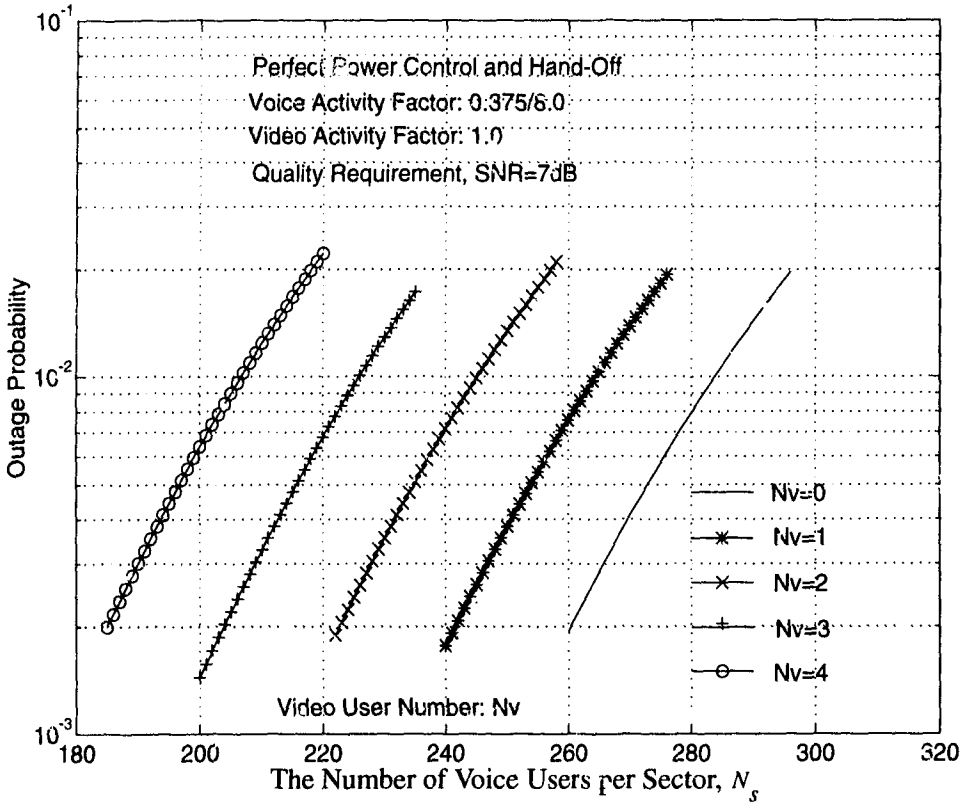

Fig. 4.29 The outage probabilities of voice traffic given certain number of mixed voice and video users. Calculation is based on the quality requirement of voice users. The quality requirement of Eb/No=7 dB is assumed for the voice. Here, Nv is the number of video users.

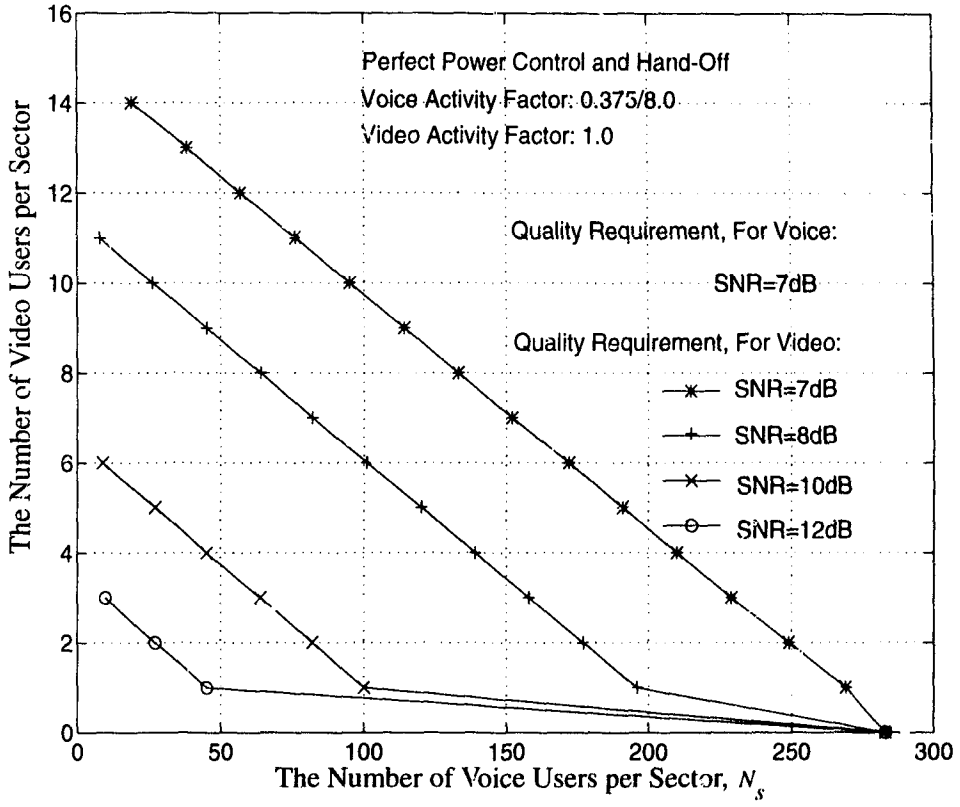

Fig. 4.30 The capacity of mixed traffic of voice and video. Calculation is based on the outage requirement of the video users assuming that efficient error control techniques are available for reducing the SNR requirement of video.

Chapter 5

Capacity and Quality of Service

5.1 Introduction

Capacity and quality of service are closely related. The capacity of a system is ultimately determined by the quality requirement of services. Normally, the capacity of a system can be measured by the radio capacity, the Erlang capacity and total throughput. It is generally accepted that the radio capacity is the maximum number of users which can be accommodated in a system while a specific quality requirement is met. When we evaluate the radio capacity, call arrival statistics are not considered. Normally, the radio capacity is obtained through an outage analysis For example, the radio capacity of a CDMA cellular system with voice users is the maximum number of users that can be accommodated with outage probability less than 0.01 [14].

For a multi-user cellular system, the measure of its effectiveness is not only the radio capacity which is the maximum number of users that can be served at one time, but also the peak load that can be supported with a given quality and with availability of service as measured by the blocking and dropping probability. The averaged traffic load in terms of average number of users requesting service resulting in a given blocking probability is defined as the Erlang capacity. The Erlang capacity of a CDMA cellular system is examined in [18]. We adopt the Poisson distribution as the call arrival statistics.

In general, for a system with heterogeneous traffic, we suggest using the criterion of total information throughput to measure the overall system capacity, in other words,

the total information bit rate handled by a cell. For convenience, we also use the packet throughput to measure the system capacity of a packet CDMA system.

In conventional FDMA or TDMA communication systems, a specific frequency or time slot is assigned to a user as a channel. In each channel, there is a corresponding transmission/reception mechanism at a base station. In a CDMA cellular system, although users all share a common spectral frequency allocation, there are separate modems or processors at a base station for each individual user. We define a modulation/demodulation and spreading/despreading mechanism for a specific user as a physical channel. In practice, there are always limited channel resources available at a base station. In addition, we would also like to reduce the complexity when we design a system.

Call blocking or dropping occurs when the number of calls arriving at a base station exceeds the number of available channels. To evaluate the required number of channels, we simply consider blocking and dropping together and assume a worst case scenario in which a call is dropped when there is no channel available for it. In addition to the outage or call blocking caused by interference, the call blocking and dropping caused by a limited number of channels also need to be investigated.

During a soft handoff, multiple channels are allocated to different base stations to perform cell site diversity [2]. Since in most cases the best reception of a mobile user comes from the base station with the strongest pilot to that user, the signal from this station is most important to the diversity selection. To ensure that the best base station always assigns a channel to the corresponding mobile, in addition to conventional soft handoff protocols, we propose a pilot assisted channel allocation method. With this method, a user has the priority to hold a channel from a base station to which it belongs. The rest of the channels are assigned to users not belonging to this station for cell site diversity following conventional protocols. The purpose of the pilot assisted channel allocation is to reduce the channel number required at a base station.

Since in the next generation of multi-media CDMA systems, both stream type and

date type traffic could be transmitted in the form of packets, the performance of a packet CDMA system is of great interest. To examine the effect of a cellular environment on packet CDMA, we evaluate the performance of a slotted ALOHA packet CDMA cellular system. The performance of a system with finite population is evaluated. The original ALOHA protocol works based on collision. For a packet CDMA system, its capacity is largely determined by the capture ability of CDMA and the medium access sublayer protocol which works based on accepted interference level.

The rest of this chapter is organized as follows. The second section is devoted to a discussion on the radio capacity and the Erlang capacity of a cellular CDMA system. In the third section, the effect of a limited number of channels on the quality of service is analyzed. The performance of a packet CDMA cellular system is evaluated in the fourth section. The last section presents summary and remarks.

5.2 Radio Capacity and the Erlang capacity

The radio capacity can be obtained through outage probability analysis. Since in Chapter 4, the effect of imperfect handoff and power control was examined, in this chapter, we assume that soft handoff and power control is perfect without loss of the generality of our results. A large amount of work have been down in capacity evaluation [14], [48], [49]. The Erlang capacity of a CDMA cellular system was evaluated in [18]. We may also obtain a closed form expression for the radio capacity following the procedure suggested in [18].

The number of active users is normally quite large at the capacity of a system. If the user number is large enough, we can apply the central limit theorem [14], [17], [18] and adopt the Gaussian approximation for simplification. With the Gaussian approximation and perfect power control, the outage probability obtained in Chapter 4 is

$$p_{out} = \frac{1}{2}\mathrm{erfc}\left(\frac{(t - M(I_t))}{\sqrt{2Var(I_t)}}\right) \tag{5.1}$$

where

$$t = \frac{PG}{(E_b/N_0)_{QR}} - \sigma_T^2, \tag{5.2}$$

$M(I_t)$ and $Var(I_t)$ are the mean and variance of the total interference, respectively. They are given in Chapter 3 for perfect handoff and power control. If handoff and power control are perfect we have

$$M(I_t) = \left(N_s - \frac{1}{3}\right) \cdot \upsilon + N_s \cdot \upsilon \cdot \overline{E(I_s)} \tag{5.3}$$

and

$$Var(I_t) = (3N_s - 1)\left(\frac{1}{3}\upsilon - \upsilon^2 \overline{E^2(\varphi)}\right) + N_s \cdot \left(2\upsilon \overline{E(I_s^2)} - \upsilon^2 \overline{E^2(I_s)}\right). \tag{5.4}$$

If the average number of users per sector, N_s, is sufficiently large, Equations (5.3) and (5.4) can be simplified to

$$M(I_t) \approx N_s \cdot \upsilon \cdot \left(1 + \overline{E(I_s)}\right) \tag{5.5}$$

and

$$Var(I_t) \approx N_s \cdot \upsilon \cdot \left(1 - 3\upsilon \overline{E^2(\varphi)} + 2\overline{E(I_s^2)} - \upsilon \overline{E^2(I_s)}\right) \tag{5.6}$$

We denote that

$$g_m = \upsilon\left(1 + \overline{E(I_s)}\right) \tag{5.7}$$

and

$$g_v = \upsilon \cdot \left(1 - 3\upsilon \overline{E^2(\varphi)} + 2\overline{E(I_s^2)} - \upsilon \overline{E^2(I_s)}\right). \tag{5.8}$$

From Equation (5.1), we have that

$$\left(\text{erfc}^{-1}(2p_{out})\right)^2 = \frac{(t - N_s \cdot g_m)^2}{2N_s \cdot g_v} \quad .$$

where $\mathrm{erfc}^{-1}(x)$ is the inverse function of the $\mathrm{erfc}(x)$. Let $\psi = \mathrm{erfc}^{-1}(2p_{out})$, we then obtain a quadratic equation in N_s:

$$2N_s \cdot \upsilon \cdot g_v \psi^2 = (t - N_s \cdot \upsilon \cdot g_m)^2 . \tag{5.9}$$

Solving Equation (5.9), we find the radio capacity to be

$$N_s = \frac{1}{g_m}\left(\frac{\psi^2 g_v + t g_m}{2} - \psi \sqrt{g_v (\psi^2 \cdot g_v + 2t \cdot g_m)} \right) . \tag{5.10}$$

Now we consider the effect of call arrival statistics. We assume that call arrival is Poisson distributed with a mean arrival rate λ (calls/s) and exponential service time $1/\mu$ [10], [18]

$$p_k(k) = \frac{(\lambda/\mu)^k}{k!} e^{-\lambda/\mu} \tag{5.11}$$

where k is the number of arrived active users per sector in service. Both the mean and variance of k are λ/μ. Note that $\lambda/\mu = N_s$ is just the average number of users per sector. It is also called the offered traffic.

Within the reference cell, taking into account the number of the active interfering calls in service, we have k active users at k different locations at each time instant. In the enlarged cell, the total intra-cell interference at each instant is

$$I_{ita} = \sum_{i=1}^{k} \Phi_v \varphi_i = \sum_{i=1}^{k} I_{rf,i} \tag{5.12}$$

where φ_i has a probability of $p(\varphi_i | r_{0i}, \theta_i)$ to be 1, Φ_v represents user activity and $I_{rf,i}$ is the intra-cell interference from one active user. Over sufficiently long period of time, active users appear at every location in the area A_0 which is covered by the reference base station. Therefore, I_{ita} is the sum of k statistically independent and identically distributed random variables, where k is itself a random variable. The variance of I_{ita} is

then given by [18], [50]

$$D(I_{ita}) = E(k)D(I_{rf,i}) + D(k)E^2(I_{rf,i}) \cdot \tag{5.13}$$

where

$$E(I_{rf,i}) = \upsilon\overline{E(\varphi)} \tag{5.14}$$

is the area averaged mean of the intra-cell interference from one active user and

$$D(I_{rf,1}) = \upsilon E\overline{(\varphi^2)} - \upsilon^2 E^2\overline{(\varphi)} \tag{5.15}$$

is the area averaged variance of the intra-cell interference with one active user in the enlarged cell area.

Since k in Equation (5.12) is a Poisson random variable in the enlarged cell area, we have that the mean and variance of the number of interfering users are given by $E(k) = D(k) = 3N_s - 1$. In addition, call arrival, membership switching and user activity are independent random variables. If the active users are uniformly distributed, the mean and variance of intra-cell interference can be expressed as

$$E(I_{ita}) = \left(N_s - \frac{1}{3}\right) \cdot \upsilon. \tag{5.16}$$

and

$$D(I_{ita}) = (3N_s - 1)\upsilon\ \overline{E(\varphi^2)} \cdot \tag{5.17}$$

For calculating the inter-cell interference, we consider that the number of users belonging to the other cells is much larger than the number of users within the reference cell and it is still assumed to be Poisson distributed. Using Equations (3.33), (3.34), (3.38) and a similar approach to evaluating $D(I_{ita})$, we have

$$D(I_{Rite}) = 2N_s\upsilon E\left(I_s^2\right) \tag{5.18}$$

and the mean of inter-cell interference is given by Equation (3.35).

Finally, $M(I_t)$ and $Var(I_t)$ can be obtained from Equations (3.49) and (3.50), and the Erlang capacity is further obtained from Equation (5.10) with

$$g_m = \upsilon\left(1 + E\overline{(I_s)}\right) \tag{5.19}$$

and

$$g_v = \upsilon \cdot \left(1 + 2E\overline{(I_s^2)}\right). \tag{5.20}$$

In Fig. 5.3, we plot the Erlang capacity versus the power control handoff sensitivity, given different processing gains and standard deviations of the lognormal shadowing. As H_p decreases from 1.0 to 0.5, the capacity decreases by about 30%.

In a system with integrated services, to support the various source rates and to simplify the system design, users with different rates can be transmitted at one or several line rates [3], [19]. How to chose the line rate becomes a design issue. More details will be discussed in Chapter 6. Here we investigate the effects of the processing gain and the ACF on the system capacity to look into one of the factors impacting the choice of the line rate. From Fig. 5.4 we can see that for a type of low rate user, e.g. voice user with an ACF of 0.375, if the processing gain is increased by 8 times from 156 to 1250, the capacity will increase by a factor of more than 10 from 31 to 330 Erlang for $H_p = 1.0$. Comparing Fig. 5.5 with Fig. 5.4, if the ACF is reduced by a factor of 8 so that 1/ACF increases from 2.7 to 21.6 for a voice user, the increase in capacity is about 8 times from 31 to 252 Erlang given that the processing gain is unchanged at 156. This result shows that more capacity can be obtained if the PG is increased instead of the 1/ACF.

When the bandwidth available is increased, the capacity of a CDMA system will be increased through an increase in the PG or a decrease of the transmission ACF by choosing a different transmission line rate. To further show how the PG and the ACF affect the capacity, we define the *processing efficiency* as the system capacity divided by PG, and *activity efficiency* as the system capacity divided by 1/ACF. The results plotted in Fig.

5.6 and Fig. 5.7 show that the capacity increases nonlinearly with increasing PG, but the capacity increases almost linearly with the increase of 1/ACF. A larger PG improves capacity more efficiently.

5.3 The Effect of Limited Number of Channels on QOS and Capacity

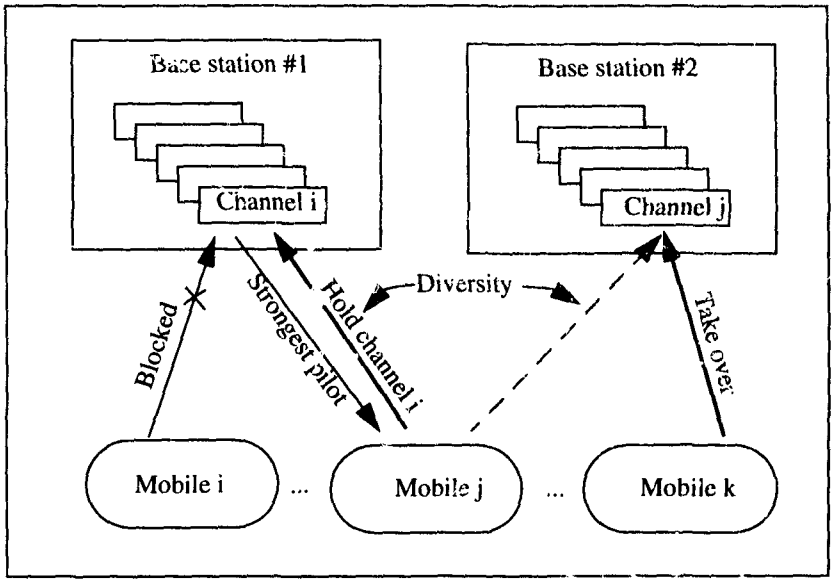

Fig. 5.1 Pilot assisted channel allocation.

A channel at a base station consists of a modulation/demodulation and spreading/ despreading mechanism for a user. If the closest three base stations are always listening to a mobile for diversity, three channels have to be assigned for each mobile. The channel number required at a base station is $3N_s$ per sector. Since the performance of cell site diversity depends on the best reception of one base station, the most important channel is the one at the reference base station. If the channel allocation is perfect, the minimum

number of channels required is determined by membership statistics. With pilot assisted channel allocation, priority is assigned to a mobile to hold a channel at a base station from which the mobile receives the highest pilot power. Then we can determine the minimum channel number required according the following steps:

The call dropping rate is related to the user membership statistics and the call arrival statistics. We adopt the Poisson arrival model. If there are k active users per sector in service, k is Poisson distributed

$$p_k(k) = \frac{N_s^k}{k!} e^{-N_s}. \tag{5.21}$$

Given that there are k active users (or calls) per sector in the soft handoff system, the conditional distribution of the user number per sector at a base station can be given by applying the Equations (3.43), (4.33), (4.34) and (4.35)

$$Var(m|k) = 3k \cdot \left(\overline{E(\varphi^2)} - E^2\overline{(\varphi)} \right), \tag{5.22}$$

$$N_{rm}(k) \approx k - \mathrm{int}\left(\frac{Var(m|k)}{1-p_{bl}} \right), \tag{5.23}$$

$$N_{ef}(k) = 3k - 3N_{rm}(k), \tag{5.24}$$

and

$$p_m(m|k) \approx \binom{N_{ef}(k)}{m} p_{bl}^m (1-p_{bl})^{N_{ef}(k)-m} \tag{5.25}$$

where $p_{bl} = 1/3$. Considering the call arrival statistics, we have that

$$p_k'(k) = \frac{(N_s(1-p_{dr}))^k}{k!} e^{-N_s(1-p_{dr})} \tag{5.26}$$

where p_{dr} is the call dropping rate which we have defined before, and

$$p_m(m) = \sum_{k=0}^{N_{kb}} p_m(m|k) \cdot p_k'(k) \tag{5.27}$$

where N_{kb} is obtained through the following equation

$$N_{ch} = N_{kb} - \text{int}\left(\frac{Var(m|N_{kb})}{1 - p_{bl}} \right). \tag{5.28}$$

Finally, the call dropping rate p_{dr} is an unknown of the following equation

$$p_{dr} = 1 - \sum_{k=0}^{N_{kb}} \sum_{m=N_{rm}(k)}^{N_{mb}} \binom{N_{ef}(k)}{m - N_{rm}(k)} \cdot p_{bl}^{\,m - N_{rm}(k)} \cdot (1 - p_{bl})^{N_{ef}(k) + N_{rm}(k) - m} \times \frac{(N_s(1 - p_{dr}))^k}{k!} e^{-N_s(1 - p_{dr})} \tag{5.29}$$

where

$$N_{mb} = \min(N_{ef}(k) + N_{rm}(k), N_{ch}) \cdot \tag{5.30}$$

Solving the nonlinear Equation (5.29), we get the call dropping rate, p_{dr}. The throughput or current traffic supported by the system after a call dropping is then

$$S_c = N_s(1 - p_{dr}) \cdot \tag{5.31}$$

Note that from Equation (5.29), the call dropping rate depends on the current throughput which is in equilibrium after a part of the call traffic drops from the offered traffic.

Fig. 5.8 shows that with a finite number of available channels, the call dropping rate increases significantly with offered traffic. If there are 100 channels, traffic of at most 60 Erlangs can be supported if a dropping rate less than 10^{-4} is to be ensured. If there are 200 channels available, 140 Erlangs can be supported, and so on. As shown in Fig. 5.9, there is little increase in throughput when the offered traffic exceeds the channel number. Note that the throughput is the mean number of the Poisson distributed simultaneous calls in service.

Since call dropping is one of the most important factors affecting quality of service, to ensure the quality of service we must consider not only the outage probability but also the call dropping rate. We propose a constraint on the outage probability and the dropping rate to jointly evaluate their effect on capacity:

$$p_{out} = p_0 10^{-wp_{dr}} \tag{5.32}$$

where $p_0 = 0.01$ and w is a weighting factor which depends on the relative importance of p_{dr} to service quality. We take $w = 1000$. The system capacity can be obtained by jointly solving the Equations (5.10) (5.29) and (5.32). In Fig. 5.10 and Fig. 5.11, we show the traffic which can be supported by the system with an acceptable service quality. Since we take $p_0 = 0.01$, if we choose w properly in Equation (5.32), the dropping rate will also be restricted to be below the level which we want. Both Fig. 5.10 and Fig. 5.11 show that when the channel number is very small, the capacity is dominated by the dropping rate, and when the channel number is large, the capacity is dominated by the outage requirement. In the case shown in Fig. 5.10, the minimum channel number required to ensure a maximum capacity is about 220 which is about $1.4N_s$. If the PG is doubled, Fig. 5.11 shows that the minimum channel number required is approximately 420 which is about $1.3N_s$. It is much smaller than $3N_s$.

5.4 Capacity of Packet CDMA

To provide insight on the performance of packet CDMA in a cellular environment, we examine a packet CDMA cellar system in this section. A micro-cellular environment is assumed. Since in a micro-cellular environment a strong line of sight often exists, we assume synchronization is available for a slotted packet system. Perfect fast power control is assumed. Slow fading, lognormal shadowing and path loss can be eliminated by power control. Correlation detection and DPSK are employed. BCH coding is used for

error correction/detection, and the automatic repeat request (ARQ) is employed for packet retransmission. In this section, a slotted ALOHA packet CDMA cellular system is studied. Fig. 5.2 shows how the packets are transmitted. Due to CDMA, the capture ability is increased, more than one packet can be successfully transmitted within the same slot.

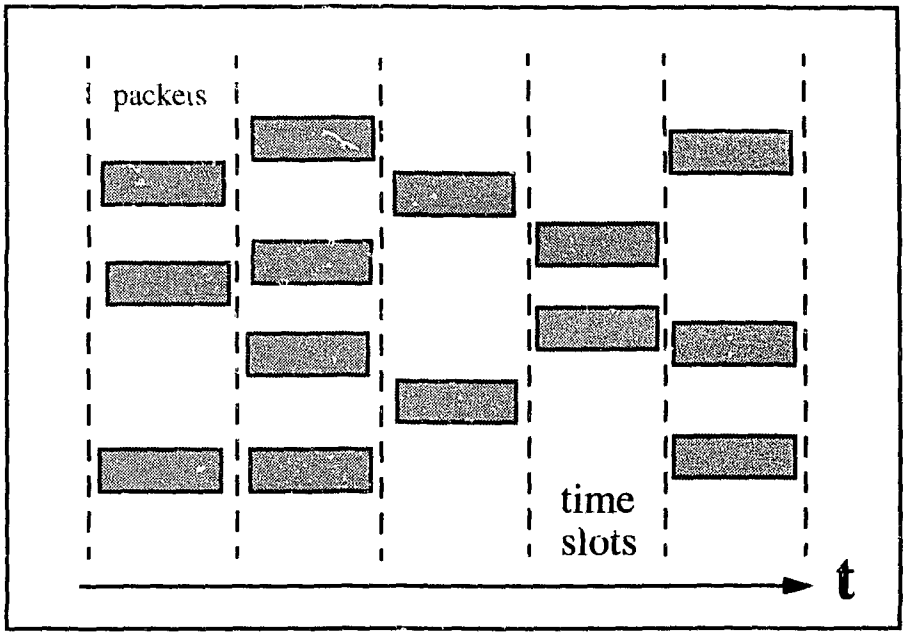

Fig. 5.2 Slotted packet CDMA

In a micro-cellular system, there are a finite number of portables communicating with a base station. The arrival of packets can be modelled as a finite state Markov process which is general but very complicated. The packet arrivals in any given slot will have a steady state. For simplicity, we adopt the binomial model for the packet arrival statistic [40], [51]. In this model, new transmission attempts and re-transmission attempts are assumed to be the same. From [51], the conditional probability distribution of the number of the packets per slot is given by

$$f_N(m|N) = \binom{N}{m} p_a^m (1-p_a)^{N-m} \qquad m \le N \tag{5.33}$$

where N is number of currently effective subscribers per sector in the reference cell, and p_a is the probability of a subscribe transmitting a packet, which equals the packet retransmission probability. Due to soft handoff, N is also a random variable. Once again, by using the binomial model proposed in Chapter 4, we modify Equation (4.33) to

$$p_N(N) = \binom{N_{ef}}{N - N_{rm}} p_{bl}^{N-N_{rm}} (1-p_{bl})^{N_{ef}+N_{rm}-N} \tag{5.34}$$

where N_{ef} and N_{rm} can be obtained by using Equations (4.34) and (4.35). Then the probability distribution of the number of packets per slot per sector is

$$f_m(m) = \sum_{N=N_{rm}}^{N_{ef}+N_{rm}} f_N(m|N)\, p_N(N) \,. \tag{5.35}$$

Due to employing CDMA techniques, the capture ability of a slotted ALOHA system is improved significantly. In a slotted ALOHA packet CDMA system, the throughput is the mean number of successful transmissions per time slot. Thus,

$$\begin{aligned} S_p &= \sum_{m=1}^{N} m f_m(m)\, p(c|m) \\ &= \sum_{N=\,}^{N_{ef}+N_{rm}} \sum_{m=1}^{N} m \cdot \binom{N}{m} p_a^m (1-p_a)^{N-m} \\ &\quad \times \binom{N_{ef}}{N-N_{rm}} p_{bl}^{N-N_{rm}} (1-p_{bl})^{N_{ef}+N_{rm}-N} p(c|m) \end{aligned} \tag{5.36}$$

where $p(c|m)$ is the probability of successful transmission of a packet given that there are m packets per slot.

The probability of a successful transmission is determined by spread spectrum sig-

nalling, error control techniques and cellular environment. To get $p(c|m)$, we first examine the bit error probability. To simplify the problem and to show the effect of cellular environment, soft handoff and power control on packet CDMA, here we assume the channel condition is very good, so that multipath fading, lognormal shadowing and the path loss can be compensated perfectly by fast power control for the reference cell. Following [52]- [54], we obtain the E_b/N_o as

$$\frac{E_b}{N_o} = \frac{PG}{\frac{m}{3} + \sigma_T^2 + \frac{I_{Pite}}{3}} \tag{5.37}$$

where m is the number of packets per slot from the subscribers belonging to the reference base station, and I_{Pite} represents the interference from the other cells. We assume that I_{Pite} is a Gaussian distributed random variable. Its mean and variance can be obtained by modifying Equations (4.14) and (4.18) to yield

$$E(I_{Pite}) = N_s p_a \cdot E(I_{pce}) \cdot E\overline{(I_s)} \tag{5.38}$$

and

$$D(I_{Pite}) = N_s p_a \cdot \left(2\overline{E(I_s^2)} E\left(I_{pce}^2 \right) - E^2\overline{(I_s)} E^2(I_{pce}) \right) \tag{5.39}$$

where N_s is the average number of users per sector, p_a is the packet transmission probability of an active user and $N_s p_a$ is the offered traffic.

Since the BER is determined by E_b/N_o and the modulation scheme employed, the conditional bit error probability for DPSK is given by

$$p_e(m|I_{Pite}) = \frac{1}{2} e^{-E_b/N_o}, \tag{5.40}$$

while for BPSK it is

$$p_e(m|I_{Pite}) = \frac{1}{2}\mathrm{erfc}\left(\sqrt{\frac{E_b}{N_o}}\right). \tag{5.41}$$

The BER of DPSK is obtained as

$$p_e(m) = \int_0^{\infty} \frac{1}{2}\exp\left\{-\frac{PG}{\frac{m}{3}+\sigma_T^2+\frac{I_{Pite}}{3}}\right\} f_{Pite}(I_{Pite})\,\mathrm{d}I_{Pite} \tag{5.42}$$

where $f_{Pite}(.)$ is the Gaussian PDF.

We use an (n,k) BCH code to perform the error detection. If an error is detected in a packet, it will be retransmitted. The probability of success of a packet is [55]

$$p(c|m) = (1-p_e(m))^n \tag{5.43}$$

and the final error rate after ARQ is employed is given by

$$p_e \le 2^{-(n-k)}\left(1-(1-p_e(m))^n\right). \tag{5.44}$$

Table 5.1 shows the performance of a slotted ALOHA packet CDMA system with mixed stream and packet traffic. The user population is finite within a cell. New transmission attempts and retransmission attempts are assumed the same. A conventional correlator, DPSK and a (255, 179, 10) BCH code are employed. We assume 64 Kbps video streams mixed with a traffic of fixed length packet. The packets are also transmitted at a 64 Kbps line rate. The performance of a conventional narrow band packet cellular system is also shown in the table. For example, if the total bandwidth of a narrow band system is 10 MHz, there are approximately 128 channels of 64 Kbps information rate. The maximum throughput of conventional slotted ALOHA is 0.368. With a frequency reuse factor of 7, the throughput is $128 \times 0.368/7 = 6.73$/packets/slot/sector. From the results, we may see that the capacity of a CDMA packet system is much larger than that of a conventional narrow band packet system. Fig. 5.12 shows the throughput of a slotted ALOHA packet CDMA system with mixed stream and random arrival packet traffic.

5.5 Summary

In this chapter, we obtain the closed form solution for radio capacity, the Erlang capacity and the throughput of a packet CDMA cellular system. Various factors which affect the system capacity are examined.

The number of simultaneous calls in service at a base station is a random variable dependent on call arrival statistics and membership statistics. Therefore, a suitable number of channels should be provided at a base station to ensure a desired quality of service. In practice, there are always a limited channel resources available at a base station. We have shown that with a limited number of channels, the call dropping rate increases drastically as the offered traffic increases. With pilot assisted channel allocation, the required number of channels can be reduced significantly. To support the Erlang capacity of a system with soft handoff and cell site diversity, a reasonably large number of channels are required; the minimum channel number required can be determined to control the cost.

The performance of the packet CDMA cellular system is of great interest. The capacity of a slotted ALOHA packet CDMA system is assessed. We show that the capacity of packet CDMA in a cellular environment is approximately 5 times larger than in a conventional FDMA system. This result supports Qaulcomm's frequency reusing efficiency of a conventional CDMA system (for voice only). We also show the effect of stream type of traffic on the throughput of packet traffic.

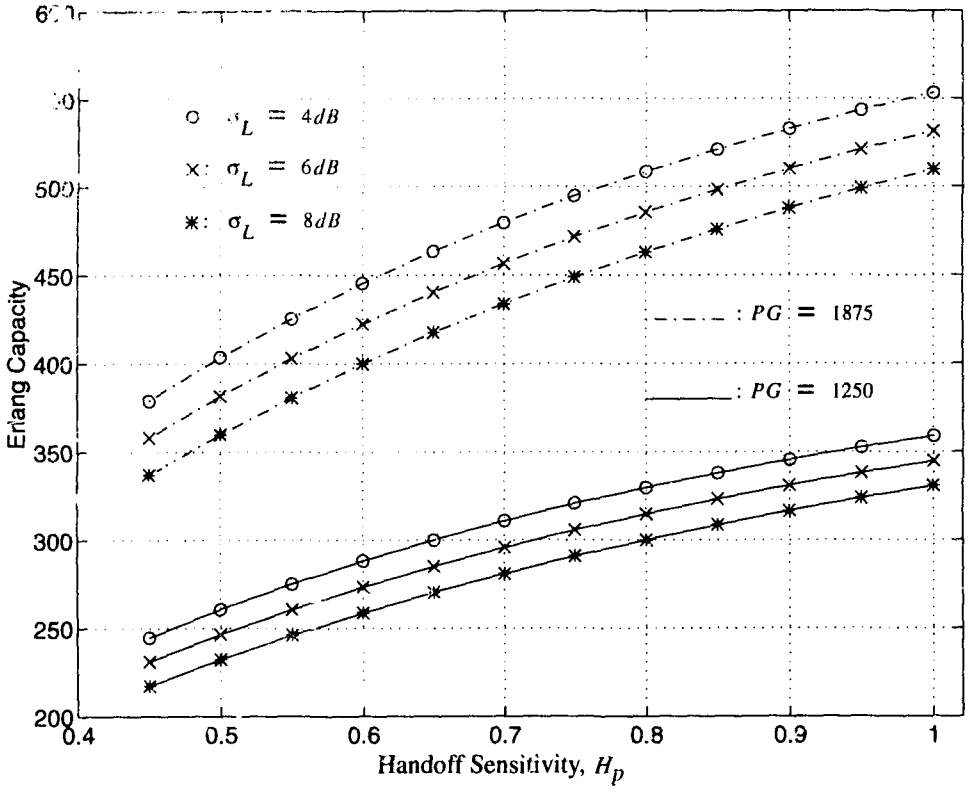

Fig. 5.3 The effect of power control switching on the Erlang capacity, given an ACF of 0.375, and an outage threshold of 7 dB.

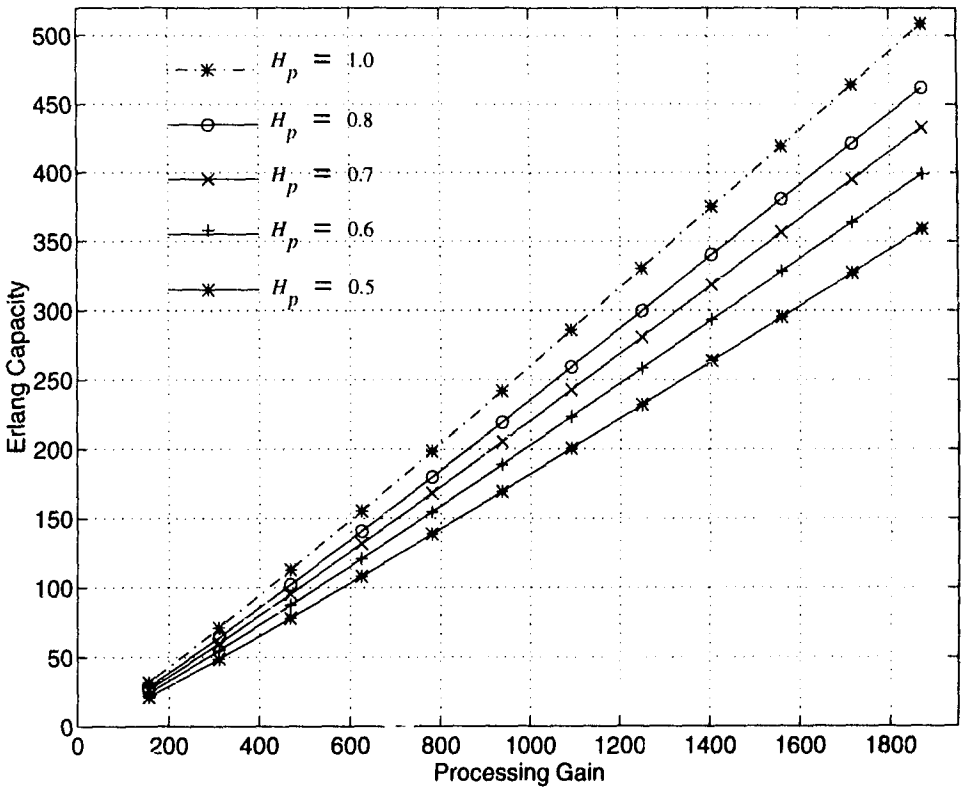

Fig. 5.4 The effect of the processing gain on the system capacity. Perfect power control. ACF is 0.375. Outage threshold is 7 dB.

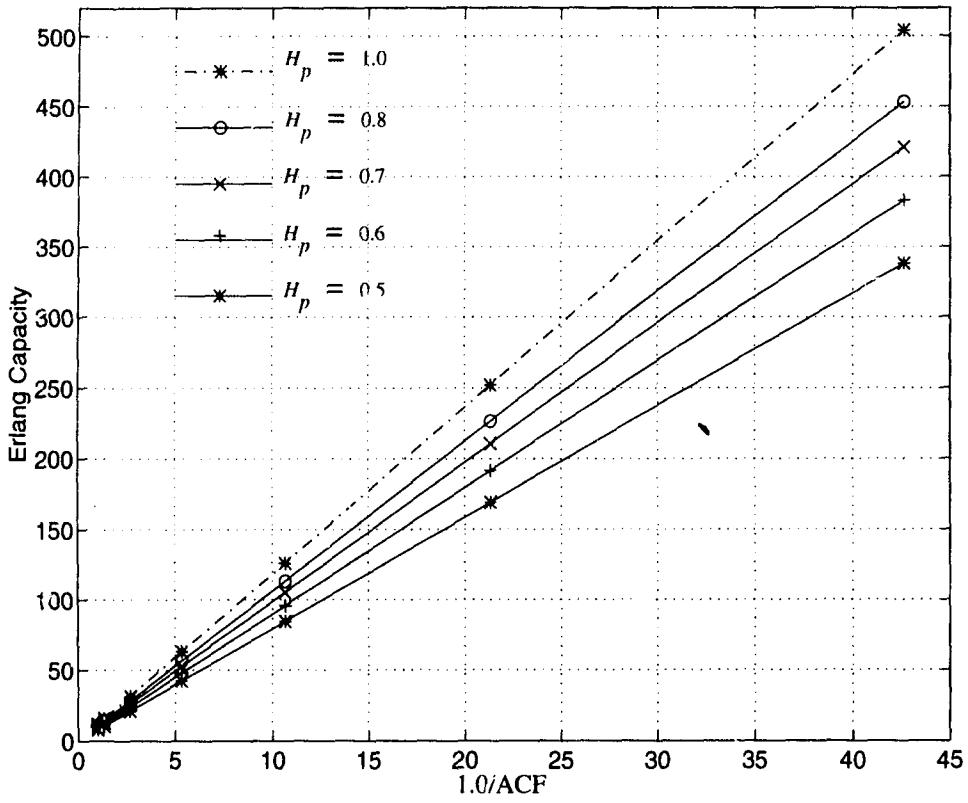

Fig. 5.5 The effect of the user ACF on the Erlang capacity. Processing gain is PG=156. Outage threshold is 7 dB.

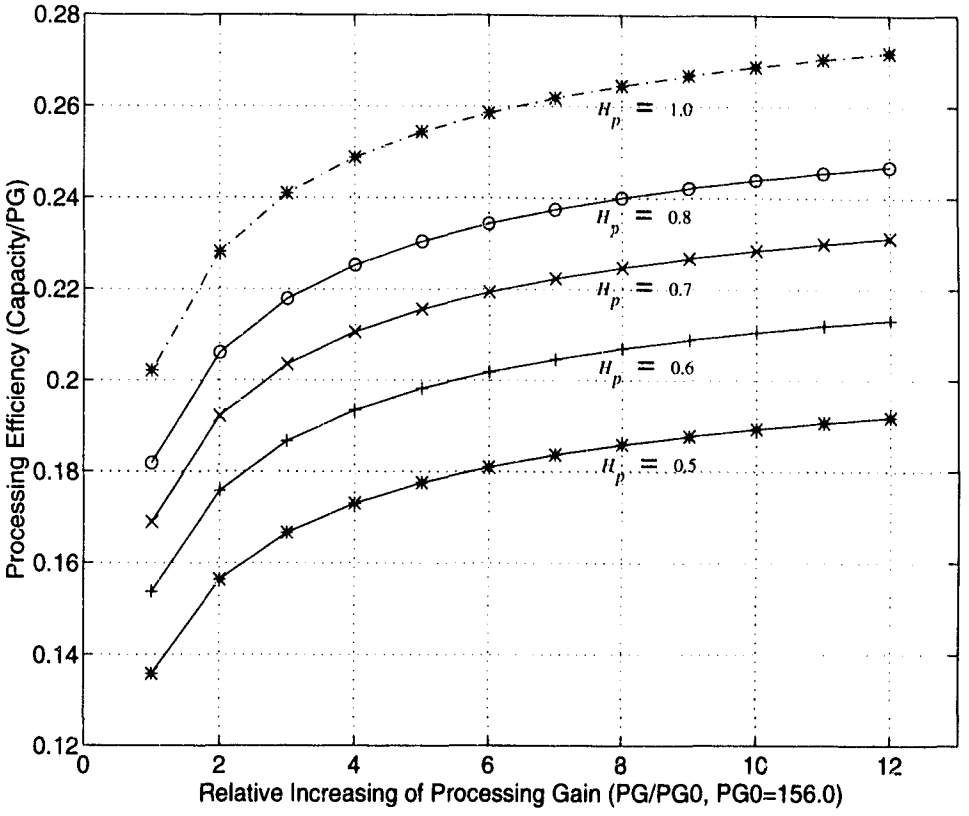

Fig. 5.6 The processing efficiency with an increasing of processing gain

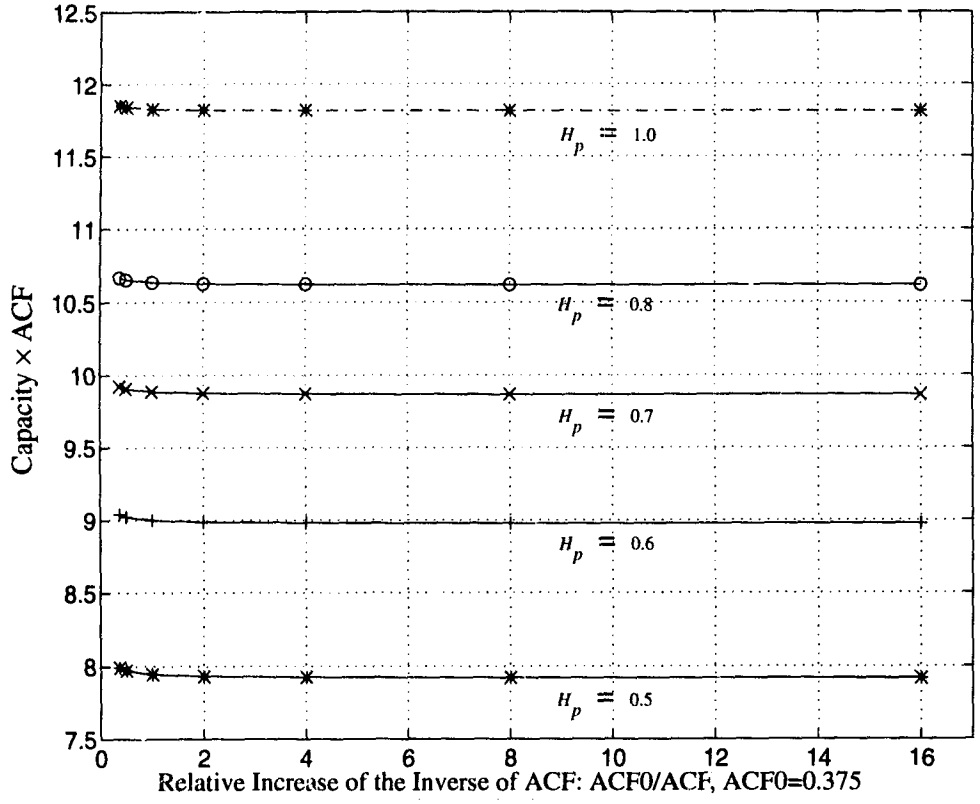

Fig. 5.7 The effect of ACF on the relative gain of capacity

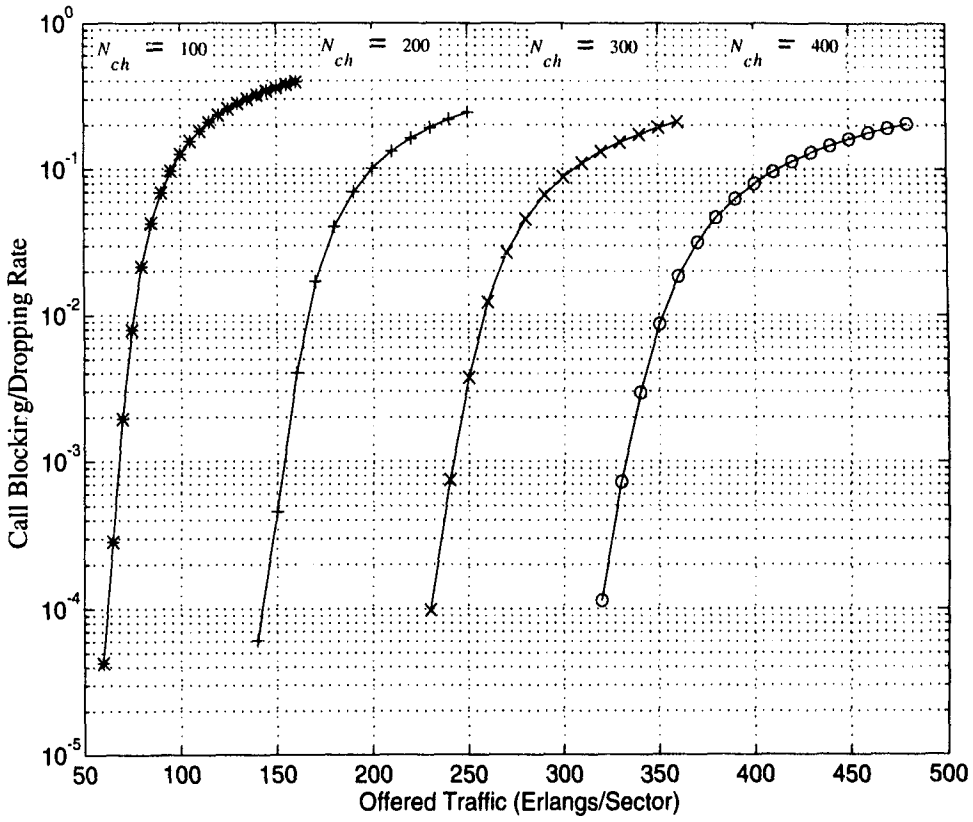

Fig. 5.8 The call blocking/dropping rate given there are finite number of channels available. Ideal handoff and power control are assumed here.

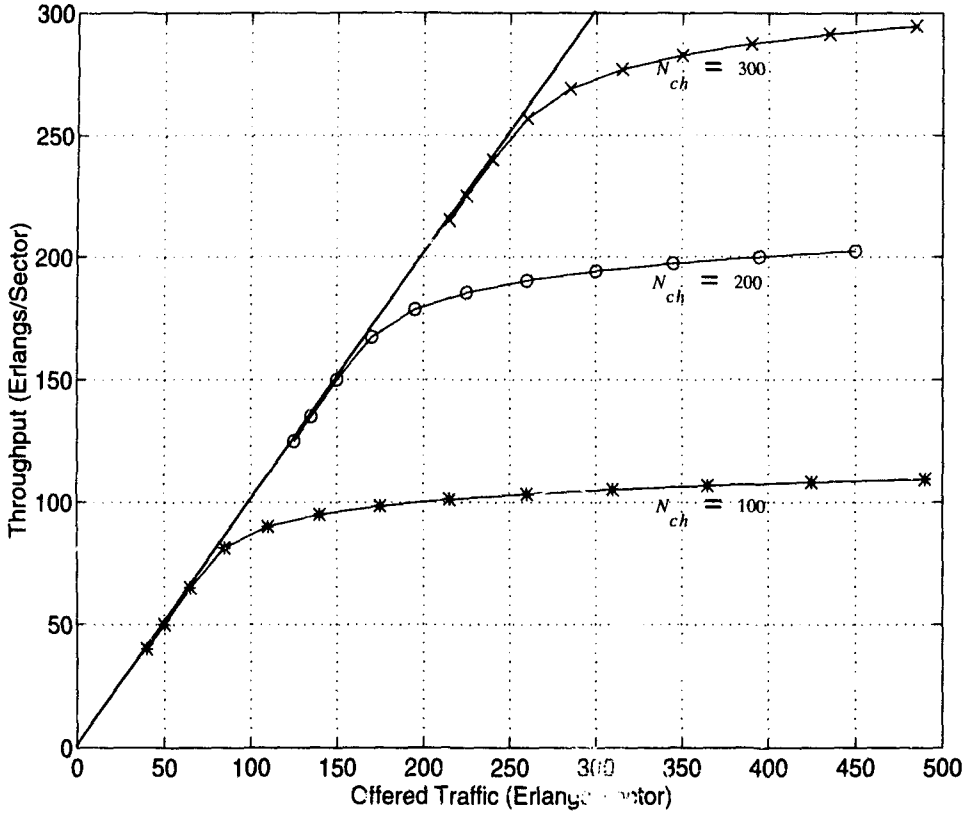

Fig. 5.9 The Erlang throughput due to finite number of channels available. Ideal handoff and perfect power control are assumed.

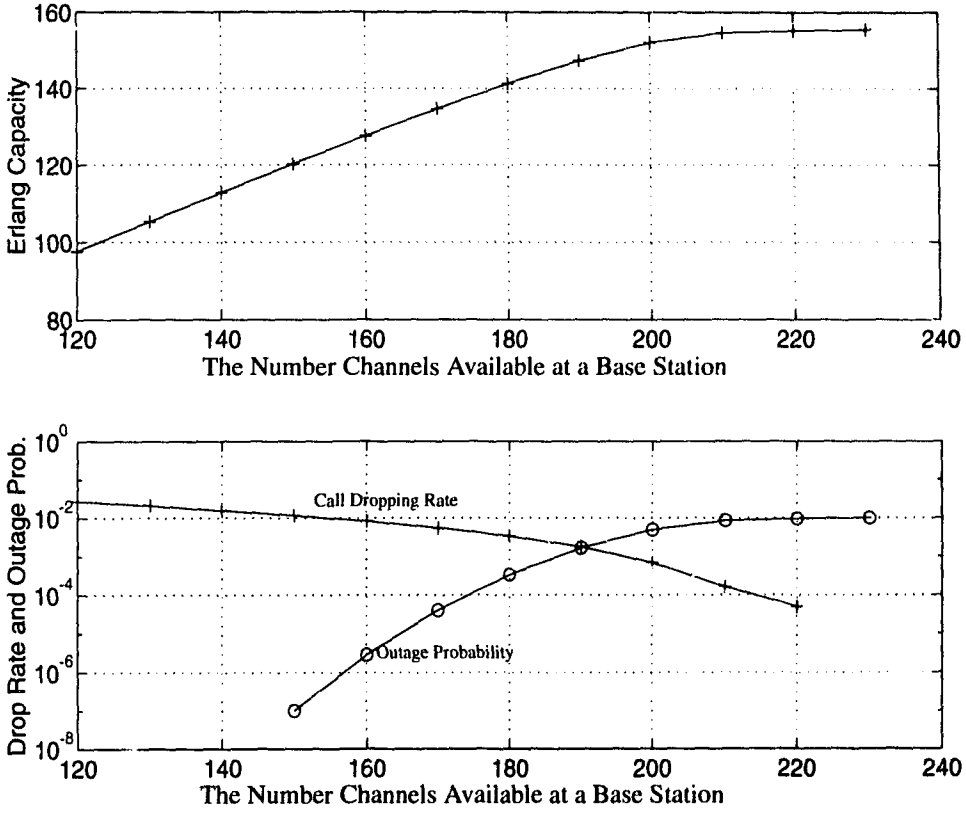

Fig. 5.10 The system capacity. Both the call dropping rate and outage probability are below the level of acceptability. PG=625, ideal handoff and perfect power control are assumed.

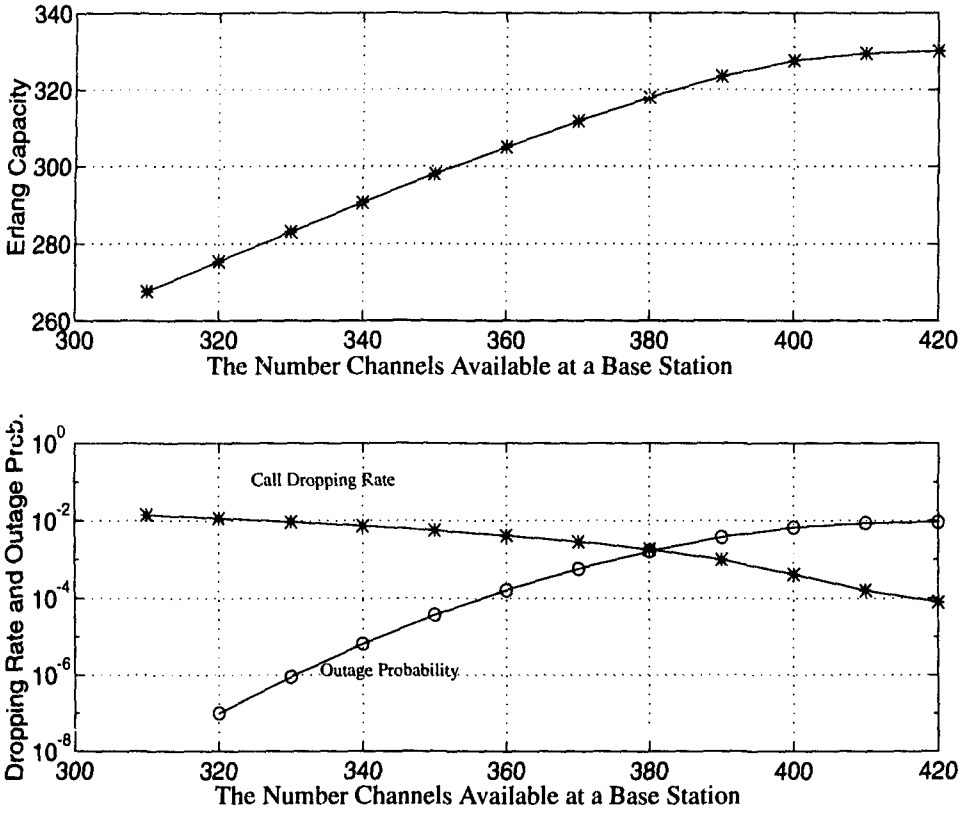

Fig. 5.11 The system capacity. Both the call dropping rate and outage probability are below the level of acceptability. PG=1250, ideal handoff and perfect power control are assumed.

Table 5.1 Capacity of A packet CDMA System with Video Stream and Packet Traffic (Maximum Packets/Slot/Sector).

Video User Number	**0**	**2**	**4**	**8**	**12**
Max. Conventional Throughput	6.73	6.62	6.52	6.31	6.10
Max. Throughput (CDMA)	34.18	32.48	30.81	27.50	24.48

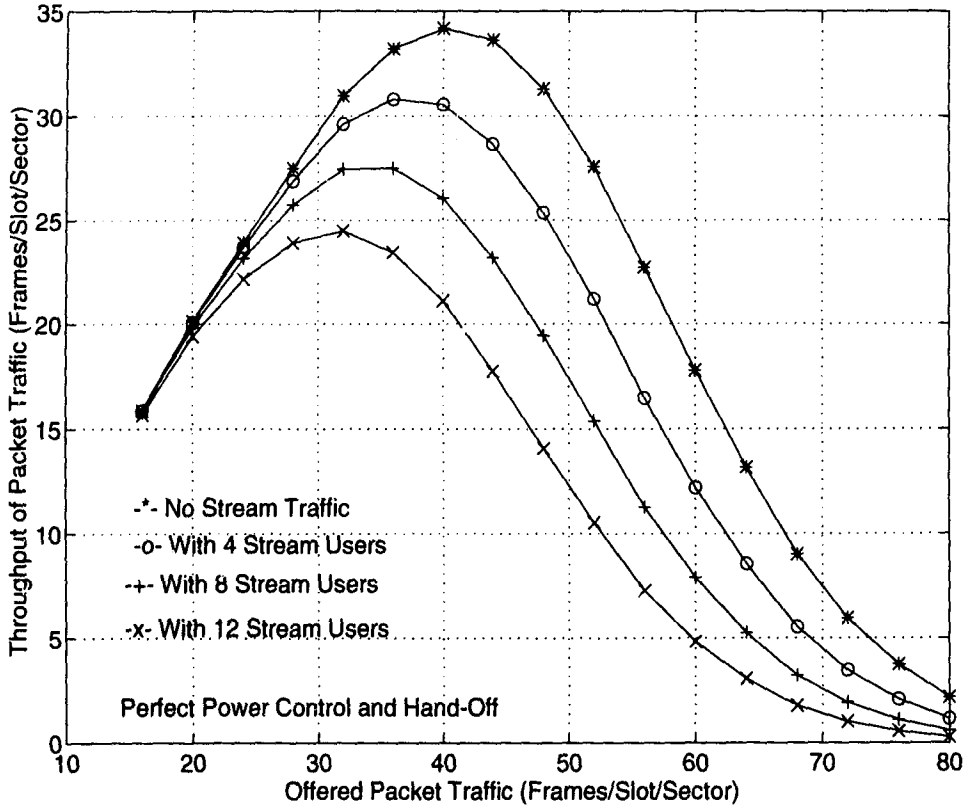

Fig. 5.12 Throughput of a slotted ALOHA packet CDMA system with mixed stream and random arrival packet traffic. Simple correlator, DPSK and (255,179,10) BCH code are employed. Both video streams and packets are transmitted at a 64 Kbps line rate.

Chapter 6

Design Issues in a CDMA Cellular System with Heterogeneous Traffic

6.1 Introduction

The Integrated Wireless Access Network (IWAN) is proposed as a structure for the third-generation of wireless PCS which will accommodate not only high quality voice services, but also data, facsimile and video services [3], [5], [6]. The design of the IWAN primarily involves greatly varying information bit rates and the communication quality requirements of various traffic types, as well as the characteristics of the wireless environment. In a multi-media wireless system, the service requirements generally include transmission rate, delay, BER/outage probability, service blocking and dropping probability.

Due to the high information rate and high transmission quality requirements of a multi-media wireless system and the severe mobile environment, improving bandwidth and power efficiency is one of the most important goals in IWAN design. Since the CDMA technique has great merits in combating multi-path fading and frequency re-use in a cellular environment, it is one of the most promising techniques proposed for the IWAN.

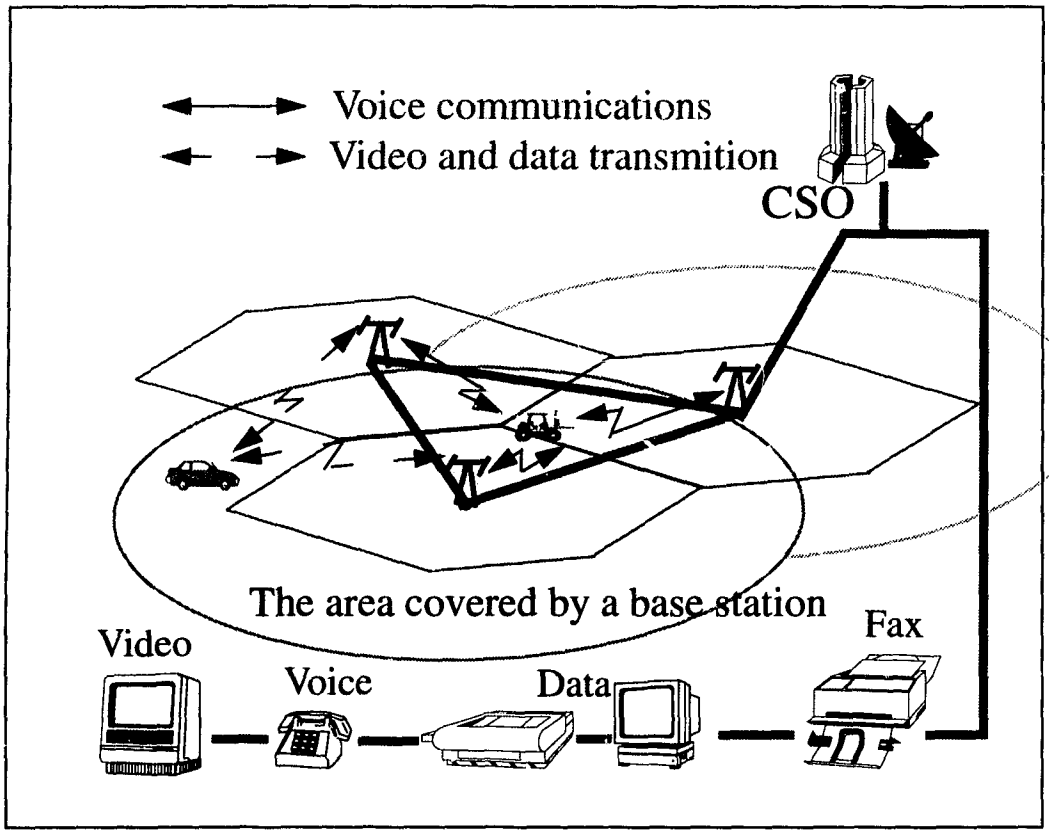

Fig. 6.1 Wireless CDMA cellular networks supporting integrated services.

Since the capacity of a CDMA cellular system is determined by multi-cell, multi-user interference, the understanding of multi-cell, multi-user interference while incorporating various traffic types is necessary. The multi-cell, multi-user interference level is largely determined by the performance of the handoff and power control which are tightly coupled to one another.

In the next generation of CDMA systems, various types of traffic will be supported by integrated services. Different traffic types may have different source rates (they may be fixed or variable) and different activity factors (ACF). To simplify system design, one or a limited number of line rates can be employed to transmit the traffic in a wide range of

source rates. A line rate is the bit transmission rate through a channel [3], [19], [20]. In these systems, the PG and ACF become design parameters determined by the choice of line rate. The impact of the choice of line rate must be investigated.

Different types of traffic may also have different quality requirements (QR) and transmission power. It is shown that for a CDMA cellular system with mixed rate traffic, its capacity is largely limited by the users with high bit rates and high QR [34]. This means that the overall system capacity can be significantly increased by using better error protection techniques for the traffic with high QR and high source rate. Normally, different traffic types received at a receiver have different power levels. Since different traffic types will also mutually interfere with each other, their power levels affect the overall capacity. In this chapter, suitable power levels which should be assigned to different traffic types need to be determined. A higher power level will provide a traffic type more error protection at the expense of the other traffic types' quality [57].

This chapter and its contribution are organized and presented as follows. The second section is devoted to a discussion of the system model in the reverse link. In the third section, the multi-cell, multi-user interference is analyzed for a CDMA cellular system with soft handoff and power control. Multiple mixed rate traffic, channel conditions in a cellular environment and traffic ACFs are taken into consideration. Both the mean and the variance of the multi-cell, multi-user interference power are obtained with an analytical method. The impact of the choice of line rate on system capacity is discussed in the fourth section. The effect of PG and ACF on capacity is compared. The design guidelines for line rate selection are provided. The fifth section addresses how to assign suitable power levels to different traffic types. A method for optimizing the power assignment for multiple traffic types is developed. Optimized power allocation is determined. The last section presents conclusions and remarks.

6.2 System Model

The IWAN supports various stream and packet traffic types. Different traffic types

with different rates are spread over the entire bandwidth available with the same chip rate. The bandwidth values considered for IWAN are 5 MHz, 10 MHz and 15 MHz [5]. Here we assume the total bandwidth is 10 MHz. We focus on stream traffic which consists of various sources with different rates, quality requirements and ACFs. Two typical stream traffic types considered here are voice and video. We assume that 8 Kbps voice with overhead yields a voice source rate of 9.6 Kbps and the video source rate is 76.8Kbps with an information rate of 64 Kbps.

To accommodate a variety of variable-rate and fixed rate sources, as well as to simplify the design, one or a few line rates are proposed for traffic transmission in the IWAN. Different traffic types with different source rates are transmitted at the line rate. A line rate is the actual bit rate used in DS spreading and de-spreading. If the source rate of a traffic type is lower than a line rate, it is increased to the fixed line rate with a corresponding reduction in ACF. If the source rate of a traffic type is higher than a line rate, it is subdivided into several parallel fixed line-rate streams [3], [19], [20].

The cellular structure is one of the most efficient structures for wireless networks. We consider the IWAN in a CDMA cellular system consisting of equal-sized hexagonal cells. The base stations are located at the centers of all cells and employ directional antennas separating a cell into three sectors as show in Fig. 3.1.

Power control is employed for compensating the propagation path loss and the channel attenuation due to shadowing and fading. Perfect power control and ideal soft handoff are assumed in this chapter without loss of generality of the results. With perfect power control, the power received at a base station from each of the station's users is the same for the same type of traffic. A nominal power pre-set is the targeted power control level for each type of traffic. With soft handoff, the strongest of the involved base stations' receptions will be utilized at the switching center. A mobile in the handoff zone is controlled by all involved adjacent cells. The mobile's power level is always set to match the lowest power requirement among these cells by responding to the pilot received with

the highest power [16], [42]. In reality, power control error always exists. The details of the effect of power control error can be found in [17], [32], [33].

As explained in Chapter 3, the final effect of fading is included in a signal to noise ratio (SNR) requirement. A conventional SNR requirement is $E_b/N_o = 7dB$ as suggested in [14] for coded voice. To ensure a specific quality of service, the required minimum E_b/N_o (or outage threshold) depends on the multipath conditions, and the coding and diversity combining techniques employed. It may vary from $5dB$ to more than $8dB$ [42]. We consider the SNR requirement as a parameter in this chapter.

6.3 Interference and Outage Analysis for Multiple Traffic Types

6.3.1 Interference Analysis for a CDMA Cellular System with a Single Type of Traffic

The interference analysis of the cellular CDMA with multiple traffic types can be derived from the analysis for a system with a single type of traffic. When there is one active user per sector, the area averaged mean inter-cell interference is obtained as $E(\overline{I_s})$ in Chapter 3. Considering the ACF and attenuation due to the Rayleigh fading, we obtain the total mean inter-cell interference

$$E(I_{Rite}) = N_s \cdot \upsilon \cdot E(\overline{I_s}) \tag{6.1}$$

where υ is the ACF of an active user. Note that the mean fading attenuation is 1.

Similar to evaluating the area averaged mean, we can also obtain the area averaged variance of the interference power of an active user. As shown in Chapter 3, we obtain $\overline{E(I_s^2)}$ and $\overline{E^2(I_s)}$ for the variance calculation. Taking the user ACF into consideration, we have that the area averaged variance of the total inter-cell interference is

$$D(I_{ite}) = N_s \cdot \left(\upsilon \overline{E(I_s^2)} - \upsilon^2 \overline{E^2(I_s)} \right). \tag{6.2}$$

We consider the inter-cell interference fluctuation caused by the Rayleigh fading as an independent random variable I_{Ry}. The total inter-cell interference is $I_{Rite} = I_{ite} \cdot I_{Ry}$, where I_{Ry} is Chi-square distributed with mean equal to 1. Therefore, with the Rayleigh fading the variance of the inter-cell interference increases to

$$\begin{aligned} D(I_{Rite}) &= N_s \cdot \left(E\left(I_{ite}^2\right) E\left(I_{Ry}^2\right) - E^2(I_{ite}) E^2(I_{Ry}) \right) \\ &= N_s \cdot \left(2\upsilon \overline{E(I_s^2)} - \upsilon^2 E^2 \overline{(I_s)} \right). \end{aligned} \tag{6.3}$$

The mean and variance of intra-cell interference are also obtained in Chapter 3. Since the membership switching and user activity are independent random variables, the mean power of intra-cell interference can be expressed as

$$\begin{aligned} E(I_{ita}) &= (3N_s - 1)\upsilon \cdot \overline{E(\varphi)} \\ &= (3N_s - 1)\upsilon \cdot \iint_{A_0} p(\varphi = 1 | r_0, \theta) f_A(r_0, \theta) r_0 dr_0 d\theta \end{aligned} \tag{6.4}$$

where $f_A(r_0, \theta) = D(r_0, \theta)/A_0$, $D(r_0, \theta)$ is the user density function over the area A_0 and A_0 is the enlarged cell area covered by a base station. With uniformly distributed users, $\overline{E(\varphi)} = 1/3$ and Equation (6.4) reduces to

$$E(I_{ita}) = \left(N_s - \frac{1}{3} \right) \cdot \upsilon \tag{6.5}$$

Similarly, the area averaged variance of the intra-cell interference with one active user is

$$\begin{aligned} D(I_{ita}) &= (3N_s - 1)\left(\upsilon \overline{E(\varphi^2)} - \upsilon^2 E^2 \overline{(\varphi)} \right) \\ &= (3N_s - 1)\left(\frac{1}{3}\upsilon - \upsilon^2 E^2 \overline{(\varphi)} \right) \end{aligned} \tag{6.6}$$

where

$$\overline{E(\varphi^2)} = \iint_{A_0} p(\varphi = 1 | r_0, \theta) f_{A_0}(r_0, \theta) r_0 dr_0 d\theta, \tag{6.7}$$

and

$$\overline{E^2(\varphi)} = \iint_{A_0} p^2(\varphi = 1 | r_0, \theta) f_{A_0}(r_0, \theta)\, r_0 dr_0 d\theta \cdot \tag{6.8}$$

Note that $\overline{E(\varphi^2)}$ is also 1/3 if users are uniformly distributed. Then the mean of total interference power is

$$M(I_t) = E(I_{ita}) + E(I_{Rite}) \tag{6.9}$$

and the variance of total interference power is

$$Var(I_t) = D(I_{ita}) + D(I_{Rite}) \tag{6.10}$$

where I_t is the total interference. Our analysis and simulation results in previous Chapters show that due to soft handoff operations the total interference approach the Gaussian distribution very quickly with an increasing number of users per cell.

6.3.2 Outage Analysis for Multiple Stream Types of Traffic

Based on the interference analysis for a single type of traffic, we can easily obtain the mean and variance of the total interference as

$$M(I_{mj}) = \sum_{i=1}^{N_t} M(I_{ti}) \tag{6.11}$$

and

$$Var(I_{mj}) = \sum_{i=1}^{N_t} Var(I_{ti}) \tag{6.12}$$

where I_{mj} is the total multi-user interference including all types of traffic to a reference user of the jth type, I_{ti} is the total interference from the ith type of traffic and N_t is the number of traffic types. Checking into details, we have

$$M(I_{mj}) = \sum_{i=1, i\neq j}^{N_t} N_{si} \cdot \upsilon_i \cdot P_i\left(1 + E\overline{(I_s)}\right) + \upsilon_j \cdot P_j\left(\left(N_{sj} - \frac{1}{3}\right) + N_{sj} \cdot E\overline{(I_s)}\right) \tag{6.13}$$

and

$$Var(I_{mj}) = \sum_{i=1, i\neq j}^{N_t} 3N_{si}P_i^2\left(\upsilon_i E\overline{(\varphi^2)} - \upsilon_i^2 E^2\overline{(\varphi)}\right)$$
$$+ \sum_{i=1}^{N_t} N_{si}\cdot P_i^2\left(2\upsilon_i E\overline{(I_s^2)} - \upsilon_i^2 E^2\overline{(I_s)}\right) + (3N_{sj}-1)P_j^2\left(\upsilon_j E\overline{(\varphi^2)} - \upsilon_j^2 E^2\overline{(\varphi)}\right) \quad (6.14)$$

where N_{si} is the number of users per sector, P_i is the targeted received power at the reference base station and υ_i is the ACF of the ith type of traffic. The reference user is from traffic type j.

For a reference user of the specific jth traffic type, the signal to noise ratio E_{bj}/N_{oj} is

$$\frac{E_{bj}}{N_{oj}} = \frac{W}{R_j}\cdot\frac{P_j}{I_{mj}+\sigma_T^2} \quad (6.15)$$

where E_{bj} is the energy per bit, N_{oj} is the total interference power density, R_j is the bit rate of a user of the jth traffic type, W is the total bandwidth available, P_j is the desired power to be received for a specific reference user of type j, and σ_T^2 represents the background noise and is taken as 1.26 (1 dB) for the case when the power of a voice user is normalized to 1 [14]. The outage probability of a reference user of the jth type is given by

$$p_{out,j} = p\left(I_{mj} > \frac{P_j\cdot W/R_j}{(E_{bj}/N_{oj})_{QR}} - \sigma_T^2\right)$$
$$= p\left(I_{mj} > \frac{P_j\cdot PG_j}{(E_{bj}/N_{oj})_{QR}} - \sigma_T^2\right) = p\,(I_{mj} > t_j) \quad (6.16)$$

where PG_j is the PG and $(E_{bj}/N_{oj})_{QR}$ is the QR of traffic type j.

If the user number is large enough, the central limit theorem can be applied [14]. In addition, due to soft handoff operations the interference approaches Gaussian more quickly than does the simple summation of multiple random variables [17]. Since the

number of active users is normally quite large at the capacity of a system, we adopt the Gaussian approximation for simplicity, and the outage probability of the reference user of type j is obtained as

$$p_{out,j} \approx \frac{1}{2}\mathrm{erfc}\left(\frac{t_j - M(I_{mj})}{\sqrt{2Var(I_{mj})}}\right) \tag{6.17}$$

where

$$t_j = \frac{P_j \cdot PG_j}{(E_{bj}/N_{oj})_{QR}} - \sigma_T^2 \tag{6.18}$$

is defined as the threshold of a user of the jth traffic type.

6.4 Effect of the Choice of Line Rate on Capacity

For efficient traffic integration, the suitable value and the number of line rates will be determined by various factors such as capacity, complexity and other system design considerations. In this section, we examine the impact of the choice of line rate on system capacity.

At first, we examine the impact of a line rate on low rate users. Since a line rate is the actual rate involved in DS spreading and de-spreading, PG and ACF become design parameters when a line rate is employed.

The PG is determined by the line rate and is given by

$$PG_{lj} = \frac{R_c}{R_l} = \frac{R_c}{R_j} \cdot \frac{R_j}{R_l} = PG_j \cdot \frac{R_j}{R_l} \tag{6.19}$$

where R_c is the spreading chip rate, R_l is line rate, and R_j is the source rate of the low rate traffic of type j. If the rate of a traffic type is lower than line rate, its ACF is reduced as

$$\upsilon_{lj} = \upsilon_j \cdot \frac{R_j}{R_l} \tag{6.20}$$

where υ_{lj} is the ACF of a low rate user with a source rate of R_j when it is transmitted at a line rate of R_l. Without loss of generality, here we consider that only a single type of low rate traffic exists. If power control is perfect and the power received at the base station from the reference user is normalized to 1, considering the effect of line rate, we have the outage probability as

$$p_{out,j} \approx \frac{1}{2}\mathrm{erfc}\left(\frac{t_{lj} - M(I_{lj})}{\sqrt{2Var(I_{lj})}}\right) \tag{6.21}$$

where

$$t_{lj} = \frac{PG_{lj}}{(E_{bj}/N_{oj})_{QR}} - \sigma_T^2 = \frac{PG_j}{(E_{bj}/N_{oj})_{QR}} \cdot \frac{R_j}{R_l} - \sigma_T^2, \tag{6.22}$$

I_{lj} is the total interference from the jth traffic type when the line rate is employed and from Equations (6.1), (6.3), (6.5) and (6.6), we have

$$M(I_{lj}) = \left(N_{sj} - \frac{1}{3}\right) \cdot \upsilon_{lj} + N_{sj} \cdot \upsilon_{lj} \cdot \overline{E(I_s)} \tag{6.23}$$

and

$$Var(I_{lj}) = N_{sj} \cdot \left(2\upsilon_{lj}\overline{E(I_s^2)} - \upsilon_{lj}^2 E^2\overline{(I_s)}\right) + (3N_{sj} - 1)\left(\frac{1}{3}\upsilon_{lj} - \upsilon_{lj}^2 E^2\overline{(\varphi)}\right) \tag{6.24}$$

Since at the capacity of a system, N_{sj} is normally very large for low rate users, Equations (6.23) and (6.24) can be simplified to

$$M(I_{lj}) = N_{sj} \cdot \upsilon_{lj}\left(1 + \overline{E(I_s)}\right) = N_{sj} \cdot \upsilon_j \cdot \frac{R_j}{R_l}\left(1 + \overline{E(I_s)}\right) \tag{6.25}$$

and

$$\begin{aligned} Var(I_{lj}) &= N_{sj} \cdot \upsilon_{lj}\left(1 - 3\upsilon_{lj}E^2\overline{(\varphi)} + 2\overline{E(I_s^2)} - \upsilon_{lj}E^2\overline{(I_s)}\right) \\ &= N_{sj} \cdot \upsilon_j\frac{R_j}{R_l}\left(1 - 3\upsilon_j\frac{R_j}{R_l}E^2\overline{(\varphi)} + 2\overline{E(I_s^2)} - \upsilon_j\frac{R_j}{R_l}E^2\overline{(I_s)}\right) \end{aligned} \tag{6.26}$$

We denote

$$g_{mj} = \upsilon_j \cdot \frac{R_j}{R_l}\left(1 + \overline{E(I_s)}\right) \tag{6.27}$$

and

$$g_{vj} = \upsilon_j \frac{R_j}{R_l}\left(1 - 3\upsilon_j \frac{R_j}{R_l} E^2\overline{(\varphi)} + 2\overline{E(I_s^2)} - \upsilon_j \frac{R_j}{R_l} E^2\overline{(I_s)}\right) \tag{6.28}$$

The key parameters for calculating the total interference are the area averaged first and second moments. Values for these parameters, obtained under the condition of ideal handoff, perfect power control, user ACF of 1 and the path loss factor $\nu = 4$ are given in Table 3.1.

Following the approach in [18], Equation (6.21) can be modified to

$$\left(\text{erfc}^{-1}(2p_{out,j})\right)^2 = \frac{(t_{lj} - N_{sj} \cdot g_{mj})^2}{2N_{vj} \cdot g_{vj}},$$

where $\text{erfc}^{-1}(x)$ is the inverse function of $\text{erfc}(x)$. Let $\psi = \text{erfc}^{-1}(2P_{out,j})$, we then obtain a quadratic equation in N_{sj}

$$2N_{sj} \cdot g_{vj}\psi^2 = (t_{lj} - N_{sj} \cdot g_{mj})^2. \tag{6.29}$$

Solving Equation (6.29), we find the radio capacity to be

$$N_{sj} = \frac{1}{g_{mj}^2}\left(\psi^2 g_{vj} + t_{lj} g_{mj} - \psi\sqrt{g_{vj}(\psi^2 \cdot g_{vj} + 2t_{lj} \cdot g_{mj})}\right). \tag{6.30}$$

When the source rate of a specific user is higher than the line rate, its transmission will be split into several parallel streams. Orthogonal sequence can be used to provide interference isolation between the sub-divided parallel transmissions[20], [56]. Here we consider a worst case scenario in which the parallel transmissions are separated by long sequences which are synchronized, with no orthogonal protection. If there is a single high rate traffic type j and we also normalize its power to 1, we have the signal to noise ratio E_{bj}/N_{oj} as

$$\frac{E_{bj}}{N_{oj}} = \frac{PG_j}{I_{tj} + \sigma_T^2 + \frac{k-2}{k}\upsilon_j + \frac{\upsilon_{lj}}{k}} \tag{6.31}$$

where k is the number of parallel streams after spliting

$$k = \left\lfloor \frac{R_j}{R_l} \right\rfloor , \tag{6.32}$$

υ_{lj} is the ACF of the last one of the streams after separation

$$\upsilon_{lj} = \frac{R_j - kR_l}{R_l} \cdot \upsilon_j \tag{6.33}$$

and I_{lj} is the total interference when no stream separation is used. Here we denote $I_{lj} = I_{ij} + \frac{k-2}{k}\upsilon_j + \frac{\upsilon_{lj}}{k}$. Then, the mean and variance of I_{lj} can be obtained as

$$M(I_{lj}) = \begin{cases} M(I_{ij}) + \frac{k-2}{k}\upsilon_j + \frac{\upsilon_{lj}}{k} & \text{If } R_j/R_l = k \\ M(I_{ij}) + \frac{k-1}{k}\upsilon_j & \text{Otherwise} \end{cases} \tag{6.34}$$

and

$$Var(I_{lj}) = \begin{cases} Var(I_{ij}) + \frac{1}{k^2}\left((k-2)^2\left(\upsilon_j - \upsilon_j^2\right) + \upsilon_{lj} - \upsilon_{lj}^2 \right) & \text{If } R_j/R_l = k \\ Var(I_{ij}) + \frac{1}{k^2}\left((k-1)^2\left(\upsilon_j - \upsilon_j^2\right)\right) & \text{Otherwise} \end{cases} \tag{6.35}$$

where we denote

$$M_{lh} = \begin{cases} \frac{k-2}{k}\upsilon_j + \frac{\upsilon_{lj}}{k} & \text{If } R_j/R_l = k \\ \frac{k-1}{k}\upsilon_j & \text{Otherwise} \end{cases}$$

and

$$\sigma_{lh}^2 = \begin{cases} \frac{1}{k^2}\left((k-2)^2\left(\upsilon_j - \upsilon_j^2\right) + \upsilon_{lj} - \upsilon_{lj}^2 \right) & \text{If } R_j/R_l = k \\ \frac{1}{k^2}\left((k-1)^2\left(\upsilon_j - \upsilon_j^2\right)\right) & \text{Otherwise.} \end{cases}$$

Using the method similar to obtaining Equation (6.30) for low rate traffic type, we can also obtain a closed form equation of radio capacity for high rate users with the effect of line rate taken into consideration as

$$N_{sj} = \frac{1}{g_{mj}^2}\left(g_{mj}\left(t_j - M_{lh} + \frac{1}{3} \right) + \psi^2 g_{vj} - \left(\left(g_{mj}\left(t_j - M_{lh} + \frac{1}{3} \right) + \psi^2 g_{vj} \right)^2 \right.\right.$$
$$\left.\left. - g_{mj}^2 \left(\left(t_j - M_{lh} + \frac{1}{3} \right)^2 - 2\psi^2 \left(\sigma_{lh}^2 - \left(\frac{1}{3} - E^2\overline{(\varphi)} \right) \right) \right) \right)^{1/2} \right). \tag{6.36}$$

where

$$g_{mj} = \upsilon_j \cdot \left(1 + E\overline{(I_s)} \right) \tag{6.37}$$

and

$$g_{vj} = \upsilon_j \left(1 - 3\upsilon_j E^2\overline{(\varphi)} + 2\overline{E(I_s^2)} - \upsilon_j E^2\overline{(I_s)} \right). \tag{6.38}$$

For a system with multiple traffic types, we may employ Equations (6.13) and (6.14), and use the procedure above to obtain the capacity in terms of a specific traffic type given a fixed number of users of all other traffic types. For simplicity, we normally choose a low rate traffic type for capacity calculation and normalize its power to 1. A general formula for the capacity of a system with multiple traffic types can be given as

$$N_{sj}^* = \frac{1}{g_{mj}^2}\left(g_{mj}(t_j - \Omega_m) + \psi^2 g_{vj} - \left(\left(g_{mj}(t_j - \Omega_m) + \psi^2 g_{vj} \right)^2 \right.\right.$$
$$\left.\left. - g_{mj}^2 \left((t_j - \Omega_m)^2 - 2\psi^2 \chi_m \right) \right)^{1/2} \right) \tag{6.39}$$

where

$$\Omega_m = \sum_{i=1, i\neq j}^{N_t} N_{si} P_i g_{mi} \tag{6.40}$$

and

$$\chi_m = \sum_{i=1, i\neq j}^{N_t} N_{si} P_i^2 g_{vi}, \tag{6.41}$$

g_{mi} and g_{vi} can be obtained in a manner similar to Equations (6.37) and (6.38). Note that Equation (6.39) is for quality requirement of traffic type j. Since it is difficult to show the overall system capacity with one type of traffic, we use the overall system throughput (in Kbps per sector) to measure the capacity

$$S_c = \sum_{i=1}^{N_t} N_{si} \cdot \upsilon_i \cdot R_{0i}. \tag{6.42}$$

where R_{0i} is the information rate of traffic type i, e.g. for voice it is 8 Kbps.

To show how PG and ACF affect the capacity, we compare the capacity increase when the PG and 1/ACF are increased. A 10 MHz system with low rate users, e.g. voice users with a rate of 9.6 Kbps and an ACF of 0.375 is considered. The results plotted in Fig. 6.2 show that a larger PG improves capacity more efficiently than a small ACF. Fig. 6.2 represents the case when bandwidth available is increased how much capacity will be increased by only increasing PG or 1/ACF.

Using a lower line rate results in a larger PG and a smaller 1/ACF, while using a higher line rate leads to a more burst traffic for low rate users and reduces capacity. Lowest possible line rate which could be the lowest rate of variable and fixed rate traffic is desired for low rate users in regard to maximizing the capacity. Fig. 6.3 shows that for single low rate traffic, capacity decreases as the line rate increases. As for high rate users, they can be subdivided into several parallel streams transmitting at the line rate [3], [19], [20]. Fig. 6.4 shows that as we use a lower line rate, the high rate traffic is subdivided into more parallel streams. The reduction in capacity is very limited even if we do not use orthogonal protection. The effects of subdivision on capacity is minimal. For mixed traffic with multiple types, we can see from Fig. 6.5 and Fig. 6.6 that the impact of the choice of line rate is dominated by its effect on low rate users. Both figures show that a line rate which is chosen as low as the lowest source rate is desired for a higher capacity. In Fig. 6.7, the radio capacity for voice and video is plotted. The capacity for using a 9.6 Kbps line rate is considered the same as the case when both voice and video are transmitted at their own source rate and capacity is reduced by about 30% if a line rate of 76.8 Kbps is employed.

6.5 Optimized Power Allocation for Mixed Rate Traffic

To examine the effect of the power level of different traffic types, we first consider that the traffic consists of two types: voice and video. We choose the power of a voice user as the reference which we normalize to 1. For simplicity, we denote voice as traffic type 1 and video as type 2. With perfect power control, the outage probability of a reference voice user is given by

$$P_{out,1} = P\left(I_{m1} > \frac{PG_1}{(E_{b1}/N_{o1})_{QR}} - \sigma_T^2 \right) = P(I_{m1} > t_1) \tag{6.43}$$

and the outage probability of a video user is

$$P_{out,2} = P\left(I_{m2} > \frac{PG_2 \cdot P_2}{(E_{b2}/N_{o2})_{QR}} - \sigma_T^2 \right) = P(I_{m2} > t_2) \tag{6.44}$$

where I_{m1} and I_{m2} are different total interferences received by a reference user, PG_1 and PG_2 are PGs, $(E_{b1}/N_{o1})_{QR}$ and $(E_{b2}/N_{o2})_{QR}$ are quality requirements of voice and video respectively, t_1 and t_2 are defined as outage thresholds, and P_2 is the relative power assigned to a video user. The outage probability of a voice user is then obtained as

$$P_{out,1} \approx \frac{1}{2}\mathrm{erfc}\left(\frac{t_1 - M(I_{m1})}{\sqrt{2Var(I_{m1})}} \right) \tag{6.45}$$

where

$$\begin{aligned} M(I_{m1}) &= (3N_1 - 1) \cdot \upsilon \cdot \overline{E(\varphi)} + N_1 \cdot \upsilon \cdot \overline{E(I_s)} + N_2 P_2 \left(1 + \overline{E(I_s)} \right) \\ &\approx (N_1 \cdot \upsilon + N_2 P_2) \left(1 + \overline{E(I_s)} \right) = N_1 g_{m1} + N_2 P_2 g_{m2} \ , \end{aligned} \tag{6.46}$$

$$\begin{aligned} Var(I_{m1}) &= (3N_1 - 1)\left(\upsilon \cdot \overline{E(\varphi^2)} - \upsilon^2 \overline{E^2(\varphi)} \right) + 3N_2 P_2^2 \left(\overline{E(\varphi^2)} - \overline{E^2(\varphi)} \right) \\ &\quad + N_1 \cdot \left(2\upsilon \overline{E(I_s^2)} - \upsilon^2 \overline{E^2(I_s)} \right) + N_2 P_2^2 \left(2\overline{E(I_s^2)} - \overline{E^2(I_s)} \right) \\ &\approx N_1 \left(3\left(\upsilon \cdot \overline{E(\varphi^2)} - \upsilon^2 \overline{E^2(\varphi)} \right) + \left(2\upsilon \overline{E(I_s^2)} - \upsilon^2 \overline{E^2(I_s)} \right) \right) \\ &\quad + N_2 P_2^2 \left(3\left(\overline{E(\varphi^2)} - \overline{E^2(\varphi)} \right) + \left(2\overline{E(I_s^2)} - \overline{E^2(I_s)} \right) \right) = N_1 g_{v1} + N_2 P_2^2 g_{v2} \ , \end{aligned} \tag{6.47}$$

N_1 is the number of voice users per sector, N_2 is the number of video users per sector and υ is the voice ACF. Using the similar approach as before, Equation (6.45) can be written as

$$\left(\text{erfc}^{-1}(2P_{out})\right)^2 = \frac{(t_1 - N_1 g_{m1} - N_2 P_2 g_{m2})^2}{2\left(N_1 g_{v1} + N_2 P_2^2 g_{v2}\right)}$$

Let $\psi = \text{erfc}^{-1}(2P_{out})$. By solving this quadratic equation in N_1, we obtain the radio capacity of voice users (traffic type 1), with the specific QR of voice users (also traffic type 1) and number of video users, as

$$N_{11}^* = \frac{1}{g_{m1}^2}\Big(g_{m1}(t_1 - N_2 g_{m2} P_2) + \psi^2 g_{v1} - \Big(\Big(g_{m1}(t_1 - N_2 g_{m2} P_2) + \psi^2 g_{v1}\Big)^2 - g_{m1}^2\Big((t_1 - N_2 g_{m2} P_2)^2 - 2\psi^2 N_2 g_{v2} P_2^2\Big)\Big)^{1/2}\Big). \tag{6.48}$$

Note that we use the radio capacity of voice users as a system capacity measurement. Similarly, the outage probability of a reference video user is

$$P_{out,2} \approx \frac{1}{2}\text{erfc}\left(\frac{t_2 - M(I_{m2})}{\sqrt{2Var(I_{m2})}}\right) \tag{6.49}$$

where

$$\begin{aligned} M(I_{m2}) &= (3N_2 - 1)P_2 E\overline{(\varphi)} + N_2 P_2 E\overline{(I_s)} + N_1 \cdot \upsilon \cdot \left(1 + E\overline{(I_s)}\right) \\ &= (N_1 \cdot \upsilon + N_2 P_2)\left(1 + E\overline{(I_s)}\right) - \frac{1}{3}P_2 = N_1 g_{m1} + N_2 P_2 g_{m2} - \frac{1}{3}P_2 \end{aligned} \tag{6.50}$$

and

$$\begin{aligned} Var(I_{m2}) &= 3N_1\left(\upsilon \cdot E\overline{(\varphi^2)} - \upsilon^2 E^2\overline{(\varphi)}\right) + (3N_2 - 1)P_2^2\left(E\overline{(\varphi^2)} - E^2\overline{(\varphi)}\right) \\ &\quad + N_1 \cdot \left(2\upsilon E\overline{(I_s^2)} - \upsilon^2 E^2\overline{(I_s)}\right) + N_2 P_2^2\left(2E\overline{(I_s^2)} - E^2\overline{(I_s)}\right) \\ &= N_1 g_{v1} + N_2 P_2^2 g_{v2} - P_2^2\left(\frac{1}{3} - E^2\overline{(\varphi)}\right). \end{aligned} \tag{6.51}$$

Next, we obtain the capacity of voice users given the specific QR of video and the number of video users.

$$N_{12}^{*} = \frac{1}{g_{m1}^{2}}\Big(g_{m1}\Big(t_2 - N_2 g_{m2} P_2 + \frac{1}{3}P_2\Big) + \psi^2 g_{v1} - \Big(\Big(g_{m1}\Big(t_2 - N_2 g_{m2} P_2 + \frac{1}{3}P_2\Big) + \psi^2 g_{v1}\Big)^2 - g_{m1}^2\Big(\Big(t_2 - N_2 g_{m2} P_2 + \frac{1}{3}P_2\Big)^2 - 2\psi^2 N_2 g_{v2} P_2^2 + 2P_2^2\Big(\frac{1}{3} - E^2\overline{(\varphi)}\Big)\Big)\Big)^{1/2}\Big). \tag{6.52}$$

Since the final system capacity is limited by the traffic which has the highest quality requirement [17], we have the actual radio capacity of voice user as

$$N_1^{*} = \min\Big(N_{11}^{*}, N_{12}^{*}\Big). \tag{6.53}$$

Fig. 6.8 shows capacity versus relative power of a video user. Since N_{11}^{*} monotonically decreases with increasing P_2 and N_{12}^{*} monotonically increases with P_2, N_1^{*} is maximum when $N_{11}^{*} = N_{12}^{*}$. We can obtain a P_2^{*} such that N_1^{*} is maximum by solving the equation

$$\begin{aligned} & g_{m1} t_1 - \psi\Big(2 g_{m1} g_{v1}(t_1 - N_2 g_{m2} P_2) + \psi^2 g_{v1}^2 + 2N_2 g_{m1}^2 g_{v2} P_2^2\Big)^{1/2} \\ &= g_{m1} t_2 + \frac{1}{3} g_{m1} - \psi\Big(2 g_{m1} g_{v1}\Big(t_2 - N_2 g_{m2} P_2 + \frac{1}{3}P_2\Big) \\ &\qquad + \psi^2 g_{v1}^2 + 2N_2 g_{m1}^2 g_{v2} P_2^2 - 2P_2^2\Big(\frac{1}{3} - E^2\overline{(\varphi)}\Big)\Big)^{1/2}. \end{aligned} \tag{6.54}$$

To show the capacity of a system with mixed traffic, we calculate the total throughput as

$$S_c = N_1^{*} \cdot \upsilon_1 \cdot R_1 + N_2 \cdot \upsilon_2 \cdot R_2 \quad . \tag{6.55}$$

Examining the optimum condition $N_{11}^{*} = N_{12}^{*}$, it can be seen that this condition is equivalent to when $P_{out,1} = P_{out,2}$. Since I_{m1} and I_{m2} are almost the same, P_2^{*} can be approximated as

$$P_2^{*} \approx \frac{PG_1 \cdot (E_{b2}/N_{o2})_{QR}}{PG_2 \cdot (E_{b1}/N_{o1})_{QR}} \tag{6.56}$$

and

$$E_{b2}^{*} \approx E_{b1} \cdot \frac{(E_{b2}/N_{o2})_{QR}}{(E_{b1}/N_{o1})_{QR}} \quad . \tag{6.57}$$

In the case that there are more than two traffic types, it becomes difficult to determine the optimum power by solving multiple nonlinear equations. However, the optimum relative power of the ith type of traffic can easily be estimated by generalizing Equations (6.56) and (6.57) as

$$P_i^* \approx P_1 \cdot \frac{PG_1 \cdot (E_b/N_0)_{QR,i}}{PG_i \cdot (E_b/N_0)_{QR,1}} \qquad i = 2, 3, \ldots \tag{6.58}$$

and

$$E_{bi}^* \approx E_{b1} \cdot \frac{(E_b/N_0)_{QR,i}}{(E_b/N_0)_{QR,1}} \qquad i = 2, 3, \ldots \tag{6.59}$$

Our results show that the traffic components and user activity have minimal effect on the value of the optimum relative power, see Fig. 6.9. Table 6.1 shows the optimum relative power and energy per bit of a video user. Equations (6.56), (6.57), (6.58) and (6.59) are justified by the numerical results. Table 6.2 shows that the capacity is improved by optimized power allocation especially when the difference between the quality requirements is large. From Fig. 6.10, we can see that the overall system throughput could be increased significantly if suitable power is assigned to different traffic types. The overall throughput decreases with an increase in the number of high rate users in the case that their quality requirements are the same.

6.6 Conclusions

Due to the soft handoff operations, our analysis and simulation results show that the Gaussian approximation of multi-cell, multi-user interference is also very good for a system with mixed traffic types.

With a higher PG, a higher capacity per MHz will be achieved. This conclusion supports and generalizes the conclusion suggested in [43] that by using a wider bandwidth, a higher bandwidth efficiency can be achieved. The impact of the choice of line

rate is examined. The value of line rate determines the PG and ACF. Since a large PG is more efficient in increasing the capacity than a small ACF. The lowest possible line rate is desired in regard to maximizing the capacity of mixed traffic. The effect of subdividing a high rate service into parallel streams on the capacity is minimal in the reverse link.

The radio capacity or overall throughput of a CDMA cellular system with multiple traffic can be increased significantly by assigning suitable power to different traffic types. The optimum power is mainly determined by the quality requirements of different traffic types. This optimal power assignment can be approximated in a very simple way as indicated by our analysis.

Table 6.1 The optimum relative power and energy per bit of video with various Quality Requirements (QR). For voice: QR is 7 dB, bit rate Rs is 9.6 Kbps, ACF is 0.375, PG is 1024; For video: Rv is 76.8 Kbps, PG=128, total bandwidth assumed is 10 MHz. Power control and handoff are assumed to be perfect.

Video QR (dB)	4	6	7	8	9	10	11	12
E_{bv}/E_{bs}	0.50	0.79	0.98	1.23	1.54	1.93	2.39	2.99
P_v/P_s	4.00	6.32	7.84	9.84	12.32	15.44	19.51	23.92
E_{bv}/E_{bs} approx.	0.50	0.80	1.00	1.26	1.59	2.00	2.52	3.17

Table 6.2 The radio capacity of voice users given certain number of video users. For voice: QR is 7 dB, bit rate Rs is 9.6 Kbps, ACF is 0.375, PG is 1024; For video: Rv is 76.8Kbps, PG is 128, total bandwidth assumed is 10 MHz. Power control and handoff are assumed to be perfect.

QR (dB) (Video)	Video No.	0	1	2	3	4	6	8	11
4	Equal E_b	302	274	247	221	195	144	94	19
	Optimum E_b	302	290	278	266	254	231	208	173
	% Improvement	0%	6%	13%	20%	30%	60%	121%	811%
7	Equal E_b	302	274	247	221	195	144	94	19
	Optimum E_b	302	275	248	223	197	147	97	24
	% Improvement	0%	0.4%	0.4%	0.9%	1.0%	2.0%	3.2%	26%
10	Equal E_b	302	117	89	62	35			
	Optimum E_b	302	239	180	125	71			
	% Improvement	0%	104%	102%	102%	103%			
12	Equal E_b	302	59	29	1				
	Optimum E_b	302	192	97	8				
	% Improvement	0%	225%	234%	700%				

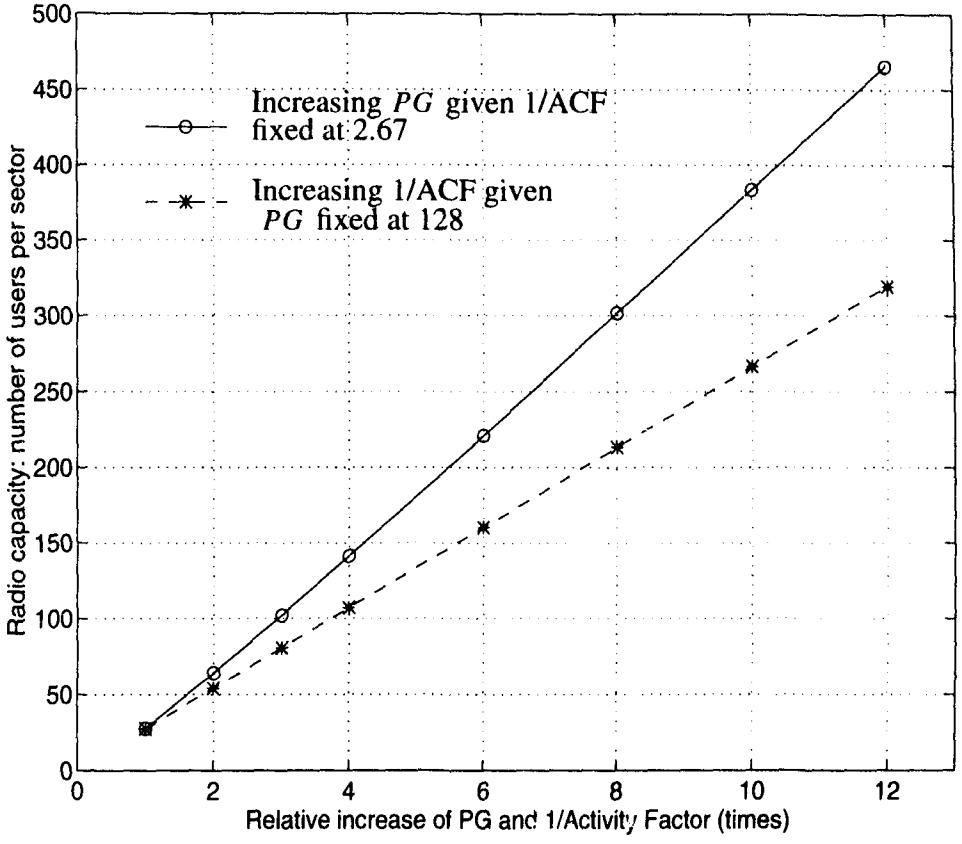

Fig. 6.2 The effect of PG and ACF on radio capacity. The start point is: PG0=128, 1/ACF0=2.67 (1/0.375), QR is 7 dB. Relative increase of PG and 1/ACF is in terms of PG/PG0 and ACF0/ACF.

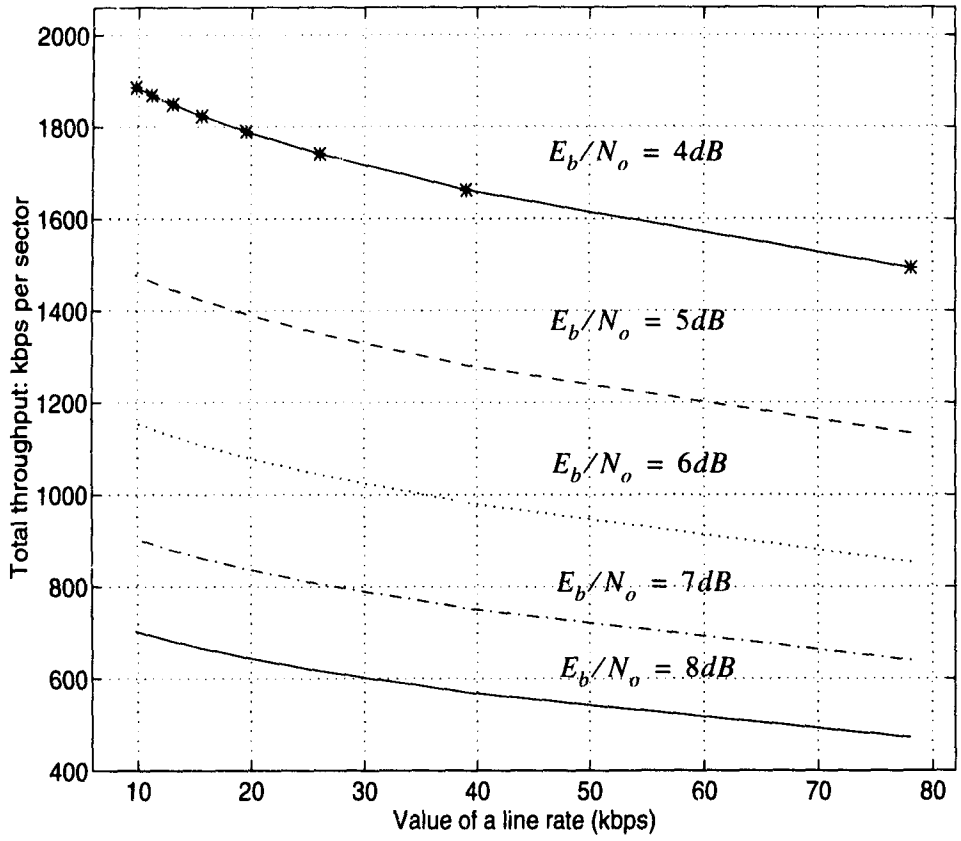

Fig. 6.3 The impact of the choice of line rate on the capacity of a system with low rate users. Voice traffic of 8 Kbps information rate (9.6 Kbps source rate) is assumed. PG is 1024. ACF is 0.375. Power control and handoff are assumed to be perfect.

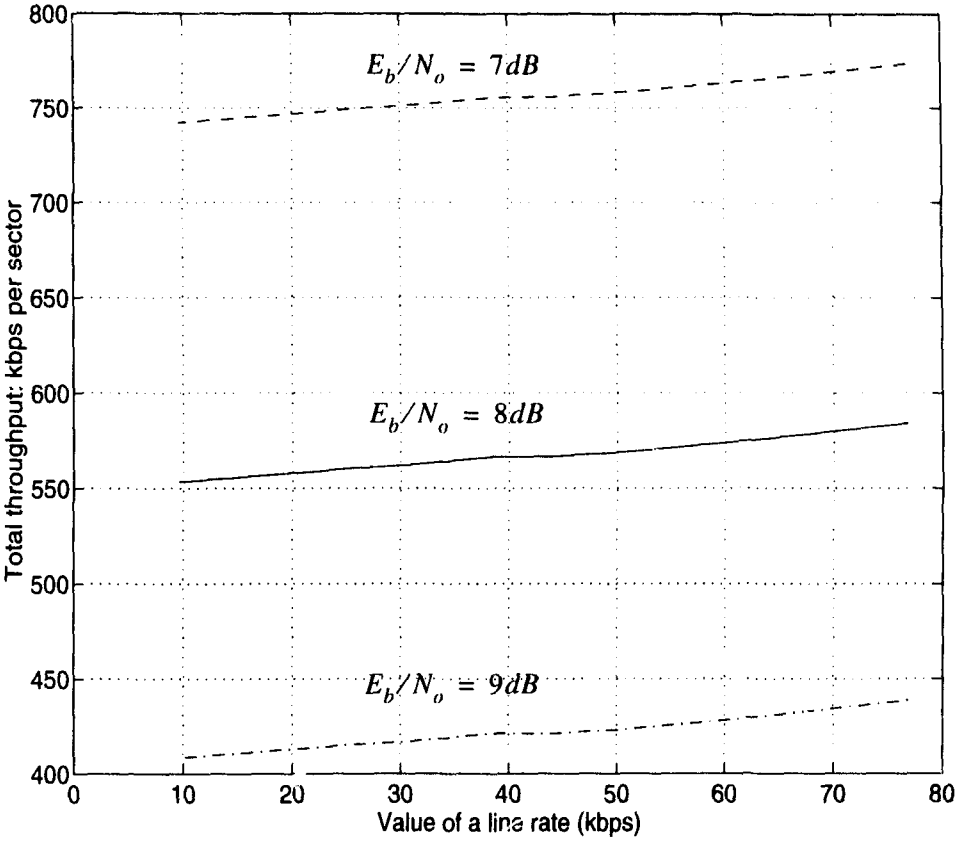

Fig. 6.4 The impact of the choice of line rate on capacity of a system with only high rate users. Video traffic of 64 Kbps information rate (76.8 Kbps source rate) is assumed. PG is 128. ACF of video is 1. No orthogonal protection is added for sub-divided parallel streams. Power control and handoff are assumed to be perfect.

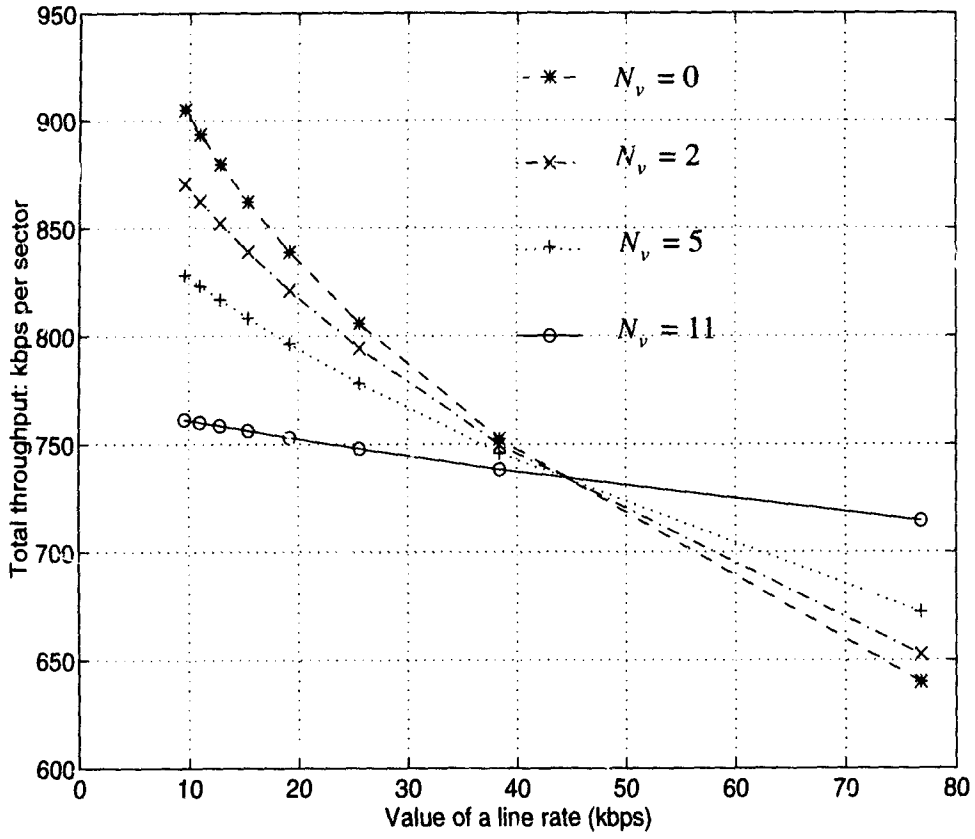

Fig. 6.5 The impact of the choice of line rate on capacity of a system with mixed rate traffic. 9.6 Kbps voice traffic and 76.8 Kbps video traffic are considered. The QR of 7 dB for both voice and video is assumed. Both are stream type of traffic with the same energy per bit.

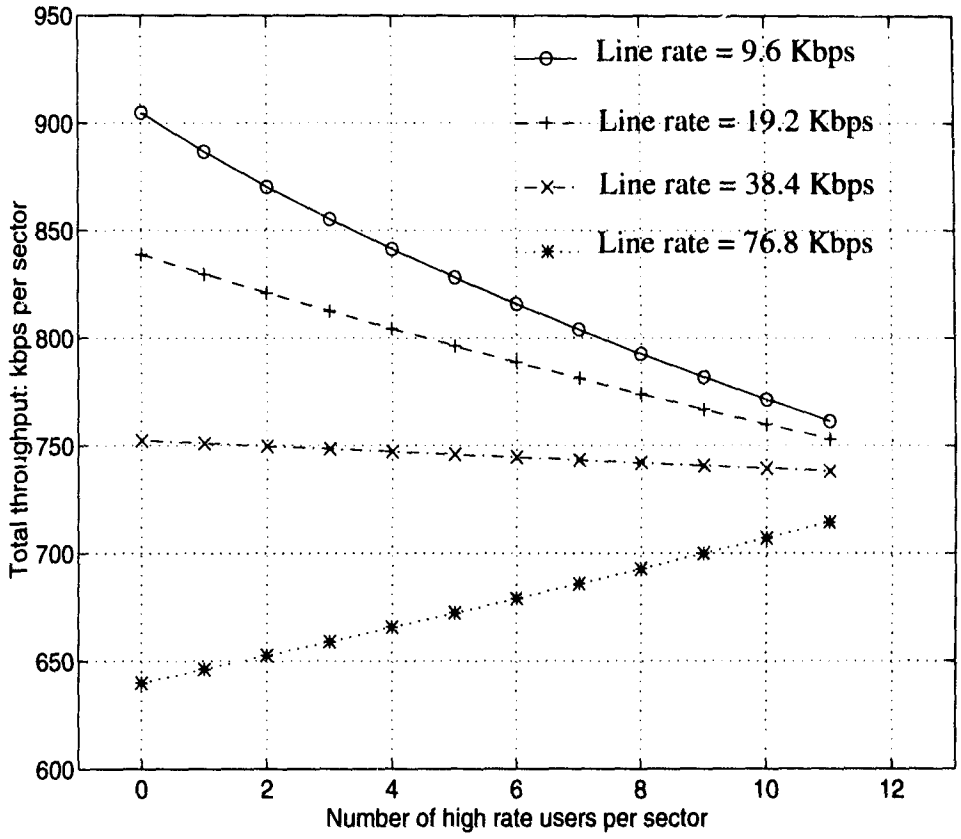

Fig. 6.6 Total throughput versus number of high rate users when different line rate is employed. 9.6 Kbps voice traffic and 76.8 Kbps video traffic are considered. The QR of 7dB for both voice and video is assumed. Both are stream type of traffic with the same energy per bit.

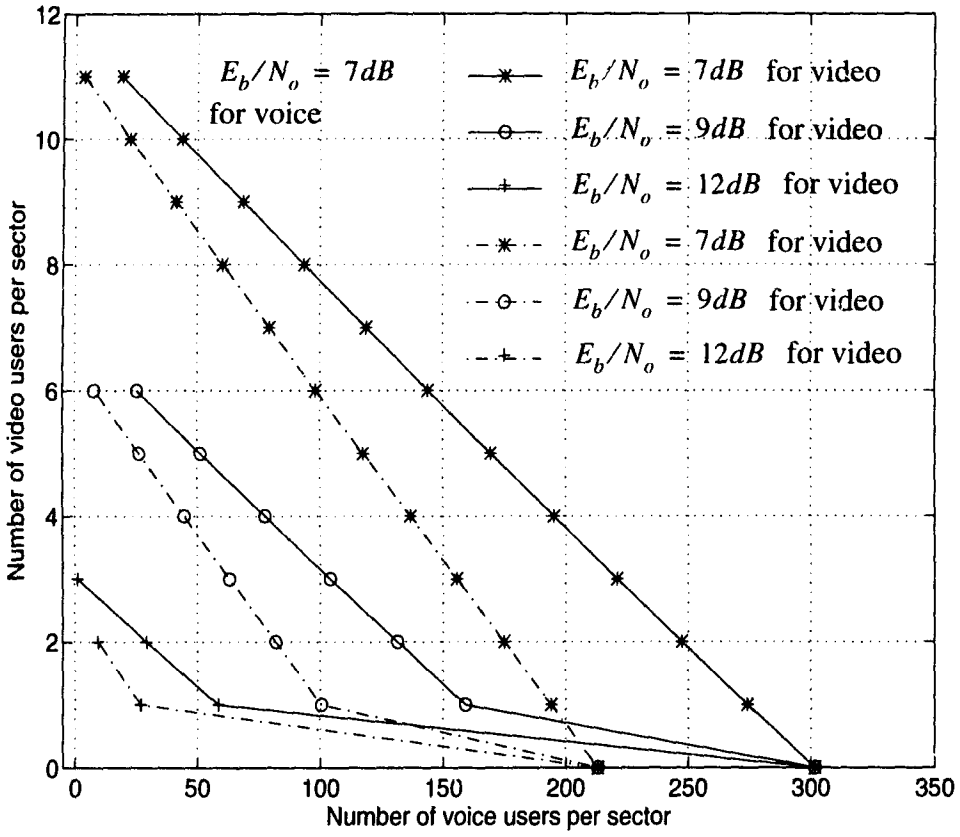

Fig. 6.7 Number of video users versus number of voice users. The solid line represents that different traffic types are transmitted at their own source rate. The dashdot line represents that voice and video are transmitted at a single line rate of 76.8 Kbps.

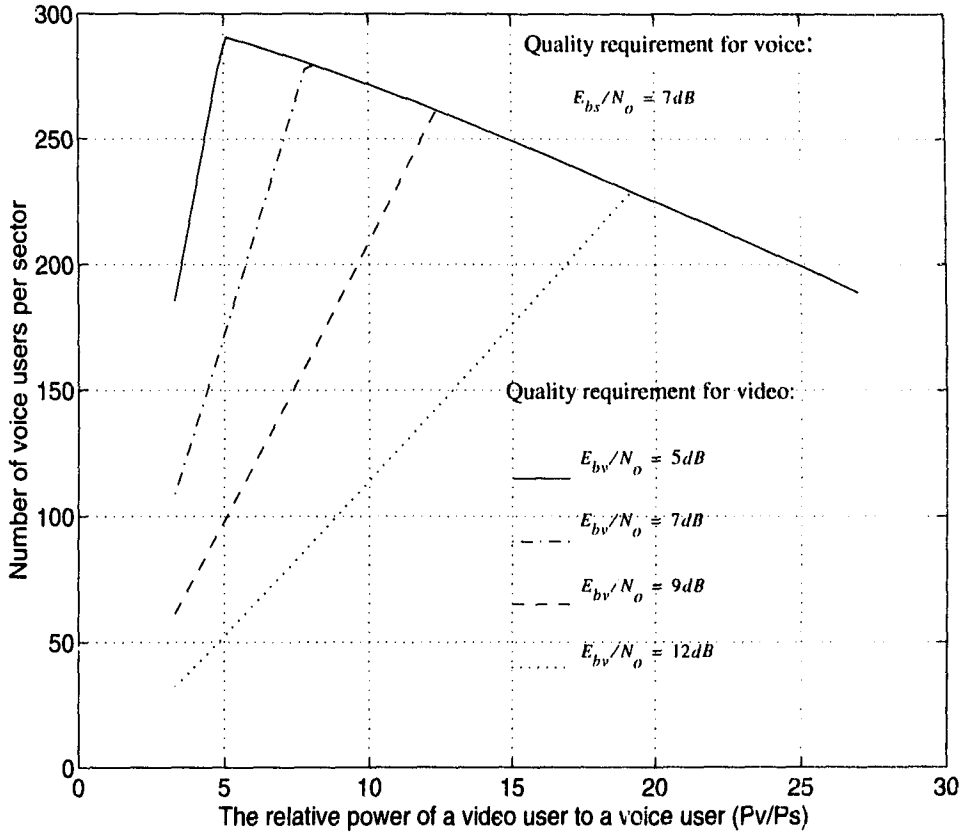

Fig. 6.8 Radio capacity of voice user per sector versus the relative power for video, Pv/Ps, given that the number of video is 1. For voice: QR is 7 dB, bit rate Rs is 9.6 Kbps, ACF is 0.375, PG is 1024; For video: Rv is 76.8 Kbps, PG is 128, total bandwidth is 10MHz. Power control and handoff are assumed to be perfect.

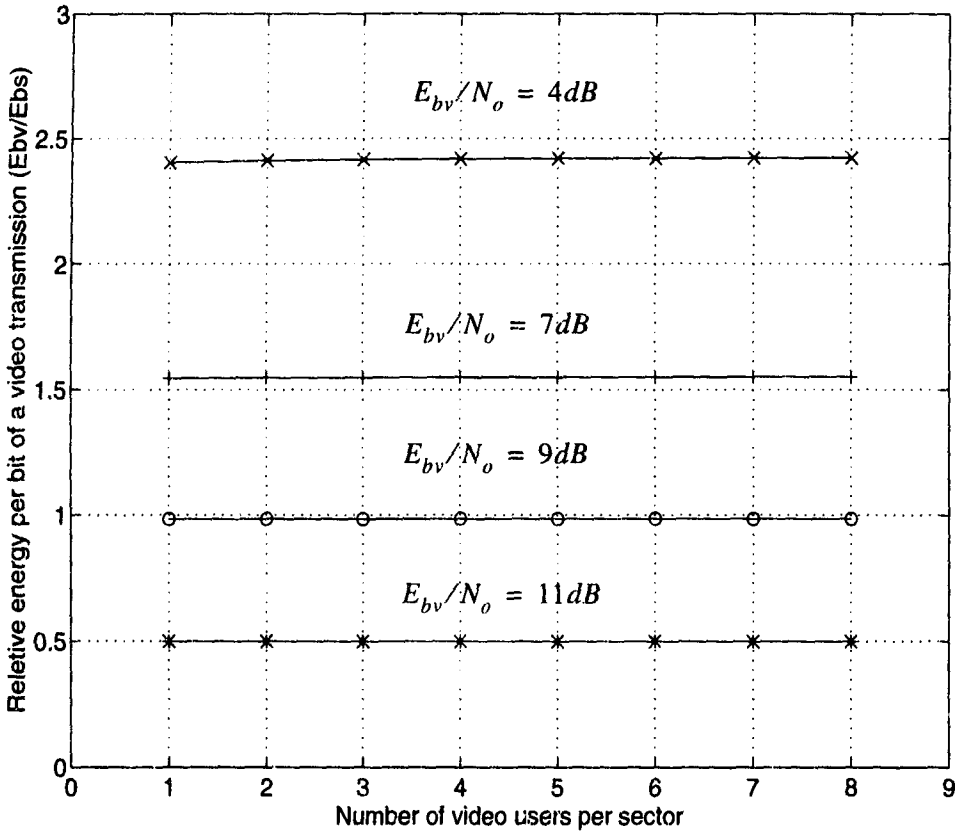

Fig. 6.9 The effect of traffic components on the optimum relative energy per bit. For voice: QR is 7 dB, bit rate Rs is 9.6 Kbps, ACF is 0.375, PG is 1024; For video: Rv is 76.8 Kbps, PG is 128, total bandwidth is 10 MHz. Power control and handoff are assumed to be perfect.

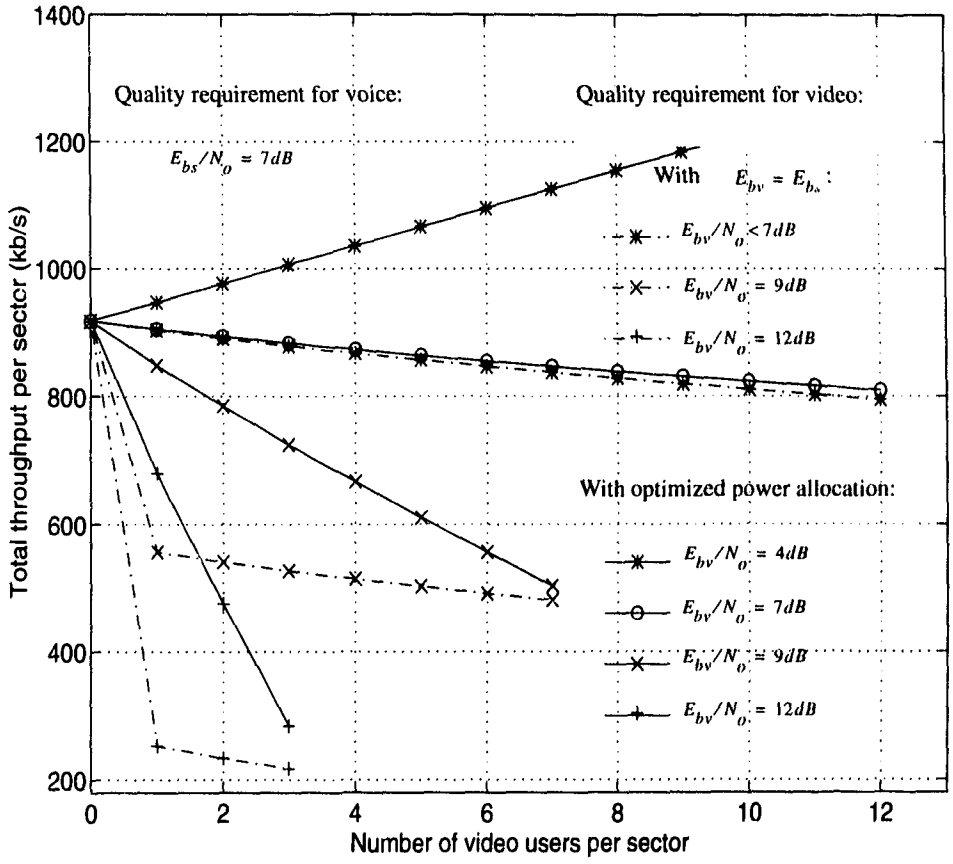

Fig. 6.10 Increasing the total throughput via optimized power allocation. For voice: QR is 7 dB, bit rate Rs is 9.6 Kbps, ACF is 0.375, PG is 1024; For video: Rv is 76.8 Kbps, PG is 128, total bandwidth is 10 MHz. Power control and handoff are assumed to be perfect.

Chapter 7

On the Simulation of CDMA Cellular Systems

7.1 Introduction

Since a communication system is usually very complicated, to evaluate a system's performance, we depend largely on simulations. The reasons for this are: 1. In a lot of cases the problems are too complicated to be analyzed, and simulations have to be employed for performance evaluation; 2. In certain situations, people want to simplify problems by developing models, making approximations and deriving bounds. All these types of analytical results have to be justified by simulations; 3. To save costs, computer simulation becomes a "must" step for system design engineers before going to the stage of prototype [58].

Due to the complexity of a communication system, simulation is a very difficult task. Enormous programming work has to be involved and large amounts of computing time and/or space are often required. With the development of computer technologies, simulating more and more complex systems becomes possible. Since simulation is often very time consuming, efficient simulation methods must be studied and developed to minimize simulation time, while keeping the accuracy of the results within an accepted range.

In a CDMA cellular system, the performance of the system is affected by many factors such as: mobile channel characteristics, location and distribution of users, cell geom-

etry, handoff and cell site diversity, power control, multipath combining schemes and coding schemes, as well as the traffic profile, etc. Therefore, a very complicated situation appears in the simulation of a CDMA cellular system. Great efforts have been made in this aspect [33], [44], [48]. Since there are a large number of random variables in a CDMA cellular system, the simulation methods used must primarily be of the Monte Carlo type. Normally, it is very time consuming to obtain the final result through the conventional Monte Carlo method. Therefore, efficient simulation methods should be used where applicable. In [44], a novel idea of the core sample technique is introduced. In essence, this method reduces simulation time from $O(n_c^2)$ to $O(n_c)$ at the expense of requiring a large memory space. We can see that in certain cases, core simulation samples can be obtained by only one simulation run, the results for different conditions can be obtained by properly processing the core samples. Repeated simulation runs are avoided and the simulation time can be significantly reduced.

Among the efficient simulation methods, the method being used most frequently is the so called Importance Sampling (IS) method. The conventional Monte Carlo method is inefficient because the estimation of events that occur infrequently may require considerable computational efforts and time. In the simulation of communication systems, K. S. Shanmugam and P. Balaban first introduced a modified Monte Carlo method to estimate error probability [59], [60]. Their basic idea was to modify the probability density function of a random process to be sampled, so as to make the "important" samples, which rarely occur, take place more frequently. Therefore, this method is called Importance Sampling. The number of samples needed for simulation can be reduced significantly by using IS.

Following [59], [60], there have been substantial research activities related to IS [61]-[69]. Most of them are related to the IS application of estimating bit error probabilities. The distribution of the random process is Gaussian, and the system is assumed to be linear and memory-less [66]. Many optimum bias schemes have been suggested, e.g., [62],

[66].

In this chapter, we will discuss several efficient simulation methods.

7.2 The Monte Carlo Method

We start our discussion on the Monte Carlo method. Assuming that the event Z happens with a probability p. The Monte Carlo estimator of p is formed on the basis of N trials:

$$\hat{p} = \frac{1}{N}\sum_{i=1}^{N} Z_i \tag{7.1}$$

where Z_i is a random variable. $Z_1 = 1$ with probability p; $Z_1 = 0$ with probability $1 = p$. The mean of this estimation is

$$E(\hat{p}) = \frac{1}{N}\sum_{i=1}^{N} E(Z_i) \approx p. \tag{7.2}$$

Now, we consider event Z which is related to a random variable x with probability density function $f(x)$. For convenience, the range of x which is denoted as Φ is divided into I and $\bar{I}$ which represent different decision regions. We have $I \cup \bar{I} = \Phi$ and $I \cap \bar{I} = 0$. Then, we have

$$Z_i = \begin{cases} 1 & x \in I \text{ with probability } p \\ 0 & x \in \bar{I} \text{ with probability } 1-p. \end{cases} \tag{7.3}$$

Ideally, we have

$$E(\hat{p}) = E(Z_i) = \int_I f(x)\,dx = p. \tag{7.4}$$

Therefore $\hat{p}$ is an unbiased estimator of p. The variance of the Monte Carlo estimation is

$$\sigma_{\hat{p}}^2 = \frac{1}{N}D(Z_i) = \frac{1}{N}(p - p^2). \tag{7.5}$$

Checking the variance of a Monte Carlo estimator, we may find that the smaller the value of p, the smaller the variance $\sigma_{\hat{p}}^2$ will be. But why for a smaller p, do we need to take more samples for estimating p? The reason is that the accuracy of an estimation is also related to p.

To show this, we should investigate the confidence interval of a Monte Carlo estimator. From [69], [58], we see that if the trial number $N \to \infty$, then the distribution of $\hat{p}$ is normal without imposing any condition on p. The mean and variance of the estimator $\hat{p}$ are p and $p(1-p)/N$, respectively. One can construct a confidence interval in the form [69]:

$$P\left\{\frac{N}{N+g_\alpha^2}\left[\hat{p}+\frac{g_\alpha^2}{2N}-g_\alpha\sqrt{\frac{\hat{p}(1-\hat{p})}{N}+\left(\frac{g_\alpha}{2N}\right)^2}\right]\le p \le \frac{N}{N+g_\alpha^2}\left[\hat{p}+\frac{g_\alpha^2}{2N}+g_\alpha\sqrt{\frac{\hat{p}(1-\hat{p})}{N}+\left(\frac{g_\alpha}{2N}\right)^2}\right]\right\} = 1-\alpha \tag{7.6}$$

where $0<\alpha<1/2$ and g_α is chosen such that

$$\int_{-g_\alpha}^{g_\alpha}\frac{1}{\sqrt{2\pi}}e^{-\frac{t^2}{2}}dt = 1-\alpha. \tag{7.7}$$

If the trial number N is large enough, the confidence interval can be well approximated by this approach. Since a simulation should be carried out with enough confidence on the results, to warrant its undertaking it can be assumed that g_α will be chosen such that $1-\alpha \approx 1$. Then the Equation (7.6) can be directly written as

$$\frac{N}{N+g_\alpha^2}\left[\hat{p}+\frac{g_\alpha^2}{2N}-g_\alpha\sqrt{\frac{\hat{p}(1-\hat{p})}{N}+\left(\frac{g_\alpha}{2N}\right)^2}\right]\le p \le \frac{N}{N+g_\alpha^2}\left[\hat{p}+\frac{g_\alpha^2}{2N}+g_\alpha\sqrt{\frac{\hat{p}(1-\hat{p})}{N}+\left(\frac{g_\alpha}{2N}\right)^2}\right]. \tag{7.8}$$

To analyze the relationship between N and $\hat{p}$, we use the upper bound without loss of generality. That is

$$p \le p + \varepsilon = kp = \frac{N}{N + g_\alpha^2}\left[\hat{p} + \frac{g_\alpha^2}{2N} + g_\alpha\sqrt{\frac{\hat{p}(1-\hat{p})}{N} + \left(\frac{g_\alpha}{2N}\right)^2}\right]. \tag{7.9}$$

If N is large enough, $\frac{N}{N + g_\alpha^2} \approx 1$. Then:

$$(k-1)\hat{p} \approx \frac{g_\alpha^2}{2N} + g_\alpha\sqrt{\frac{\hat{p}(1-\hat{p})}{N} + \left(\frac{g_\alpha}{2N}\right)^2} \tag{7.10}$$

where k is a constant related to the estimation accuracy required. It is generally accepted that k should be in a range of $1 \sim 2$ [69]. From Equation (7.10) we have

$$N = \frac{kg_\alpha^2}{\hat{p}(k-1)^2} - \frac{g_\alpha^2}{(k-1)^2}. \tag{7.11}$$

Obviously, if $\hat{p}$ is larger, the required N is less for a given confidence interval and level. This means that if an estimation is accurate enough, a larger $\hat{p}$ results from a larger p. To estimate a larger p, a smaller sample number, N, is required. We can also see that if more confidence is required, thus to increase g_α^2, a larger number of trails, N, is needed. A narrower confidence interval requires a smaller k, and in that case also, a larger N is required. From this, we can see that if we modify the distribution of the random variables to be sampled such that we make the random variable x occur in I with a higher probability $\hat{p}$, the number of trials required can be reduced for the same relative confidence interval.

7.3 Importance Sampling

From the previous discussion, we show that the Monte Carlo method is inefficient because the trial (or sample) number is related to the probability, p, which we are going

to estimate. When p is very small, a large number of trials, N, is required. If samples are within I with probability p, and p is very small, samples which belong to I are considered to be more "important". It will take an extremely long time to wait for the samples which belong to I to come. To solve this problem, K.S. Shanmugan and P. Balaban have introduced a modified Monte Carlo method to estimate error probabilities in digital communication systems. The number of samples needed for simulation is reduced considerably by using IS. The reason, as was previously analyzed, is that the probability to be estimated is artificially increased. Most of the works are limited on the IS application of estimating bit error probabilities, and the PDF of the random variable is Gaussian. As well, the system is assumed to be linear and memory-less [66]. Under these conditions, the problem becomes relatively simple. The reason for this is that if the input of a linear memory-less system is Gaussian, the output of the system is also Gaussian. The distribution of the input process can be modified based on the requirement of the decision making part at the system output end. Thus, if we know how much an input process is adjusted, then we know how much the PDF of the output process is affected. There are some works related to applying IS to non-Gaussian problems [59]. G.C. Orusk and B. Aazhang applied IS to simulate multiuser communication systems in a most recent paper [65]. Their work is still based on the assumption of the Gaussian distribution.

Following [60], the distribution of a random process is modified in an approach called biasing by modifying the distribution function $f(x)$ in Equation (7.4) to a new distribution $g(x)$. $g(x)$ will be chosen such that the bias function $B(x) = g(x)/f(x) > 1$ for $x \in I$. As a result, the event that x is in I will occur more frequently. Considering a new event Z_i^I which is related to x with a new PDF $g(x)$, we have

$$Z_i^I = \begin{cases} \dfrac{1}{B(x)} & x \in I \text{ with probability } p^* \\ 0 & x \in \bar{I} \text{ with probability } 1-p^* \end{cases} \tag{7.12}$$

where p^* is the probability that x belongs to I. The mean of this new estimator is

$$E\left(Z_i^I(x)\right) = \int_I \frac{g(x)}{B(x)}\mathrm{d}x = \int_I f(x)\,\mathrm{d}x. \tag{7.13}$$

The new estimator based on the transformation of the random process is formed as

$$\hat{p}^I = \frac{1}{N}\sum_{i=1}^{N} Z_i^I(x). \tag{7.14}$$

Because $E(\hat{p}^I) = E\left(Z_i^I\right) = p$, $\hat{p}^I$ is also an unbiased estimator of p. The variance of the estimator $\hat{p}^I$ is

$$\sigma_{\hat{p}^I}^2 = \frac{E\left(\left(Z_i^I(x)\right)^2\right) - \left(E\left(Z_i^I(x)\right)\right)^2}{N} = \frac{\int_I \frac{f(x)}{B(x)}\mathrm{d}x - p^2}{N}. \tag{7.15}$$

Comparing Equations (7.15) and (7.5), we see that if N is the same, as long as $\int_I \frac{f(x)}{B(x)}\mathrm{d}x < p$, there is $\sigma_{\hat{p}}^2 > \sigma_{\hat{p}^I}^2$. Specifically, if $B(x) > 1$, $\forall x \in I$, $\sigma_{\hat{p}}^2 > \sigma_{\hat{p}^I}^2$. If we take $1/p$ as $B(x)$, $\sigma_{\hat{p}^I}^2 = 0$. Comparing IS with the conventional Monte Carlo method, if the variance of the estimators accepted is the same, from Equations (7.5) and (7.15), we have

$$\frac{p(1-p)}{N} = \frac{\int_I \frac{f(x)}{B(x)}\mathrm{d}x - p^2}{N_{IS}}. \tag{7.16}$$

The sample size savings factor is

$$r = \frac{N}{N_{IS}} = \frac{p(1-p)}{\int_I \frac{f(x)}{B(x)}\mathrm{d}x - p^2} = \frac{\sigma_{\hat{p}}^2}{\sigma_{\hat{p}^I}^2}. \tag{7.17}$$

The above is the conventional approach to the IS method. In practice, the samples which

belong to either I or $\bar{I}$ may be taken for further processing. To estimate the statistic effect based on the region division of I and $\bar{I}$ to the further sample usage, we form an equivalent IS estimator as follows

$$Z_i^* = \begin{cases} 1 & x \in I \text{ with probability } p^* \\ 0 & x \in \bar{I} \text{ with probability } 1 - p^*, \end{cases} \tag{7.18}$$

and

$$\hat{p}^* = \frac{1}{N} \sum_{i=1}^{N} Z_i^*. \tag{7.19}$$

The mean of this estimator is

$$E\left(Z_i^* \right) = \int_I g(x)\, dx = p^* \tag{7.20}$$

where $g(x) = B(x) f(x)$ and $B(x) > 1$, $\forall x \in I$. Let

$$k = \frac{p^*}{p} = \frac{\int_I B(x) f(x)\, dx}{\int_I f(x)\, dx}. \tag{7.21}$$

We may get the estimation of p from the estimation of p^*, given that $\hat{p}^*$ is accurate enough, thus

$$\hat{p}_o = \frac{1}{k} \hat{p}^* \tag{7.22}$$

where $\hat{p}_o$ is the estimation of p using this new IS approach. The variance of the estimator $\hat{p}^*$ is

$$\sigma_{\hat{p}^*}^2 = \frac{p^*(1 - p^*)}{N} = \frac{kp(1 - kp)}{N}. \tag{7.23}$$

The variance of the estimator $\hat{p}_o$ is

$$\sigma^2_{\hat{p}_o} = E((\hat{p}-p)^2) = \frac{1}{k^2}E((\hat{p}^*-p^*)^2) = \frac{1}{k^2}\sigma^2_{\hat{p}^*}, \tag{7.24}$$

and thus

$$\sigma^2_{\hat{p}_o} = \frac{\frac{p}{k}-p^2}{N} = \frac{p^2\left(\frac{1}{p^*}-1\right)}{N}. \tag{7.25}$$

Then we get the sample number saving factor as

$$r = \frac{\sigma^2_{\hat{p}}}{\sigma^2_{\hat{p}_o}}. \tag{7.26}$$

Comparing Equations (7.25) and (7.5), we can also see if $B(x) > 1$, $\sigma^2_{\hat{p}_o} < \sigma^2_{\hat{p}}$, $\forall x \in I$. After comparing Equations (7.25) and (7.15), we find that if $B(x)$ is a constant they are identical. For the estimator $\hat{p}_o$, $\sigma^2_{\hat{p}_o}$ is only affected by the result of $\int_I B(x)f(x)\,dx$. A different $B(x)$ may lead to the same variance of the estimator, as long as p^* is the same.

An IS estimator is normally focused on the estimation of p. People always try to optimize the estimator in terms of the accuracy of $\hat{p}^I$. We often find a lot of optimum bias schemes [66] which tend to modify $f(x)$ to

$$g(x) = \begin{cases} B(x)f(x) & x \in I \\ 0 & x \in \bar{I}. \end{cases} \tag{7.27}$$

This means that all the samples from the modified process belong to I. No sample belonging to $\bar{I}$ is available. In practice, the samples belonging to $\bar{I}$ are usually of the same importance as the samples belonging to I, especially in the cases that the samples are reused by the system. The straight forward idea is to find a $B(x)$ such that

$$\int_I g(x)\,dx = \int_I B(x)f(x)\,dx$$
$$= \int_{\bar{I}} g(x)\,dx = \int_{\bar{I}} B(x)f(x)\,dx = \frac{1}{2}. \tag{7.28}$$

We find it is an optimum modification by analyze the "whole" estimator [70].

7.4 The Whole Estimator

For a conventional estimator, if an accurate $\hat{p}^I$ is obtained, its reverse part, $\hat{q}^I = 1 - \hat{p}^I$, will also be obtained with the same accuracy. But if the samples are taken for further usage in the same simulation process, the performance of the system will be affected. For example, when simulating a system with ARQ, the system may not work properly if the noise is over biased. To show the statistical effect of the bias on the whole system, we use two independent estimators to estimate both p and q at the same time. We call this pair of estimators the whole estimator. The performance of the whole estimator is discussed in this section.

To investigate the reverse part of a Monte Carlo estimator, we have

$$R_i = \begin{cases} 1 & x \in I \text{ with probability } q = 1-p \\ 0 & x \in \bar{I} \text{ with probability } p \end{cases} \tag{7.29}$$

and the estimator is

$$\hat{q} = \frac{1}{N}\sum_{i=1}^{N} R_i, \tag{7.30}$$

then similar to the estimator $\hat{p}$

$$E(R_i) = q = 1-p, \tag{7.31}$$

$$D(R_i) = E\left(R_i^2\right) - E^2(R_i) = p - p^2 \tag{7.32}$$

and

$$\sigma_{\hat{q}}^2 = \frac{D(R_i)}{N} = \frac{p - p^2}{N}. \tag{7.33}$$

Comparing Equations (7.33) and (7.5), it is obvious that for a conventional Monte Carlo estimator, $\sigma_{\hat{q}}^2 = \sigma_{\hat{p}}^2$. Because $\hat{p}$ and $\hat{q}$ are independent Gaussian random variables, the variance of the whole estimator should be:

$$\sigma_w^2 = \sigma_{\hat{p}}^2 + \sigma_{\hat{q}}^2 = \frac{2}{N}(p(1-p)). \tag{7.34}$$

When we apply the IS method, after biasing, we have:

$$R_i = \begin{cases} 1 & x \in I \text{ with probability } q^* = 1 - p^* \\ 0 & x \in \bar{I} \text{ with probability } p^*. \end{cases} \tag{7.35}$$

and

$$k_1 = \frac{q^*}{q} = \frac{\int_I g(x)\,dx}{\int_I f(x)\,dx}. \tag{7.36}$$

then similar to $\hat{p}_o$,

$$\hat{q}_o = \frac{1}{k_1}\hat{q}^*. \tag{7.37}$$

The variance of the estimator at the reverse part is:

$$\sigma_{\hat{q}^*}^2 = \frac{q^*(1-q^*)}{N} \simeq \frac{k_1 q(1 - k_1 q)}{N} \tag{7.38}$$

and

$$\sigma_{\hat{q}_o}^2 = \frac{\sigma_{\hat{q}^*}^2}{k_1^2} = \frac{\frac{q}{k_1} - q^2}{N} = \frac{q^2\left(\frac{1}{q^*} - 1\right)}{N} = \frac{(1-p)^2\left(\frac{1}{1-p^*} - 1\right)}{N}. \tag{7.39}$$

The variance of the whole IS estimator is

$$\begin{aligned}\sigma_w^2 &= \sigma_{\hat{p}_o}^2 + \sigma_{\hat{q}_o}^2 \\ &= \frac{1}{N}\left(p^2\left(\frac{1}{p^*}-1\right)+(1-p)^2\left(\frac{1}{1-p^*}-1\right)\right).\end{aligned} \tag{7.40}$$

We want to find a p_o^* such that σ_w^2 is minimum. This forms an optimization problem. Note that p and p^* are under the constraint $0 \le p \le 1$ and $0 \le p^* \le 1$. Let $J = N\sigma_w^2$, we have

$$J = \frac{1}{(1-p^*)p^*}(p^2 - 2p^2p^* + p^{*2} - 2pp^{*2} + 2p^2p^{*2}), \tag{7.41}$$

then

$$\frac{dJ}{dp^*} = (p^{*2} - 2pp^{*2} + 2p^2p^* - p^2)\frac{1}{(p^* - p^{*2})^2}. \tag{7.42}$$

Solving

$$p^{*2} - 2pp^{*2} + 2p^2p^* - p^2 = 0, \tag{7.43}$$

we get the only valid solution $p_o^* = p$. This means that any modification of the distribution of a random process to be sampled will lead to increasing the variance of the whole estimator. In the case that samples are reused by a system, as long as you do the biasing, the variance of the estimation will be increased. There is a statistic effect on the overall system performance when we employ the biasing.

The question is whether an increased variance is acceptable. In practice, we are concerned more with the estimation accuracy than with the variance. For example, to estimate a large p, say, $p = 0.3$, the error of $\hat{p}$ may be acceptable within a range of 10^{-2}. If $p = 10^{-6}$ and the error of $\hat{p}$ is at a degree of 10^{-4}, this error of $\hat{p}$ is not acceptable, although the variance of the later is smaller than the former. From section 3.1, we know that for a specific relative confidence interval and confidence level, an increased p leads

to reducing the sample number N (see Equation (7.11)), although at the same time, the variance of a Monte Carlo estimator is increased (see Equation (7.5)). Therefore, here we examine if a better bias manner can be found in terms of minimizing the sample number required and keeping the relative confidence interval unchanged.

Here we only consider the upper bound of a confidence interval without loss of generality. Rewriting Equation (7.9), we have

$$p^* \le p^* + \varepsilon_1 = k_1 \hat{p}^* \tag{7.44}$$

and

$$q^* \le q^* + \varepsilon_2 = k_2 \hat{q}^*. \tag{7.45}$$

We assume the requirement on the confidence interval for both $\hat{p}^*$ and $\hat{q}^*$ is the same, thus, $k_1 = k_2 = k$. The confidence level is also g_α. From Equation (7.11) the sample number required for $\hat{p}^*$ is

$$N_1 = \frac{k g_\alpha^2}{\hat{p}^* (k-1)^2} - \frac{g_\alpha^2}{(k-1)^2} \tag{7.46}$$

and for $\hat{q}^*$ is

$$N_2 = \frac{k g_\alpha^2}{\hat{q}^* (k-1)^2} - \frac{g_\alpha^2}{(k-1)^2}. \tag{7.47}$$

We form an objective function

$$J_N = N_1 + N_2 = \frac{k g_\alpha^2}{\hat{p}^* (1-\hat{p}^*) (k-1)^2} - \frac{2 g_\alpha^2}{(k-1)^2} \tag{7.48}$$

Because $0 \le \hat{p}^* \le 1$, obviously, when $\hat{p}^* = 1 - \hat{p}^* = 1/2$, $\hat{p}^* (1-\hat{p}^*)$ is a maximum, then J_N is minimum. Note that if the estimation is accurate enough, $p^* \approx \hat{p}^*$. This result suggests that an optimum biased scheme should make samples occur in I and $\bar{I}$ with equal probability, thus, $p^* = 1/2$. This optimum is in terms of saving the number of

samples required under an unchanged relative confidence interval and confidence level.

7.5 Core Sample Techniques

In [44], a core sample technique is proposed for the simulation of a CDMA cellular system. The basic idea of this core sample technique is to use the additive nature of total interference in cellular CDMA. Specifically, to simulate a system of N_c cells and N_s mobiles per cell, we randomly distribute $N_c \cdot N_s$ users in N_c cells and collect simulation data. If the performance of a CDMA system with different N_s is going to be evaluated, conventional brute force simulation has to be performed for every different N_s to be concerned. A huge amount of simulation time is required. Since every user follows the same location distribution statistics and the total interference is additive, notice that $N_s \times N_c = N_s(1 \times N_c) = N_s(N_0 \times N_c)$, one simulation run for N_s users per cell is equivalent to N_s simulation runs for $N_0 = 1$, and summing N_s samples from different simulation runs. Data obtained by one simulation run for $N_0 = 1$ is referred to as a core sample. Data needed for different values of N_s can be deduced from the core samples. The resultant variance for different N_s is dependent on the total number of core samples and the value of N_s.

In the core sample method, a two-column array is employed for recording the simulation data including the power of the reference signal and total power of interference received at the reference base station.

The procedures and data structure of the core sample technique are basically as follows:

For $N_s = N_0$

i	total power received $I_{pi} = I_i + s_i$	desired signal s_i
1	I_{p1}	s_1
2	I_{p2}	s_2
⋮		

the interference to signal ratio (ISR) can then be obtained as $ISR_i = I_{pi}/s_i$ for $s_i \neq 0$.

Since the interference is additive, the simulation data for $N_s = 2N_0$ can be obtained from the simulation for $N_s = N_0$ in the following way:

For $N_s = 2N_0$

i	total power received $I_{pi}^{(2)} = I_{p2i-1} + I_{p2i}$	desired signal $s_i^{(2)}$
1	$I_{p1}^{(2)}$	$s_1^{(2)}$
2	$I_{p2}^{(2)}$	$s_2^{(2)}$
⋮		

where $s_i^{(2)}$ is randomly chosen to be either s_{2i-1} or s_{2i} if both s_{2i-1} and s_{2i} are non-zero; $s_i^{(2)}$ is zero if both s_{2i-1} and s_{2i} are zero; $s_i^{(2)} = s_{2i-1} + s_{2i}$ otherwise. Follow-

ing the same procedure, the final simulation results can be obtained when $N_s = nN_0$.

7.6 Common Random Numbers

The basic idea of the Common Random Numbers (CRN) method is that we can compare the different systems by inputting the same random sequence to different systems [71]. We will be more confident on simulation results if any observed differences in performance are due to the differences in the choice of system parameters.

Assuming that Y_{1j} and Y_{2j} are the observations from the first and the second system, and that we want to observe the random variable $Z_j = Y_{1j} - Y_{2j}$ for $j = 1, 2, \ldots, n$, we have

$$E(Z_j) = E(Y_{1j}) - E(Y_{2j}) \tag{7.49}$$

and

$$E(Z_j) \approx \overline{Z}_n = \sum_{j=1}^{n} \frac{Z_i}{n}, \tag{7.50}$$

then

$$Var\left(\overline{Z}_n\right) = \frac{Var(Z_j)}{n} = \frac{Var(Y_{1j}) + Var(Y_{2j}) - 2Cov(Y_{1j}, Y_{2j})}{n}. \tag{7.51}$$

If $Cov(Y_{1j}, Y_{2j}) > 0$, then the variance $Var(\bar{Z}_n)$ can be reduced.

Whether the CRN method can be used depends on different systems and their relations. The CRN method works if and only if the covariance of the outputs of the two systems is greater than 0. The degree of the simulation variance reduction depends on the degree of the correlation of the outputs of the systems. If it is affordable, a preliminary check on the covariances or correlations between the output random variables of alternative systems should be made.

The drawback of the CRN method is that if the covariance of the two outputs is nega-

tive, it will increase the variance of the whole estimation. If the covariance or correlation of the outputs of the different systems can not be determined analytically before the simulation starts, extra computations have to be involved. It may also be time consuming. Great advantages can be obtained when CRN is used for parallel processing. For serial processing, the advantage in time saving will be reduced. The CRN method requires the synchronization of the inputs and the outputs of the alternative systems.

Because we will compare the performance of different schemes including different diversity, power control and cell geometry etc., the CRN method may be very useful for us. Usually, we only change some parameters to see the performance of the modified system. Therefore, the performance of the modified system may have a high probability of having positive correlation with the performance of the original system. As long as the requirements of CRN on the system's outputs can be met, the CRN method can be used in a straight forward manner.

7.7 Simulation Results of a CDMA Cellular System

Our analysis and modelling methods developed in previous chapters are justified by the simulation results. Figs. 7.1-7.4 show the PDFs of total interference power with different user number per sector. Similarly to what is shown in the previous analysis, here we can also see that the multi-cell, multi-user interference approaches the Gaussian distribution very rapidly due to soft handoff. Figs. 7.5 and 7.6 show the outage probability of an IS-95 CDMA cellular system. From these figures we can get the radio capacity of this system to be 28 and 36 voice users per sector for PG = 128 and PG = 156 respectively. When the total bandwidth is increased to 10 MHz, the outage probability of a CDMA cellular system with voice users is shown in Figs. 7.7 and 7.8 for PG = 1024 and PG = 1248 respectively. With the bandwidth of 10 MHz, if we use a line rate of 64Kbps to transmit voice signals, the voice activity factor changes from 0.375 to 0.047. The outage probability is shown in Figs. 7.9 and 7.10 when we use the 64 Kbps line rate

for transmission and keep the processing gain to be 128 and 156 respectively. Comparing Figs. 7.7 and 7.8 with Figs. 7.9 and 7.10, we show that there is about a 25% reduction in capacity due to using the 64 Kbps line rate. This confirms our conclusion obtained through previous analysis that for low rate users, a higher transmission line rate will lead to a more burst traffic, as a result, reduce the capacity of low rate users. Fig. 7.11 shows the outage probability when lognormal shadowing is weak with a standard deviation of $\sigma_{LN} = 2.5dB$. Comparing Figs. 7.11 with 7.6, we see that the effect of shadowing is greatly reduced by soft handoff and power control.

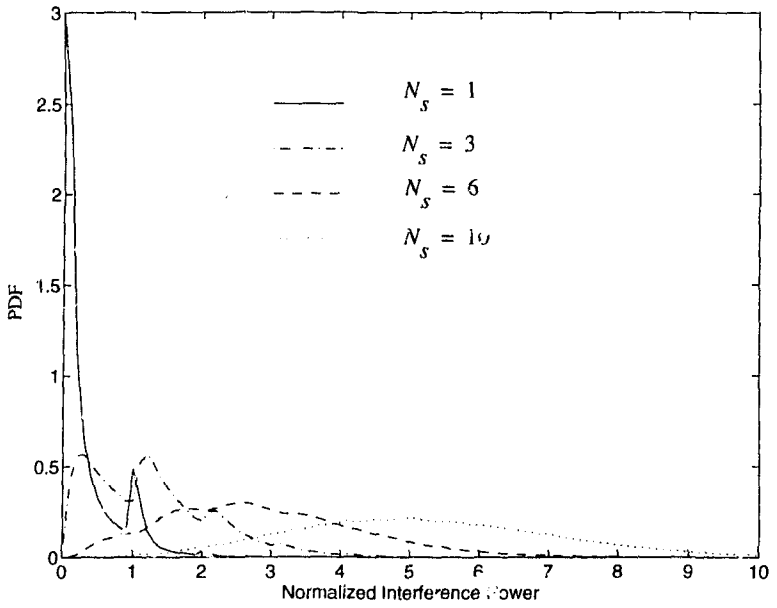

Fig. 7.1 Simulation results of PDFs of multi-cell, multi-user interference with different number of users per sector. Standard deviation of lognormal shadowing is σ_{LN} = 8 dB, Rs is 9.6 kb/s, activity factor is 0.375.

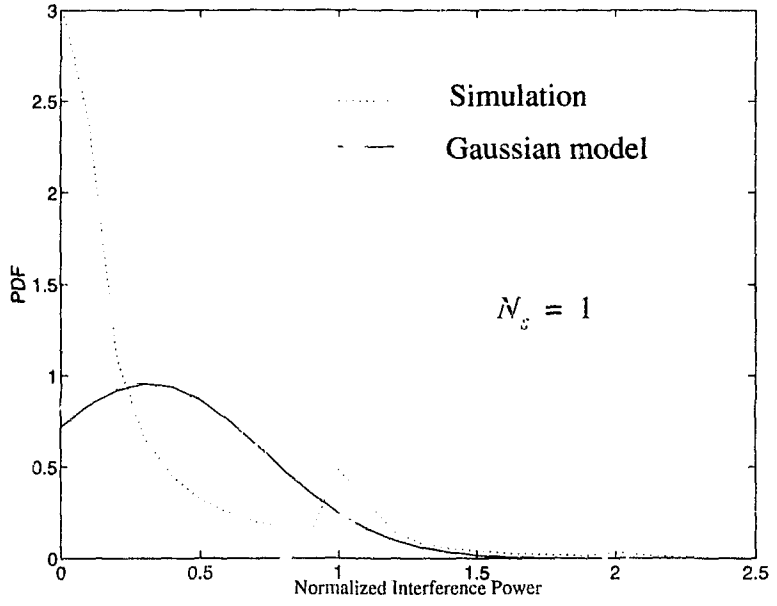

Fig. 7.2 PDF of the total interference. Standard deviation of log-normal shadowing is σ_{LN} = 8 dB, Rs is 9.6 kb/s, activity factor is 0.375, Ns=1.

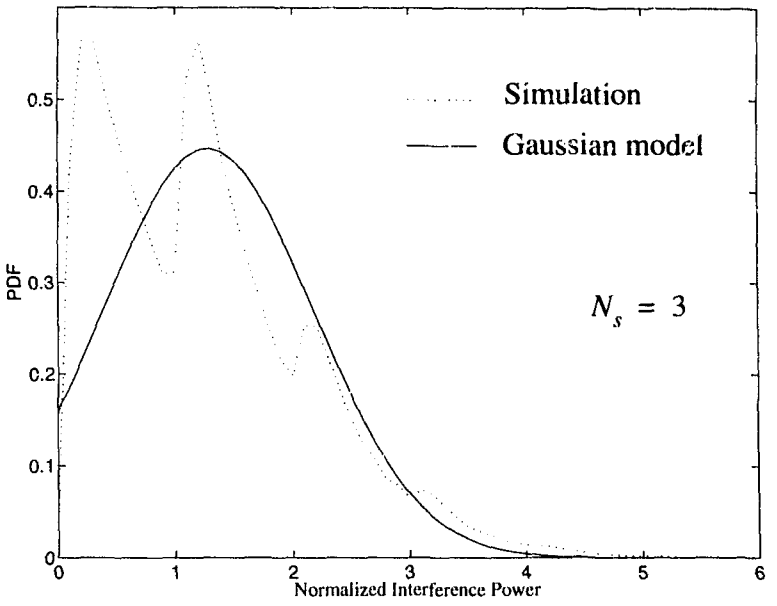

Fig. 7.3 PDF of the total interference. Standard deviation of lognormal shadowing is σ_{LN} = 8 dB, Rs is 9.6 kb/s, activity factor is 0.375, Ns=3.

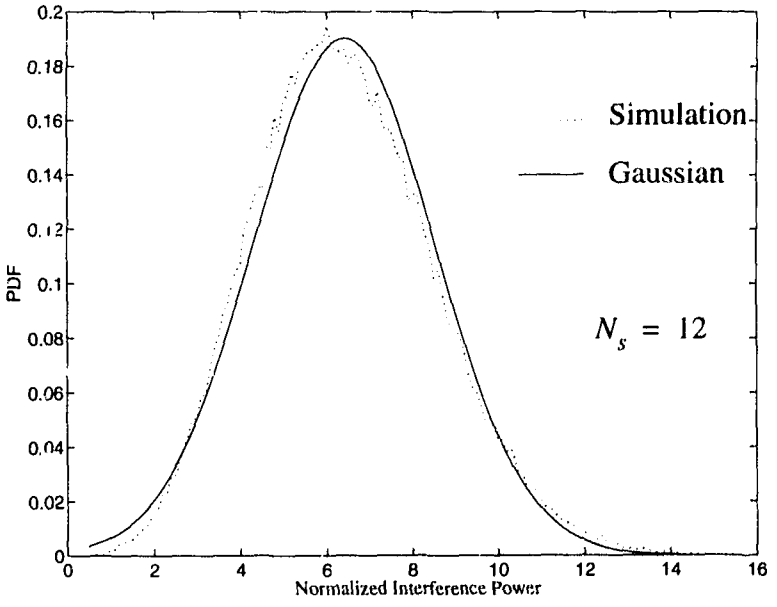

Fig. 7.4 PDF of the total interference. Standard deviation of lognormal shadowing is σ_{LN} = 8 dB, Rs is 9.6 kb/s, activity factor is 0.375, Ns=12.

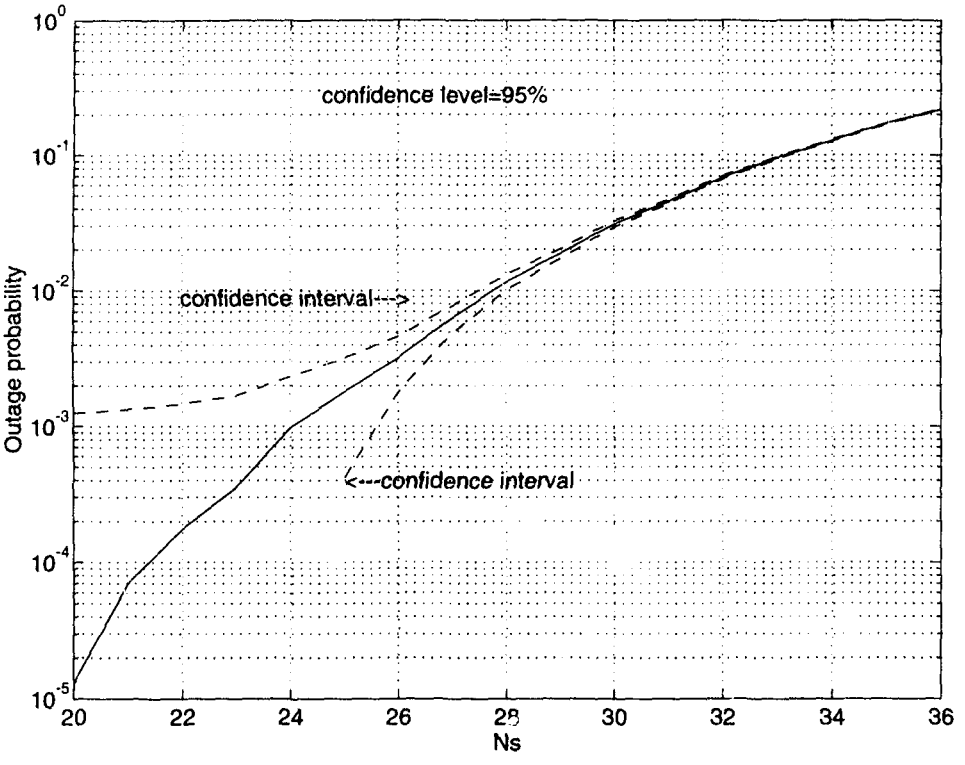

Fig. 7.5 The outage probability of a CDMA cellular system with voice users. Standard deviation of lognormal shadowing is σ_{LN} = 8 dB, QR is 7 dB, Rs is 9.6 kb/s, activity factor is 0.375, bandwidth available is 1.25 MHz, PG=128.

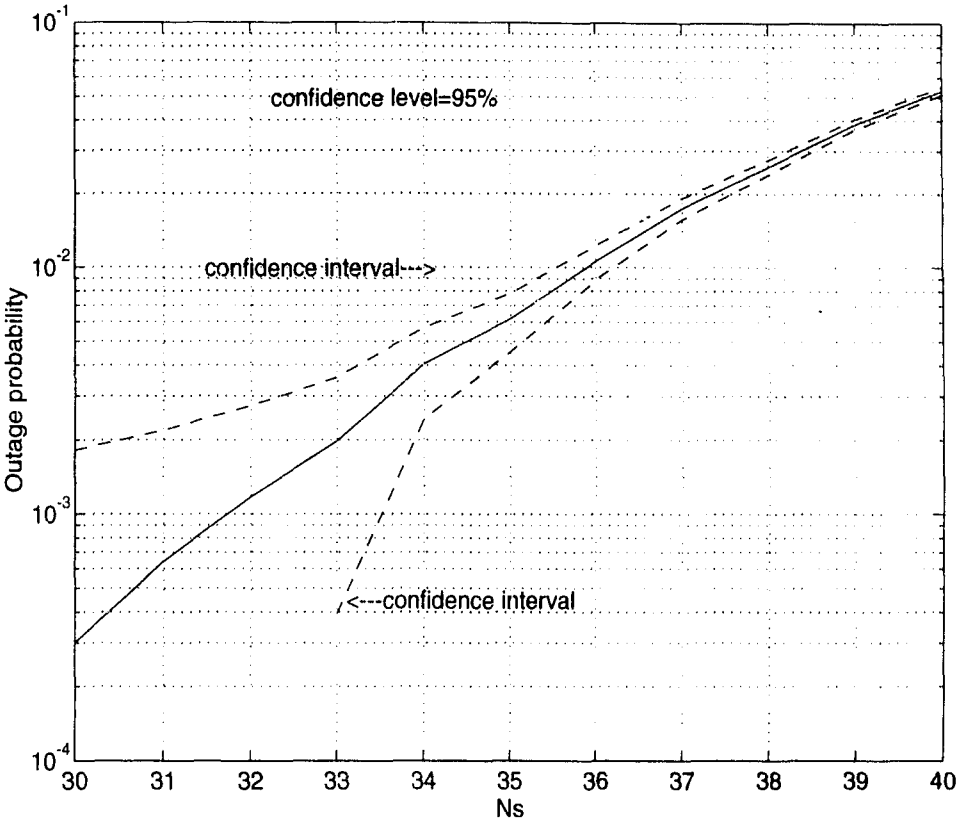

Fig. 7.6 The outage probability of a CDMA cellular system with voice users. Standard deviation of lognormal shadowing is σ_{LN} = 8 dB, QR is 7 dB, Rs is 9.6 kb/s, activity factor is 0.375, bandwidth available is 1.25 MHz, PG=156.

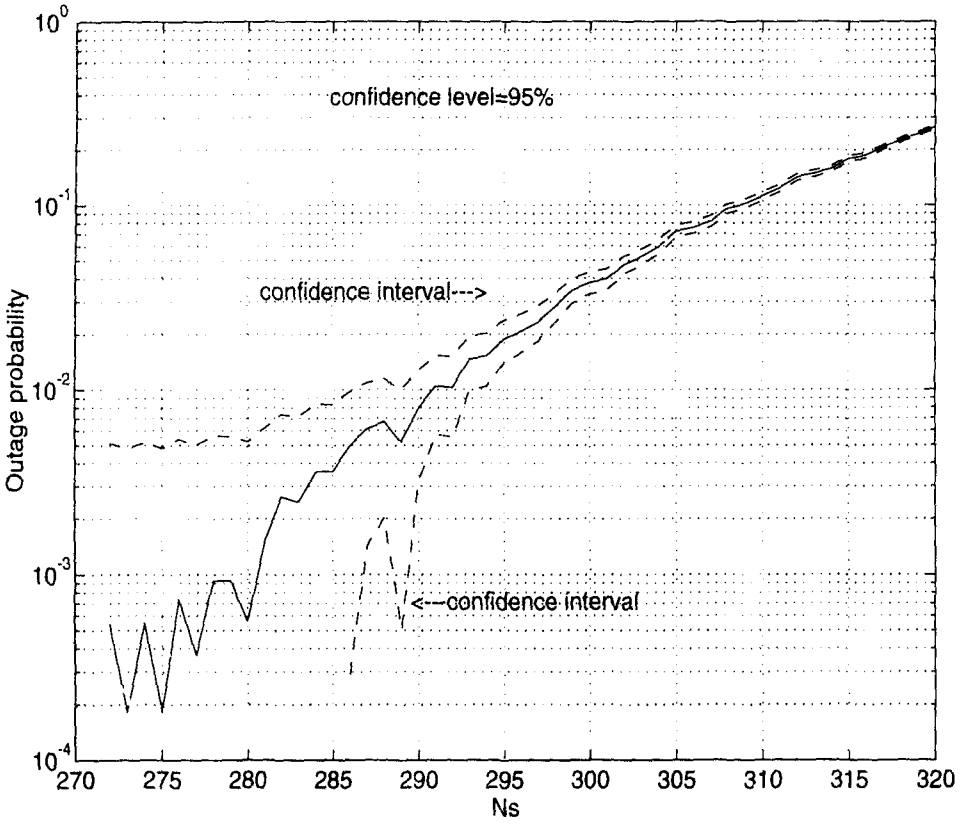

Fig. 7.7 The outage probability of a CDMA cellular system with voice users. Standard deviation of lognormal shadowing is σ_{LN} = 8 dB, QR is 7 dB, Rs is 9.6 kb/s, activity factor is 0.375, bandwidth available is 10 MHz, PG=1024.

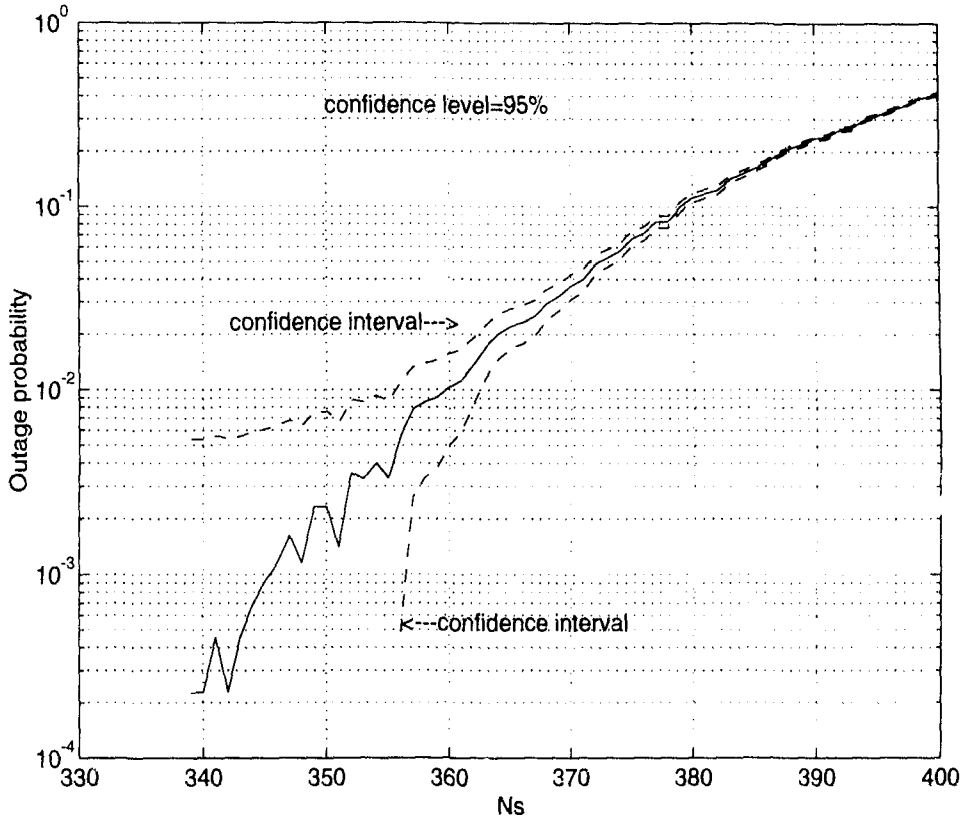

Fig. 7.8 The outage probability of a CDMA cellular system with voice users. Standard deviation of lognormal shadowing is σ_{LN} = 8 dB, QR is 7 dB, Rs is 9.6 kb/s, activity factor is 0.375, bandwidth available is 10 MHz, PG=1248.

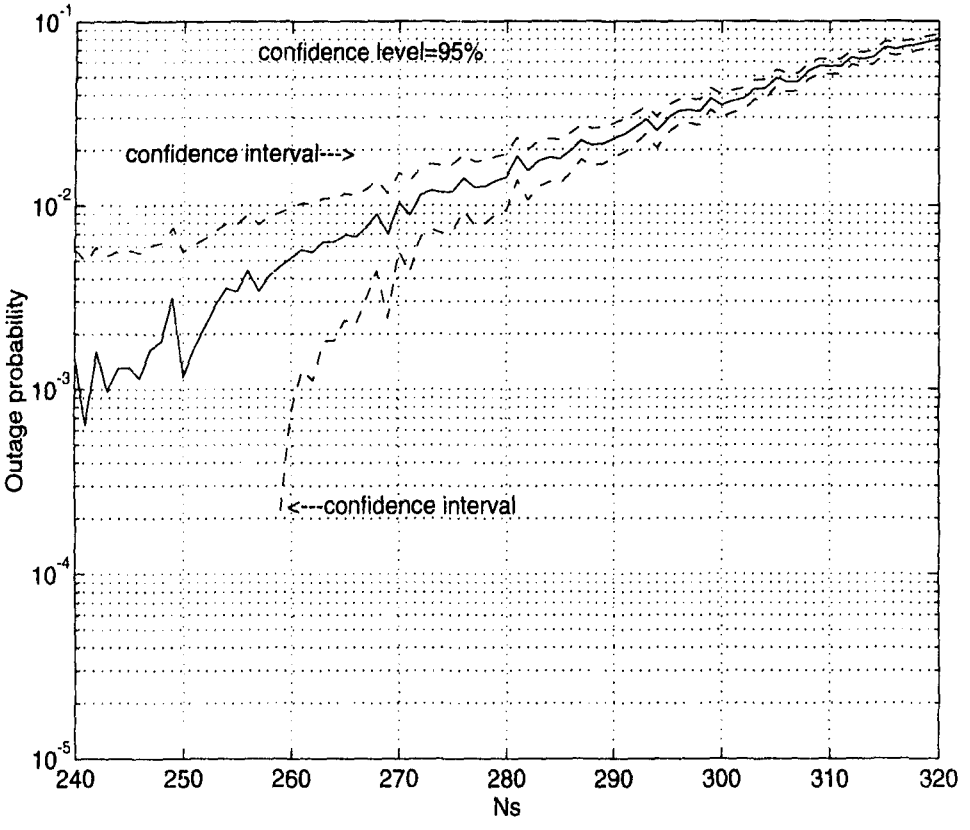

Fig. 7.9 The outage probability of a CDMA cellular system with voice users. Standard deviation of lognormal shadowing is σ_{LN} = 8 dB, QR is 7 dB, Rs is 9.6 kb/s, transmission line rate is 64 Kbps, activity factor is 0.047, bandwidth available is 10 MHz, PG=156.

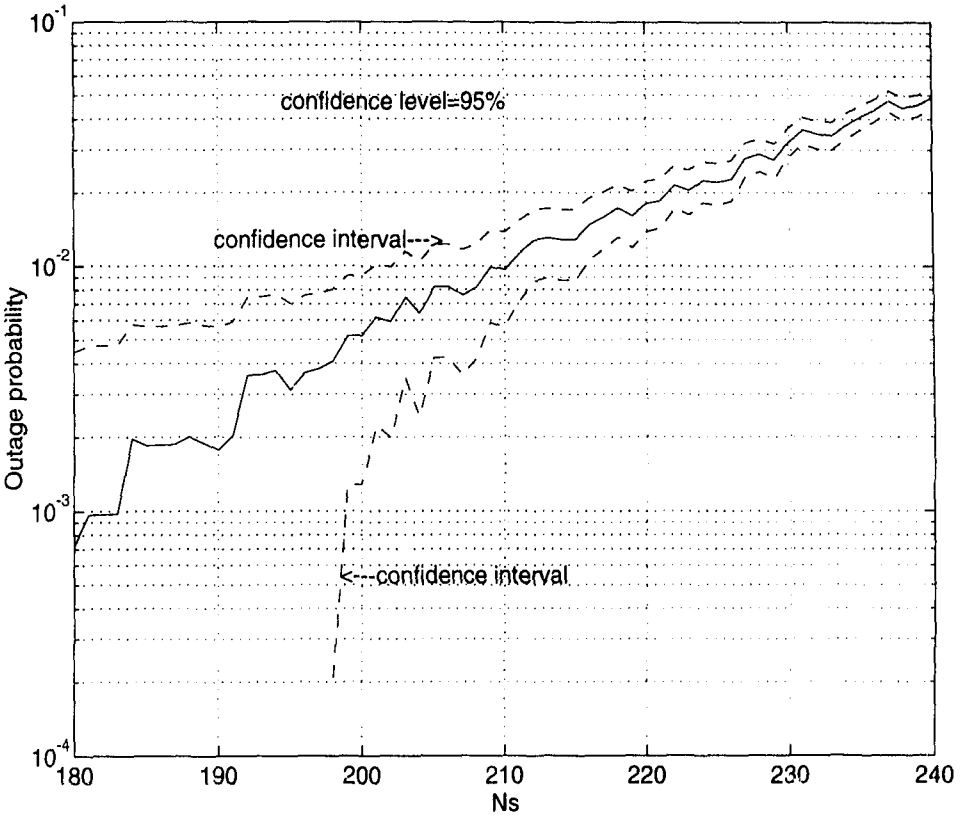

Fig. 7.10 The outage probability of a CDMA cellular system with voice users. Standard deviation of lognormal shadowing is σ_{LN} = 8 dB, QR is 7 dB, Rs is 9.6 kb/s, transmission line rate is 64 Kbps, activity factor is 0.047, bandwidth available is 10 MHz, PG=128.

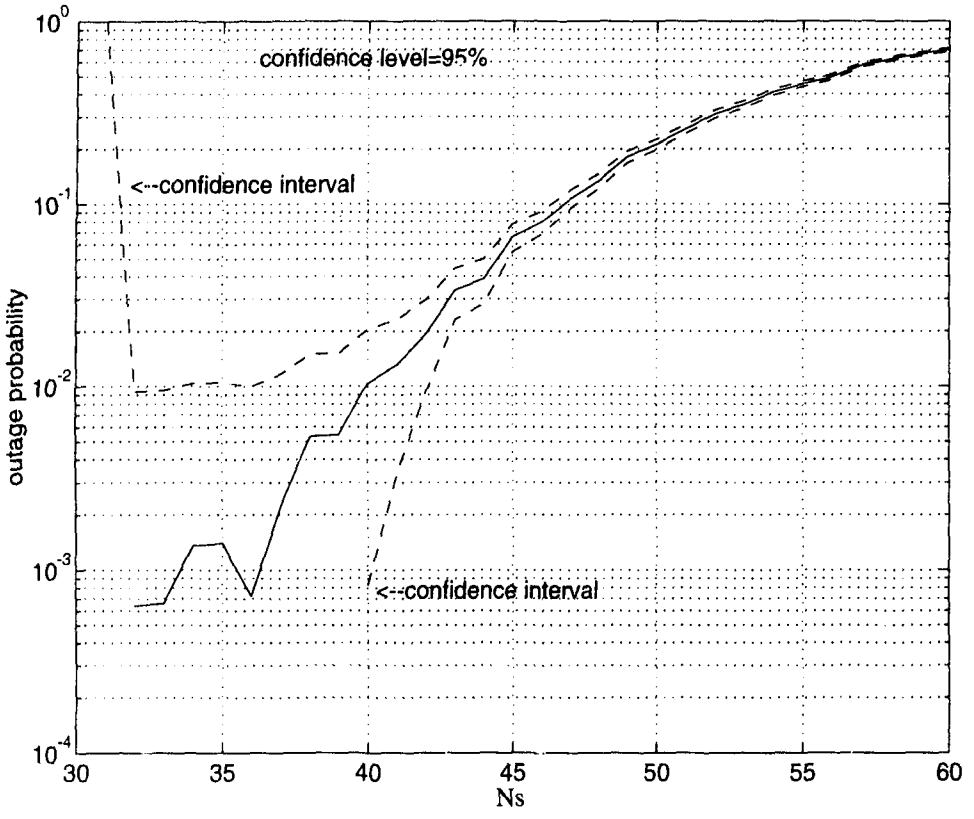

Fig. 7.11 The outage probability of a CDMA cellular system with voice users. Standard deviation of lognormal shadowing is σ_{LN} = 2.5 dB, QR is 7 dB, Rs is 9.6 kb/s, activity factor is 0.375, PG=156.

Chapter 8

Conclusion and Future Work

8.1 Summary

In order to provide the design recommendations for the next generation multimedia wireless networks, the performance of a CDMA cellular system with homogeneous and/or heterogeneous traffic has been studied in details.

Since the capacity of a CDMA cellular system is interference limited, we have developed an analytical method for modelling the multi-cell, multi-user co-channel interference in a CDMA cellular system for both a large number and a small number of users. Through analysis and simulation, we have shown that the Gaussian approximation of the multi-cell, multi-user interference is valid in most cases for cellular CDMA. The reason is that due to soft handoff operations, the interference approaches the Gaussian distribution much faster than a simple summation of random variables.

We have also show that soft handoff and power control are closely related to each other. Power control should match on the best reception of the desired signal to minimize the interference and maximize the capacity. Our results support the conclusion on imperfect power control, which has been obtained by several other researchers. Our results show that the power control error will reduce the system capacity significantly.

To facilitate the system performance and QOS evaluation, we have developed a new model for membership statistics in a CDMA cellular system. The membership statistics which are determined by soft handoff operations affect the intra-cell interference and

QOS. Our results show that the results obtained by the proposed model closely agree with the simulation results.

We have evaluated the radio capacity, Erlang capacity and the QOS of a CDMA cellular system with integrated traffic via an analytical method and simulations. We have shown the effect of a limited number of channels on capacity and QOS. To ensure the Erlang capacity of a system with satisfied QOS, much more channels than the Erlang capacity must be provided.

We have discussed the design considerations for CDMA cellular system with heterogeneous traffic. The impact of the choice of line rate on system capacity has been examined. Our results suggest that the lowest possible line rate is desired in order to maximizing the capacity. We have also determined the optimized power allocation for different types of traffic. The capacity or overall throughput of a CDMA cellular system with multiple traffic can be increased significantly by simply assigning suitable power to different traffic types. Optimum power allocation suggests that the different power assignments to different traffic types are mainly determined by their quality requirements.

8.2 Future Work

This work is emphasized on system analysis, modelling and simulation to provide design recommendations at the system level. Future work will be more focused on study of system management and resource management for a CDMA cellular system with heterogeneous traffic.

Delay-related system performance of a packet CDMA cellular system should be further investigated. The relationship between delay and error probability for stream type of traffic need to be studied.

Soft handoff and power control should be further studied together for multiple traffic types in both the forward and reverse link.

Resource management including the assignment of physical channels, power, band-

width and space diversity should be optimized to maximize the capacity.

Efficient simulation techniques will be further employed in simulation of system performance to further save time and computer memory space.

Bibliography

[1] Victor O. K. Li and Xiaoxin Qiu, "Personal communications systems (PCS)," *Proceedings of the IEEE*, pp. 1210-1243, Sept. 1995.

[2] Per-Göran Andermo and Lars-Magnus Ewerbring, "A CDMA-Based Radio Access Design for UMTS," *IEEE Personal Communications*, pp. 48-53, Feb. 1995.

[3] V. K. Bhargava, "Efficient methods for high rate wireless transmission of integrated traffic," *Proc. of IEEE PIMRC '94*, pp. 1106-1113, Sept. 1994.

[4] D. Raychaudhuri and N. D. Wilson, "ATM-based transport architecture for multi-services wireless personal communication networks," *IEEE Journal on Selected Areas in Communications*, vol. 12, pp. 1401-1414, Aug. 1994.

[5] P. Mermelstein and S. Kandala, "Capacity estimates for mixed-rate traffic on the integrated wireless access network," *Proc. of IEEE PIMRC '95*, pp. 228-232, Sept. 1995

[6] P. Mermelstein, A. Jalali and H. Leib, "Integrated Services on Wireless Multiple Access Networks," *Proc. of ICC '93*, pp. 863-867, June, 1993.

[7] D. L. Schilling, R. Pickholtz, and L. Milstein, "Spread spectrum goes commercial," *IEEE spectrum*, pp. 40-45. Aug. 1990.

[8] R. Kohno, R. Meidan, and L. B. Milstein, "Spread spectrum access methods for wireless communications," *IEEE communications magazine*, pp. 58-67, Jan. 1995.

[9] W.C.Y. Lee, "Overview of cellular CDMA," *IEEE Trans. Vel. Technol.*, vol. 40, pp. 291-302, May 1991.

[10] A. J. Viterbi "Very Low Rate Convolutional Codes for Maximum Theoretical Performance of Spread-Spectrum Multiple-Access Channels," *IEEE Journal on Selected Areas in Communications*, Vol. 8, No. 4, pp. 641-649, May 1990.

[11] R. Padovani, "Reverse link performance of IS-95 based cellular systems," *IEEE Personal Communications*, pp. 28-34, Third Quarter 1994.

[12] A. Salmasi and K. S. Gilhousen, "On the system design aspects of Code Division Multiple Access (CDMA) applied to digital cellular and personal communications networks," *Proc. 41st IEEE Vehicular Tech. Conf.*, St. Louis, MO., pp. 57-62, 1991.

[13] Qualcomm, "CDMA technology for digital cellular and personal communications network," Presented at Cellular Technologies TecForum, Chicago, IL, June 3, 1992.

[14] K.S. Gilhousen, I. M. Jacobs, R. Padovani, A. J. Viterbi, L. A. Weaver, Jr., and C. E. Wheatley, III, "On the capacity of a cellular CDMA system," *IEEE Trans. Vel. Technol.*, vol. 40, pp. 303-312, May 1991.

[15] A. M. Viterbi, A. J Viterbi and E. Zehavi, "Other-cell interference in cellular power-controlled CDMA," *IEEE Trans. Commun.*, vol. 42, pp. 1501-1504, Feb./ Mar./Apr. 1994.

[16] A. J. Viterbi and A. M. Viterbi, K. S. Gilhousen and E. Zehavi, "Soft handoff extends CDMA cell coverage and increases reverse link capacity," *IEEE Journal on Selected Areas in Communications*, vol. 12, pp. 1281-1288, Oct. 1994.

[17] J. Zou, V. K. Bhargava and Q. Wang, "Reverse link interference modelling and outage analysis for DS-CDMA cellular systems," to appear in the *International Journal of Wireless Personal Communications.*

[18] A. M. Viterbi and A. J. Viterbi, "Erlang capacity of a power controlled CDMA system," *IEEE Journal on Selected Areas in Communications*, vol. 11, pp. 892-899, Aug. 1993.

[19] J. Zou, R. Pichna, Q. Wang and V. K. Bhargava, "Efficient methods for high rate data transmission in mobile and personal communications," *Proc. of IEEE MEXICON '94,* Puebla, Mexico, pp. 140-145, Mar, 1994.

[20] Mo-Han Fong, Vijay K. Bhargava and Qiang Wang, "Concatenated orthogonal/ PN spreading scheme for cellular DS-CDMA systems with integrated traffic," *Proc. of IEEE ICC '95,* June 1995.

[21] F. Knebelkamp, B. Eylert, W. Schutters, M. Chang, K. Gilhousen, "Field test of a CDMA system," *Proc. 44th IEEE Vehicular Tech. Conf.*, Stockholm, Sweden, pp. 1-5, June 1994.

[22] R. Padovani, B. Butler and R. Boesel, "CDMA digital cellular: field test results," *Proc. 44th IEEE Vehicular Tech. Conf.*, Stockholm, Sweden, pp. 11-15, June 1994.

[23] J.G. Proakis, *Digital Communications.* New York: McGraw-Hill, 1989.

[24] R. C. French, "The effect of fading and shadowing on channel reuse in mobile radio," *IEEE Trans. Veh. Technol.*, Vol. 28,pp.171-181, 1979.

[25] Chun Loo and Norman Secord, "Computer Models for Fading Channels with Applications to Digital Transmission," *IEEE Trans. on Vehicular Technology*, Vol. 40, No. 4, Nov. 1991.

[26] A. Papoulis, *Probability, Random Variables, and Stochastic Processes*, 2nd ed., NewYork: McGraw-Hill 1984.

[27] M. Nakagami, "The m-distribution--a general formula of intensity distribution of rapid fading," *Statistical Methods of Radio Wave Propagation*, Pergamon Press, 1960.

[28] W. C. Y. Lee, *Mobile Communications Design Fundamentals*, Indianapolis, IN Sams, 1986.

[29] William C. Jakes, Jr., *Microwave Mobile Communications*, NJ: IEEE Press, 1994.

[30] S.C. Schwartz and Y.S. Yeh, "On the distribution function and moments of power sums with log-normal components," *Bell Syst. Tech. J.*, pp.1441-1462, Sept. 1982.

[31] Y.-S. Yeh and S. C. Schwartz, "Outage probability in mobile telephony due to multiple Log-Normal interferes," *IEEE Trans. on Comm.*, Vol. 32, pp. 380-388, Apr. 1984.

[32] R. Prasad, M. G. Jansen and A. Kegel, "Capacity analysis of a cellular direct sequence code division multiple access system with imperfect power control," *IEICE Trans. Commun.*, vol. E76-B, pp. 894-905, Aug. 1993.

[33] E. Kudoh and T. Matsumoto, "On the capacity of DS-CDMA cellular mobile radios under imperfect transmitter power control." *IEICE Trans. Commun.*, vol. E76-B, pp. 886-893, Aug. 1993.

[34] J. Zou, V. K. Bhargava and Q. Wang, "Reverse link analysis and performance evaluation for DS-CDMA cellular systems," *Proc. of IEEE PIMRC '94*, pp. 50-54, Sept. 1994.

[35] G.L. Stuber and C. Kchao, "Analysis of a multiple-cell direct-sequence CDMA cellular mobile radio system," *IEEE Journal on Selected Areas in Communications*, vol. 10, No. 4, pp. 659-679, May 1992.

[36] C. Kchao and G.L. Stuber, "Analysis of a direct-sequence spread-spectrum cellular radio system," *IEEE Trans. Commun.*, vol. 41, No. 10, pp.1507-1516, Oct. 1993.

[37] W.-P. Yung, "Direct-sequence spread-spectrum code-division-multiple access cellular systems in Rayleigh fading and log-normal shadowing channel," *Proc. IEEE ICC '91*, pp. 28.2.1-28.2.6, 1991.

[38] L.B. Milstein, T.S. Rappaport, and R. Barghouti, "Performance evaluation for cellular CDMA," *IEEE Journal on Selected Areas in Communications*, vol. 10, No. 4 pp.-680-689, May 1992

[39] A. J. Viterbi, A. M. Viterbi and E. Zehavi, "Performance of power-controlled wide-band terrestrial digital communication," *IEEE Trans. Commun.*, vol. 41, pp. 559-568, Apr. 1993.

[40] C. A. F. J. Wijffels, H. S. Misser and R. Prasad, "A micro-cellular CDMA system over slow and fast Rician fading radio channels with forward error correcting coding and diversity," *IEEE Trans. Vel. Technol.*, Vol. 42, No. 4, pp. 570-580, Nov. 1993.

[41] R. Pichna, Q. Wang and V. K. Bhargava, "Non-ideal power control in DS-CDMA cellular," *Proc. IEEE Pac. Rim Conf '93*, pp. 686-689, May 1993.

[42] J. Shapira, "Microcell engineering in CDMA cellular networks," *IEEE Trans. Vel. Technol.*, vol. 43, pp. 817-825, Nov. 1994.

[43] .A. Jalali and P. Mermelstein, "Effects of Diversity, Power Control, and Bandwidth on the Capacity of Micro-cellular CDMA Systems," *IEEE Journal on Selected Areas in Communications*, vol. 12, pp. 952-961, June 1994.

[44] Q. Wang and V. K. Bhargava, "A versatile simulation tool for cellular CDMA communications," *Final Report prepared for Science Council of British Columbia under Technology B. C. Grant\#52(T-3)*, Nov. 1993.

[45] R. Vijayan and J. M. Holtzman, "A model for analyzing handoff algorithms," *IEEE Trans. Vel. Technol.*, vol. 42, pp.351-356, Aug. 1993.

[46] J. Zou and V. K. Bhargava, "On soft handoff, Erlang capacity and service quality of a CDMA cellular system: reverse link analysis," *Proc. of IEEE PIMRC '95*, Toronto, Ont., pp. 603-607, Sept. 1995.

[47] U. Charash, "Reception through Nakagami fading multi-path channels with random delays," *IEEE Trans. on Comm.*, Vol. COM-27, pp. 657-670, April 1979.

[48] R. Pichna, Q. Wang, V. K. Bhargava, J. Zou and R. Kerr "Simulation of power control and diversity of cellular CDMA," *Journal of China Institute of Communications,* pp. 94-98, July 1995.

[49] R. Kerr, Q. Wang and V. K. Bhargava, "Capacity Analysis of Cellular CDMA," *Proc. ISSSTA '92*, pp. 235-238, Mar. 1992

[50] W. Feller, *An Introduction to Probability Theory and Its Applications*, Vol. I, 3rd ed. New York: Wiley 1968.

[51] D. Raychaudhuri, "Performance analysis of random access packet-switched code division multiple access systems," *IEEE Trans. Commun.*, vol. COM-29, pp895-901, June 1981.

[52] M. B. Pursly, "Performance evaluation for phase-coded spread-spectrum multiple-access communication--Part I: System analysis," *IEEE Trans. Commun.*, vol. COM-25, pp. 795-799, Aug. 1977.

[53] G. Turin, "The effects of multipath and fading on the performance of direct-sequence CDMA systems," *IEEE Journal on Selected Areas in Communications*, vol. SAC.-2, No. 4, pp. 597-603, July 1984.

[54] N. D. Wilson, R. Ganesh, K. Joseph, and D. Raychaudhuri, "Packet CDMA versus dynamic TDMA for multi-access in an integrated voice/data PCN," *IEEE Journal on Selected Areas in Communications*, vol. SAC.-11, No. 6, pp. 870-883, Aug. 1993.

[55] S. Lin and D. J. Costello, Jr., *Error Control Coding: Fundamentals and Applications*, Prentice-Hall, Inc. Englewood Cliffs, New Jersey 1983.

[56] Mo-Han Fong, Qiang Wang and Vijay K. Bhargava, "Concatenated Orthogonal/ PN Codes for DS-CDMA Systems in a Multi-user and Multipath Fading Environment," *Proc. of IEEE Globecom '94*, pp. 1642-1646, Dec. 1994.

[57] J. Zou and V. K. Bhargava, "Optimized power allocation for mixed rate traffic in a DS-CDMA cellular system," *IEE Electronic Letters*, vol. 31, No. 22, pp. 1902-1903, Oct. 1995.

[58] M. C. Jeruchim, P. Balaban, and K. S. Shanmugan, *Simulation of Communication Systems*, New York: Plenum Press, 1992.

[59] P. Balaban, "Statistical Evaluation of the Error Rate of the Fiber-guide Repeater Using Importance Sampling," *BSTJ*, Vol. 55, pp. 745-766, July-August 1976.

[60] K. S. Shanmugam and P. Balaban, "A Modified Monte-Carlo Simulation Technique for The Evaluation of Error Rate in Digital Communication Systems," In *IEEE Trans. on Comm.*, Vol. 28, No. 11, Nov. 1980.

[61] P. M. Hahn and M. C. Jeruchim, "Developments in The Theory and Application of importance Sampling," *In IEEE Trans. Comm.*, Vol. 35, pp. 706-714, No. 7, July 1987.

[62] D. Liu and K. Yao, "Improved Importance Sampling Technique for Efficient Simulation of Digital Communication Systems," *IEEE J. Select Areas Comm.*, Jan. 1988.

[63] G. C. Orsak and B. Aazhang, "Constrained Solutions in Importance Sampling via Robust Statistics," *IEEE Trans. on Information Theory*, Vol. IT-37, pp. 307-316, No.3, Mar. 1991.

[64] G. C. Orsak and B. Aazhang, "On The Theory of Importance Sampling Applied to The Analysis of Detection System," *IEEE Trans. on Comm.*, Vol. 30, pp. 332-339, No. 4, Apr. 1989.

[65] G. C. Orsak and B. Aazhang, "Efficient importance sampling techniques for simulation of multiuser communication systems," *IEEE Trans. on Comm.*, Vol. 40, pp. 1111-1118, June 1992.

[66] N. C. Beaulieu, "A Composite Importance Sampling Technique for Digital Communication System Simulation," *IEEE Trans. on Comm.*, Vol. 38, pp. 393-396, No. 4, Apr. 1990.

[67] Jyun-Cheng Chen, D. Lu, J. S. Sadowsky and K. Yao, "On Biasing Gaussian Noise in Importance Sampling: Optimization and Implementation," *Proc. of ICC'92*, pp. 344.5.1-344.5.5, 1992.

[68] Q. Wang and V.K. Bhargava, "On the Application of Importance Sampling to BER Estimation in the Simulation of Digital Communication Systems," *IEEE Trans. on Comm.*, Vol. 35, pp.1231-1233, No. 11, Nov. 1987.

[69] M.C. Jeruchim, "Techniques for Estimating the Bit Error Rate in the Simulation of Digital Communication Systems," *IEEE J. Select Areas Comm.*, Vol. SAC-2, pp. 153-170, Jan. 1984.

[70] J. Zou, and V. K. Bhargava, "On the optimum biasing of importance sampling for simulation of communication systems," *Proc. of Canadian Conference on Electrical and Computer Engineering*, Vancouver, B.C., pp. 515-518, Sept. 1993.

[71] A. W. Law and W. D. Kelton, *Simulation Modeling and Analysis*, New York: McGraw-Hill Book Company, 1982.

Appendix

List of Abbreviations

ACF	Activity Factor
ARQ	automatic repeat request
ATM	Asynchronous Transfer Mode
BER	bit error probability
B-ISDN	Broadband-Integrated Services Digital Networks
CDMA	Code Division Multiple Access
CITR	The Canadian Institute for Telecommunications Research
CODIT	COde DIvision Testbed project under RACE
CRN	Common Random Numbers
CRT	cathode ray tube
DPSK	differential phase shift keying
DS/CDMA	Direct Sequence CDMA
FDMA	Frequency Division Multiple Access
HF	High Frequency
IS	Importance Sampling
IS-95	TIA/EIA Interim Standard proposed by Qualcomm
IWAN	Integrated Wireless Access Network
MTSO	mobile telephone switching office
PC	power control
PCS	personal communications system
PDF	probability density function
PG	Processing Gain
PN	pseudo-noise
QOS	quality of services

QR	quality requirement
RACE	The R & D in Advanced Communications Technologies in Europe program
SNR	signal to noise ratio
TDMA	Time Division Multiple Access
VLSI	Very Large Scale Integration